ALKYNE CYCLIZATION INVOLVING A ZWITTERIONIC HEXARUTHENIUM CARBIDO CARBONYL COMPLEX AND THE SYNTHESIS OF THE FIRST-NITRIDO HETEROMETALLIC CARBONYL CLUSTER COMPLEXES

by

Nutan Damodhar Wakdikar

Bachelor of Science
University of Mumbai, 2011

Master of Science
University of Mumbai, 2014

Submitted in Partial Fulfillment of the Requirements

For the Degree of Doctor of Philosophy in

Chemistry

College of Arts & Science

University of South Carolina

2021

Accepted by:

Richard D. Adams, Major Professor

Dmitry V. Peryshkov, Committee Member

Sheryl L. Wiskur, Committee Member

Christopher Williams, Committee Member

Tracey L. Weldon, Interim Vice Provost and Dean of the Graduate School

© Copyright by Nutan Damodhar Wakdikar, 2021
All Rights Reserved.

DEDICATION

This is for you, Papa.

ACKNOWLEDGEMENTS

The task of completing the doctoral studies requires patience, guidance, and a constant motivation. It is certainly not an easy one. That is why, at first, I would like to express a sincere gratitude and heartfelt thanks to my advisor Prof. Richard D. Adams for helping me to undertake my Ph.D. studies in his lab. His in-depth knowledge of chemistry, the zeal and passion towards doing research, the discipline to stay focused and work hard have been a constant source of encouragement throughout my time as a graduate student at the University of South Carolina. Also, I am and will always be deeply grateful to him for teaching me valuable lessons under his supervision and mentorship that helped me become a resilient and diligent person that I am today in my work and prepared me for my future endeavors.

I would like to extend my ineffable gratitude to my research committee: Professors Dmitry Peryshkov, Sheryl Wiskur and Christopher Williams for accepting to review my work and for taking the time to be there for all my comprehensive exams and dissertation defense. Thank you, Prof. Peryshkov, to help me understand the concepts of Organometallic Chemistry and build up my presentation skills as a first-year graduate student that I was in your coursework studies at UofSC. It was a great experience working on the collaborative projects and with your students, Prof. Williams.

I would also like to acknowledge the help and support from former members and current members in the Adams group: Dr. Joseph Kiprotich for giving me research

advice, Dr. Jonathan Tedder for training me in lab work and crystal structure solving, Dr. Poonam Dhull for always encouraging me, Meenal Kaushal, Humaiara Akter, Morteza Maleki, Claire Prince and Wilson Edenfield for being great friends. I wish all you guys good luck for your future endeavours! Special recognition goes to Dr. Mark D. Smith for his help with crystals that were difficult to handle, Dr. Perry J. Pellechia and Toni Johnson for assistance with VT-NMR and all other complex NMR studies and Dr. Mike Walla and Dr. William E. Cotham for excellent technical support with mass spectrometer.

I would like to thank the Graduate School and the Department of Chemistry & Biochemistry for giving me the opportunity to study here at the University of South Carolina. I really appreciate the help I received from the members and my colleagues at this department.

Finally, I would like to acknowledge and express my gratitude to my family members and friends for just being there for me all the time. A big THANK YOU to my parents for believing in me. Thank you, Papa, for showing constant support and encouragement, for pushing me to pursue all my dreams and to help me attain a never give up attitude. To my mom, who taught me kindness and love. Special thanks to my brother, Akash, and my sister, Yugeshri, for filling up my life with joyful and exciting moments, you guys are world to me!

ABSTRACT

Chapter 1 introduces two related topics with the primary focus on the background of zwitterions and the conceptual understanding of a metal-complexed zwitterion. It also discusses the potential of a metal-complexed zwitterion for a carbon-carbon bond formation reaction. Synthesis of the metal carbonyl cluster, $Ru_6(\mu_6\text{-}C)(\mu\text{-}CO)(CO)_{16,}$ is also discussed in detail. Then, the background with the importance of heterometallic cluster complexes is discussed with the help of various examples used for catalysis.

The reaction of hexaruthenium carbido carbonyl cluster, $Ru_6(\mu_6\text{-}C)(\mu\text{-}CO)(CO)_{16}$, with C_2H_2 and Me_3NO yielding first examples of two new zwitterionic complexes, $Ru_6C(CO)_{15}(\mu\text{–}\eta^2\text{–}C_2H_2NMe_3)$, **2.2**, and $Ru_6C(CO)_{14}(\mu_3\text{–}\eta^4\text{–}C_4H_4NMe_3)$, **2.3**, are presented in Chapter 2. Addition of CO to **2.2** yields the complex $Ru_6C(CO)_{16}(\eta^1\text{–}\textit{E}\text{–}C_2H_2NMe_3)$, **2.4. t**hat involves the transformation of a bridging-$C_2H_2NMe_3$ ligand to a terminally coordinated position. On heating the complex **2.2,** it undergoes thermal transformation to the complex $Ru_6C(CO)_{15}(\mu_3\text{-}C_2H_2)$, **2.5** and similarly the complex **2.3** transforms to the complex $Ru_6C(CO)_{14}(\mu_3\text{–}\eta^4\text{–}C_4H_4)$, **2.6**. Similarly, the reaction of $Ru_6(\mu_6\text{-}C)(\mu\text{-}CO)(CO)_{16}$ with methyl propiolate and Me_3NO yields the zwitterionic metal complex $Ru_6C(CO)_{16}[\eta^1\text{-}\textit{E}\text{-}C(CO_2Me)\text{=}C(H)NMe_3]$, **2.7**. The compound **2.7** thermally transforms to the complex $Ru_6C(CO)_{15}[\mu_3\text{-}HC_2(CO_2Me)]$, **2.8.** The structure, and transformations involved within the new complexes are described.

Reaction of $Ru_6(\mu_6\text{-}C)(CO)_{14}(\mu_3{-}\eta^4\text{-}C_4H_4)$, **3.2** with dimethyl acetylene dicarboxylate are presented in Chapter 3. Th namely, $Ru_6(\mu_6\text{-}C)(CO)_{16}(\mu{-}\eta^4{-}C_4H_4)$, **3.3**, $Ru_6(\mu_6\text{-}C)(CO)_{14}[\eta^6\text{-}C_6H_4(CO_2Me)_2]$, **3.4**, $Ru_6(\mu_6\text{-}C)(CO)_{14}(\mu{-}\eta^4{-}C_4H_4)[\mu_3{-}C_2(CO_2Me)_2]$, **3.5**, $Ru_6(\mu_6\text{-}C)(CO)_{14}(\mu{-}\eta^4{-}C_4H_4)[\mu_3{-}C_2(CO_2Me)_2]$, **3.6** and $Ru_6(\mu_6\text{-}C)(CO)_{14}[\mu_3{-}\eta^6\text{-}C_6H_4(CO_2Me)_2]$, **3.7.** Compound **3.4** and **3.7** contains a metal-coordinated arene ring formed by cycloaddition reaction. Addition of dimethyl acetylene dicarboxylate to **3.3** yields the compound $Ru_6C(CO)_{15}(\mu{-}\eta^4{-}C_4H_4)[\mu{-}C_2(CO_2Me)_2]$, **3.8**. by replacing one of its bridging CO ligands with DMAD. On heating, compound **3.5** undergoes C-C coupling between the DMAD and the butadiendiyl ligand to give the complex $Ru_6C(CO)_{14}[\mu_4{-}\eta^6{-}CHCHCHCC(CO_2Me)C(CO_2Me)](\mu\text{-}H)$, **3.9**. Compound **3.3** was decarbonylated with Me_3NO to compound $Ru_6C\ (CO)_{15}(\mu{-}\eta^4{-}C_4H_4)(NMe_3)$, **3.10.**

The reactions of the pentaruthenium nitride carbonyl cluster complex, $[PPN][Ru_5(\mu_5\text{-}N)(CO)_{14}]$, **4.1,** with the gold complex, $Au(PPh_3)]NO_3$, and copper complexes, $[Cu(PPh_3)Br]_4$, and $[Cu(NCMe)_4][BF_4]$ are presented in Chapter 4. The reaction of $[PPN][Ru_5(\mu_5\text{-}N)(CO)_{14}]$, **4.1,** with $Au(PPh_3)]NO_3$ yielded three ruthenium-gold heterometallic nitrido carbonyl cluster complexes namely $Ru_4(\mu_4\text{-}N)(CO)_{12}(\mu\text{-}AuPPh_3)$, **4.2,** $Ru_5(\mu_5\text{-}N)(CO)_{14}(\mu\text{-}AuPPh_3)$, **4.3** and $Ru_5(\mu_5\text{-}N)(CO)_{13}(\mu\text{-}AuPPh_3)[\mu_3\text{-}(AuPPh_3)_2]$, **4.4.** The reaction of $[PPN][Ru_5(\mu_5\text{-}N)(CO)_{14}]$, **4.1**, with $[Cu(PPh_3)Br]$ in presence of $Tl[PF_6]$ yielded three new ruthenium-copper heterometallic nitrido carbonyl cluster complexes namely $Ru_4(\mu_4\text{-}N)(CO)_{12}[\mu\text{-}Cu(PPh_3)]$, **4.5,** $Ru_5(\mu_5\text{-}N)(CO)_{13}(PPh_3)[\mu_3\text{-}Cu(PPh_3)]$, **4.6**, and $Ru_5(\mu_5\text{-}N)(CO)_{13}[\mu\text{-}Cu(PPh_3)][(\mu_3\text{-}Cu(PPh_3)]_2$, **4.7.** The reaction of $[PPN][Ru_5(\mu_5\text{-}N)(CO)_{14}]$, **4.1,** with $[Cu(NCMe)_4][BF_4]$

yield $Ru_5(\mu_5\text{-}N)(CO)_{14}[\mu_3\text{-}Cu(NCMe)]$, **4.8.** The synthesis and structures of new complexes are discussed herein.

The synthesis of the new dicopper cation of $[\{(IPr)Cu\}_2(\mu\text{-}Cl)][PF_6]$, **5.1** and its reaction with the complex $[PPN][HOs_3(CO)_{11}]$, **5.2** are presented in Chapter 5. The reaction of **5.1** with the salt complex $[PPN][HOs_3(CO)_{11}]$, **5.2** yielded the new osmium-copper heterometallic complex $Os_3(CO)_{11}(H)[\mu\text{-}Cu(IPr)]$, **5.3**, the first example of Cu – Os carbonyl cluster complex containing a N-heterocyclic carbene ligand.

TABLE OF CONTENTS

LIST OF TABLES

LIST OF FIGURES

CHAPTER 1

INTRODUCTION

This dissertation covers two related topics of study with the primary focus on the chemistry of zwitterionic trimethylammonio-alkenyl ligands in ruthenium carbido carbonyl cluster complexes and the second on the synthesis and characterization of novel heterometallic carbonyl cluster complexes for their potential use in catalysis.

1.1 ZWITTERION

Zwitterions, in general, are neutral compounds containing formal unit electrical charges of opposite sign.[1] In a zwitterion, formally a positive charge and a negative charge could be present on either adjacent or non-adjacent atoms. Some examples for zwitterionic compounds include dipolar compounds such as amino acids [$H_3N^+CH_2C(=O)O^-$ ammonioacetate (glycine)] which contains formally a positive charge and a negative charge on non-adjacent atoms. Hydrocarbylonium zwitterions have been known for many years. [2,3] The best examples include, ylides, such as phosphonium ylides [R_3P^+-$^-CR'_2$], **A**,[2] or sulfonium ylides [R_3S^+-$^-CR'_2$], **B**,[3] containing formally a positive and a negative charge on adjacent atoms, see Scheme 1.1.1

Scheme 1.1.1 Phosphonium and Sulfonium Ylides

They were among the first reported ones and are known as Wittig reagents after their discovery.[2] Along with these zwitterions, there are numerous examples of metal-complexed zwitterions.

Metal-Complexed Zwitterions

In a typical metal-complexed zwitterion, the negative charge on carbon atom is formally transferred to the metal atom upon coordination, see Scheme 1.1.2. It involves an exclusive coordination through carbon atom only.

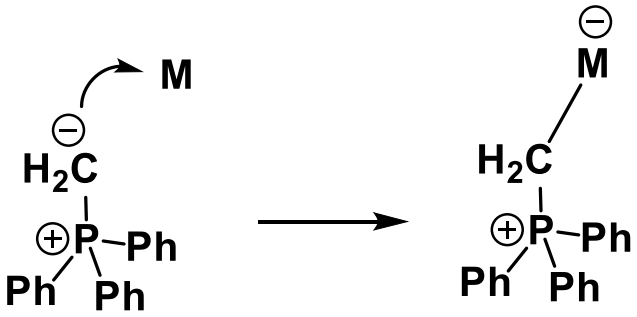

Scheme 1.1.2. Formation of a Metal-Complexed Zwitterion

The ylides are known to coordinate very well with the metal atoms through the formal transfer of negative charge on the carbon atom to the metal atom to form zwitterion complexes, see **C** and **D** in Scheme 1.1.3.[4,5]

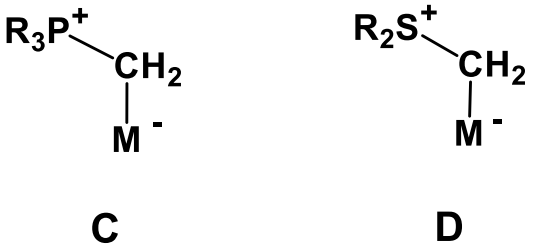

Scheme 1.1.3. Metal-Complexed Ylides

In recent years, many examples of the extended metal-complexed zwitterionic hydrocarbylonium species have also been synthesized, see Scheme 1.1.4. The most common examples are the ones containing phosphonium alkenyl ligands, see **E**.[6-8]

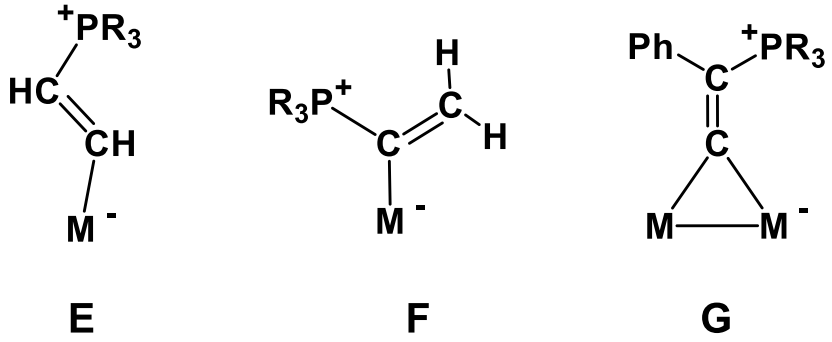

Scheme 1.1.4. Examples of Metal-Complexed Zwitterion

However, there are very few examples of metal-complexed zwitterions containing ammonium alkenyl ligands, **H**, see Scheme 1.1.5.[9] These ylides or zwitterions serve as valuable reagents in many organic syntheses.[3] They find applications in many carbon – carbon bond forming coupling reactions.

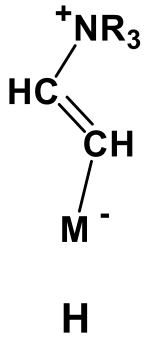

Scheme 1.1.5. Zwitterion Complex with an Ammonium Alkenyl Ligand

Carbon – Carbon Coupling Bond Formation in Zwitterion

A very well-known example of the synthetic use of ylides is the Wittig reaction. It involves reaction of a ketone and a phosphonium ylide with oxygen atom exchange to make an alkene,

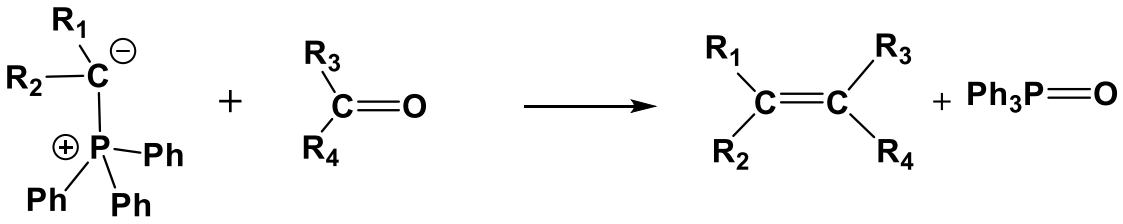

Scheme 1.1.6. Wittig reaction

see Scheme 1.1.6.[2] In recent years, there has been great deal of interest in the use of tertiary phosphines as reagents to perform organic syntheses.[10] Zwitterionic species such as phosphonium ylides are known to play valuable roles in phosphine-mediated organic reactions. Phosphine-mediated organic reactions have become an important tool for the synthesis of carbon-carbon bonds.[11]

In a typical phosphine-catalyzed organic reaction, zwitterionic species can follow two pathways as represented in Scheme 1.1.7.[10] One pathway would lead to the formation of stoichiometric product while the other one will result in the formation of catalyzed product. The mechanism begins with the nucleophilic addition of phosphine to an electrophilic unsaturated species (usually electron-deficient olefins or alkynes) to form zwitterionic intermediate. The zwitterionic intermediate formed can further react with an appropriate coupling partner (a second molecule of olefin or alkyne) to form second intermediate. At this point the second intermediate can follow either a catalytic or a stoichiometric pathway. Thus, it can release the final product in catalytic or stoichiometric fashion by elimination of phosphine catalyst. In the mechanism, deoxygenated product will be formed by elimination of phosphine oxide in stoichiometric amounts when the oxophilicity of phosphine takes effect over the leaving group ability and with the help of other functional group such as carbonyl involved in the transformation. In particular, the phosphine-mediated approach involving zwitterionic intermediates has been an effective method for performing cycloaddition reactions.[12] An interesting example of a cycloaddition reaction is the Alkyne Cyclotrimerization, a (2+2+2) cycloaddition reaction, that can be used to synthesize arene rings.[13] Arenes are a versatile and an important class of compounds having applications in the field of pharmaceuticals, medicine, fuels and many more.[14]

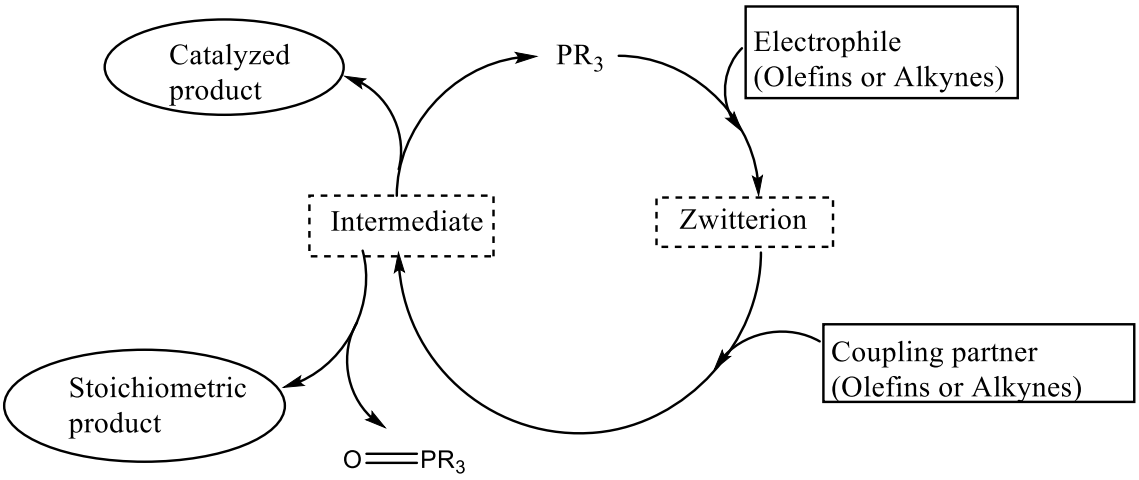

Scheme 1.1.7. Pathways for phosphine-mediated carbon-carbon coupling reactions.

A transition-metal-catalyzed [2+2+2] cycloaddition reaction is highly efficient method for the synthesis of 6 membered cyclic ring compounds with high atom economy.[13d] Ruthenium have been known as an excellent transition metal to promote [2+2+2] cycloaddition reactions due to its tendency for multiple metal bonding and through coupling with alkynes to produce different metallacyclic complexes.[13e-f] Therefore, with this background, the synthesis of two novel zwitterionic compounds containing ammonium alkenyl ligands and how these compounds were used as intermediates to achieve tertiary-amine mediated alkyne coupling cycloaddition reactions to synthesize arene rings by using the metal cluster complex $Ru_6(\mu_6\text{-}C)(\mu\text{-}CO)(CO)_{16}$ as the starting material will be discussed.

Synthesis of $Ru_6(\mu_6\text{-}C)(\mu\text{-}CO)(CO)_{16}$ and its Importance

The synthesis for the high nuclearity cluster of $Ru_6(\mu_6\text{-}C)(\mu\text{-}CO)(CO)_{16}$ is a slightly modified version of the procedure originally reported by Brian F. G. Johnson and Jack Lewis, see Scheme 1.1.8.[15] Much of the early chemistry developed for this cluster

complex was investigated by Johnson and Lewis. The octahedral hexaruthenium carbido cluster, $Ru_6(\mu_6\text{-}C)(CO)_{17}$, was initially synthesized by the thermal decomposition of triruthenium dodecacarbonyl, $Ru_3(CO)_{12}$, in nonane solvent in low yield (18.7 %). It is believed that the encapsulated carbido atom is formed by the reduction of a carbonyl (CO) ligand with the release of carbon dioxide (CO_2) during the pyrolysis.[15] An improved synthesis was developed by Johnson and Lewis where $Ru_3(CO)_{12}$ is loaded into a high-pressure reactor, dissolved in octane solvent, and pressurized to 30 atm of ethylene and heated at 150 °C for 6 h.[16] As compared to the low yields (18.7%) produced by the previously reported pyrolysis of $Ru_3(CO)_{12}$, yields of 70% for $Ru_6(\mu_6\text{-}C)(\mu\text{-}CO)(CO)_{16}$ was obtained by using this method.

The octahedral hexaruthenium carbido cluster complex $Ru_6(\mu_6\text{-}C)(\mu\text{-}CO)(CO)_{16}$ was synthesized by loading $Ru_3(CO)_{12}$ in a high-pressure reactor and dissolving in octane solvent. The reactor was pressurized to 350psi of ethylene and heated at 180°C for 6h. The octahedral Ru_6 cluster contains 16 terminal and one bridging CO ligands. The interstitial carbido carbon atom bonds to all six ruthenium atoms of the Ru_6 cluster. With each CO contributing two electrons and four electrons from the interstitial carbido carbon atom, and 48 from the six ruthenium atoms the total valence electron count for the cluster is 86 which is in accord with the observed octahedral cluster six metal atoms.[17]

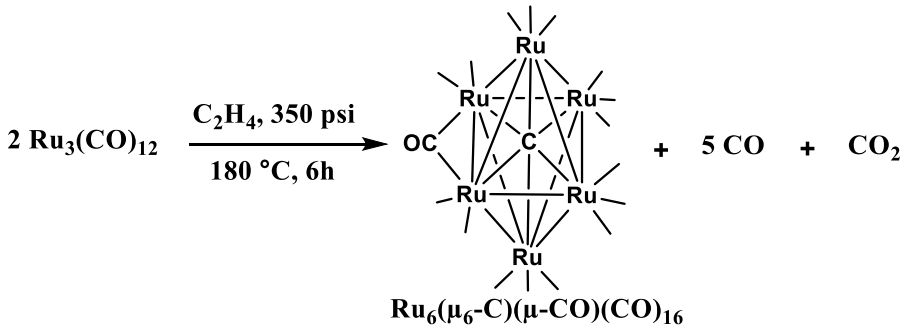

Scheme. 1.1.8 Synthesis of $Ru_6(\mu_6\text{-}C)(\mu\text{-}CO)(CO)_{16}$

The Ru_6 carbido cluster is known to undergo a wide range of reactions from substitution to addition and insertion reactions. The ability of the cluster polyhedron to rearrange itself and the carbide carbon that keeps the octahedral structure intact makes it an attractive choice for many organic reactions. The scope of the Ru_6 carbido cluster chemistry widens as many organic transformations can occur on the surface of the cluster core. This allows the synthesis of many new compounds and the study of their intramolecular transformations.[18]

1.2 Heterometallic Carbonyl Cluster Compounds

Cluster complexes are compounds containing an ensemble of metal atoms (usually same but different metals may also be involved) and supporting ligands. The former is homometallic cluster complexes see Scheme 1.2.1, and the latter are heterometallic cluster complexes, see Scheme 1.2.2 for examples.[19]

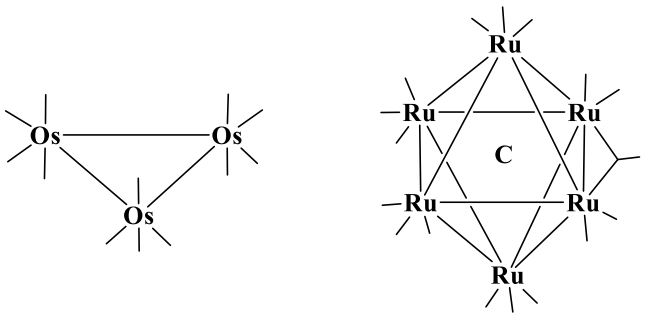

$Os_3(CO)_{12}$ $Ru_6C(CO)_{17}$

Scheme 1.2.1. Homometallic Carbonyl Cluster Complexes

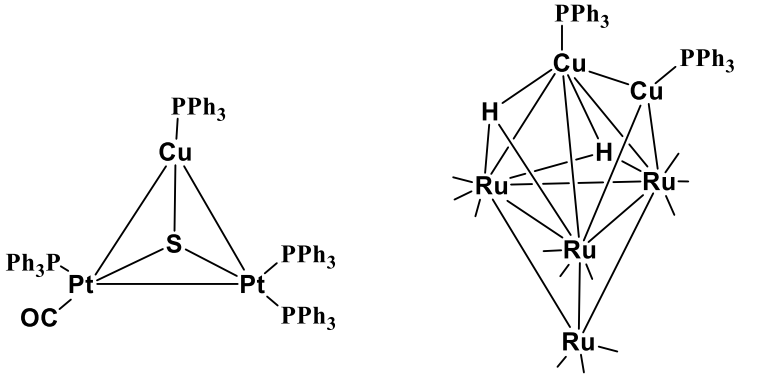

$[CuPt_2(\mu_3\text{-}S)(CO)(PPh_3)_4][PF_6]$ $[Cu_2Ru_4(H)_2(CO)_{12}(PPh_3)_2]$

Scheme 1.2.2. Heterometallic Carbonyl Cluster Complexes

Importance of Heterometallic Cluster Complexes of Group 8-IB metals in Catalysis

In the field of catalysis, a variety of heterometallic catalysts have proven to be more useful than homometallic catalysts for certain types of catalytic reactions. An important example of this has been the use of Pt-Ir, Pt-Sn and Pt-Re heterometallic systems dispersed on alumina as a petroleum reforming catalyst for the production of aromatic compounds for use in the formation of unleaded gasolines.[20] These catalysts exhibit higher activities and better lifetimes than pure Pt catalysts.[21] Also,heterometallic

catalysts containing group 8 and IB metals are known to exhibit better catalytic activity than pure group 8 metals for the dehydrogenation of cyclohexane.[21] (see Scheme 1.2.3). The concept of heterometallization involves addition of a second metal to the first one in order to enhance the catalytic properties of the original metal catalyst through "synergism" that can create a catalyst that is superior to the original metal catalyst.[22]

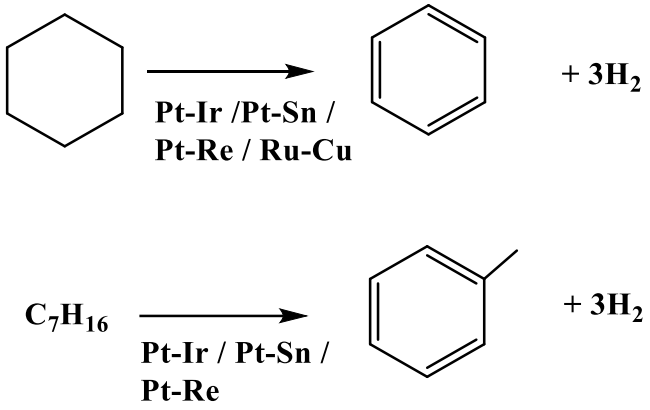

Scheme 1.2.3 Aromatics formed by dehydrogenation of saturated hydrocarbons by heterometallic catalysts.

A heterometallic catalyst can provide two active sites that can function in concert or in tandem to perform a desired reaction.[23] Bimetallic and polymetallic cluster complexes serve as an excellent precursor to heterometallic catalysts.[24] Therefore, synthesis of the heterometallic cluster complexes becomes important. Heterobimetallic cluster catalysts containing group 11 elements, also known as the coinage metals (Cu, Ag or Au), are known to exhibit superior activity and selectivity as compared to their monometallic counterparts.[25,26] Much interest has been developed over the past few years to synthesize bimetallic complexes involving coinage metals to study their structure and catalytic properties.[27] Indeed, some of first successful examples of the synthesis of

hetero-bimetallic complexes involved ligated-gold groupings bonded to transition metals carbonyl groups.[28] Copper has also been shown to be an effective modifier and cocatalyst in heterometallic complexes.[29] Many ligated forms of copper ions have been synthesized and have been used as catalysts in many organic reactions.[30-32] N-heterocyclic carbenes have been shown be very effective ligands for the ions of copper.[33] Therefore, this led us to prepare heterometallic cluster complexes containing copper and gold metal groupings.

One of the successful methods to prepare heterometallic cluster complexes has been through reactions of polynuclear metal carbonyl anions with metal halide complexes or complex metal cations.[34] Many heterobimetallic cluster complexes have been prepared containing interstitial carbido[35] or interstitial borido ligands.[36] Only a few have been prepared with interstitial oxo ligands.[37] There is only one example of a heterometallic complex containing nitrido ligand.[38] This prompted us to prepare a series of new heterometallic complexes containing an interstitial nitrido ligand by using $[PPN][Ru_5(\mu_5\text{-}N)(CO)_{14}]$[39] {PPN = $[Ph_3PNPPh_3]^+$} as the starting material.

Similarly, we have made a new carbene-ligated copper and osmium heterometallic complex from the triosmium carbonyl anion $[HOs_3(CO)_{11}]^-$ obtained from the salt, $[PPN][Os_3(CO)_{11}(\mu\text{-}H)]$.[40] {PPN = $[Ph_3PNPPh_3]^+$}. The reagents used to introduce gold and copper as metal groupings into the new heterometallic complexes are $Au(PPh_3)NO_3]$ [41], $CuPPh_3Br$[42], $[\{(IPr)Cu\}_2(\mu\text{-}Cl)][PF_6]$[43] {IPr = [N,N′-bis(2,6-diisopropylphenyl)imidazolin-2- ylidene]} and $[(MeCN)_4Cu][BF_4]$.

1.3 References

1. Moss, G. P.; Smith, P. A. S.; Tavernier, D. *Pure & Appl. Chem.* **1995**, *67*, 1307-1375

2. (a) Wittig, G.; Schöllkopf, U. Ü ber Triphenyl-phosphinmethylene als olefinbildende Reagenzien I. *Chem. Ber.* **1954**, *87*, 1318−1330. (b) Wittig, G.; Haag, W. Über Triphenyl-phosphinmethylene als olefinbildende Reagenzien II. *Chem. Ber.* **1955**, *88*, 1654−1666. (c) Bart, J. C. J. Structure of the Non-stabilized Phosphonium Ylid Methylenetriphenylphosphorane. *J. Chem. Soc. B* **1969**, 350−365

3. (a) Trost, B. M.; Melvin, L. S., "Sulfur Ylides. Emerging Synthetic Intermediates", Academic Press, New York, **1975**. (b) Neuhaus, J. D.; Oost, R.; Merad, J.; Maulide, N. Sulfur-Based Ylides in Transition-Metal-Catalysed Processes. *Top. Curr. Chem*. **2018**, *376*, 15. (c) Lu, L.-Q.; Li, T.-R.; Wang, Q.; Xiao, W.-J. Beyond Sulfide-Centric Catalysis: Recent Advances in the Catalytic Cyclization Reactions of Sulfur Ylides. *Chem. Soc. Rev*. **2017**, *46*, 4135−4149. (d) Zhang, Y.; Wang, J. Catalytic [2,3]-Sigmatropic Rearrangement of Sulfur Ylide Derived from Metal Carbene, *Coord. Chem. Rev*. **2010**, *254*, 941−953. (e) Burtoloso, A. C. B.; Dias, R. M. P.; Leonarczyk, I. A. Sulfoxonium and Sulfonium Ylides as Diazocarbonyl Equivalents in Metal-Catalyzed Insertion Reactions, *Eur. J. Org. Chem*. **2013**, 5005−5016. (f) Li, A.-H.; Dai, L.-X.; Aggarwal, V. K. Asymmetric Ylide Reactions: Epoxidation, Cyclopropanation, Aziridination, Olefination, and Rearrangement, *Chem. Rev*. **1997**, *97*, 2341−2372.

4. (a) Selected examples include: (a) Pattacini, R.; Jie, S.; Braunstein, P. Facile dichloromethane activation and phosphine methylation. Isolation of unprecedented zwitterionic organozinc and organocobalt Intermediates. *Chem. Commun.* **2009**, 890−892. (b) Engelter, C.; Moss, J. R.; Niven, M. L.; Nassimbeni, L. R.; Reid, G. A cationic ylide complex of platinum (II): its structure and formation from a chloromethyl-platinum complex. *J. Organomet. Chem.* **1982**, *232*, C78−C80. (c) Kermode, N. J.; Lappert, M. F.; Skelton, B. W.; White, A. H.; Holton, J. Synthesis of ylideplatinum(II) complexes via αfunctionalised alkylplatinum(II) intermediates and some comparative data on palladium(II) complexes; X-ray structure of trans-[Pt- (CH_2PEt_3)I(PEt_3)$_2$]I. *J. Organomet.* Chem. **1982**, *228*, C71−C75. (d) Azam, K. A.; Frew, A. A.; Lloyd, B. R.; Manojlovic-Muir, L.; Muir, K. W.; Puddephatt, R. J. μ-Methylene) diplatinum complexes: their syntheses, structures, and properties. *Organometallics* **1985**, *4*, 1400−1406. (e) Churchill, M. R.; Wasserman, H. J. Crystal and molecular structure of [W(CH_2PMe_3)$(CO)_2$Cl(PMe_3)$_3$][CF_3SO_3], a sevencoordinate tungsten(II) complex produced by transfer of trimethylphosphine to the W:CH2 system. *Inorg. Chem.* **1982**, *21*, 3913−3916. (f) Toupet, L.; Weinberger, B.; Des Abbayes, H.; Grosse, U. Structure du Complexe Tetracarbonyle- (methylenetriphenylphosphorane-C)fer(II), [Fe($C_{19}H_{17}P$)$(CO)_4$]. *Acta Crystallogr., Sect. C: Cryst. Struct. Commun.* **1984**, *40*, 2056-2058. (g) Moss, J. R.; Niven, M. L.; Stretch, P. M. Haloalkyl complexes of the transition metals. Part 5. The synthesis and reactions of some new pentamethylcyclopentadienyl halomethyl and methoxymethyl complexes of molybdenum(II) and tungsten(II) and the Xray crystal structure of the cationic ylide complex [η-C_5Me_5W- $(CO)_3CH_2PPh_3$]I. *Inorg. Chim. Acta* **1986**, *119*, 177−186. (h) Porter, L. C.; Knachel, H.; Fackler Jnr, J. P. A Mononuelear Gold (l) Complex Containing a Covalently Bound Ylide Ligand. The

Structure of Chloro[methyl(methylene)diphenylphosphoranyI-C]gold(I). *Acta Crystallogr., Sect. C: Cryst. Struct. Commun.* **1987**, *43*, 1833−1835. (i) Uson, R.; Laguna, A.; Uson, A.; Jones, P. G.; Meyer-Base, K. Synthesis of Pentafluorophenyl(ylide)silver (l) Complexes: X-Ray Structures of two Modifications of $[Ag(C_6F_5)(CH_2PPh_3)]$. *J. Chem. Soc., Dalton Trans.* **1988**, 341−345. (j) Usón, R.; Laguna, A.; Laguna, M.; Gimeno, M.C.; Pablo, A.; Jones, P. G.; Meyer-Bäse, K.; Erdbrügger, C.F. Synthesis and reactivity of neutral complexes of the types $[AuX_3(ylide)]$and trans-$[Au(C_6F_5)X_2(ylide)]$ (X = halide or pseudohalide). X-ray structure of $[Au(SCN)_3(CH_2PPh_3)]$. *J. Organomet. Chem.* **1987**, *336*, 461−468. (k) Hoover, J. F.; Stryker, J. M. Synthesis of Platinum Bis(phosphonium ylide) Complexes from -Halomethyl Precursors. *Organometallics* **1988**, *7*, 2082−2084. (l) Cerrada, E.; Concepcion Gimeno, M.; Laguna, A.; Laguna, M.; Orera, V.; Jones, P. G. Charge-transfer salts with mononuclear and dinuclear ylide gold(I) complexes: x-ray structure of [Au- $(CH_2PPh_3)_2$](TCNQ), (TCNQ = 7,7′,8,8′-tetracyanoquinodimethane). *J. Organomet. Chem.* **1996**, *506*, 203−210.

5. Selected examples include: (a) O'Connor, E. J.; Helquist, P. Stable precursors of transition-metal carbene complexes. Simplified preparation and crystal structure of η5 -cyclopentadienyl)- [(dimethylsulfonium)methyl]dicarbonyliron(II) fluorosulfonate. *J. Am. Chem. Soc.* **1982**, *104*, 1869−1874. (b) Hevia, E.; Perez, J.; Riera, V.; Miguel, D. Manganese(I) and Rhenium(I) Tricarbonyl- (Alkylthio)methyl and Alkylidenesulfonium Complexes. *Organometallics* **2002**, *21*, 5312−5319. (c) Leoni, P.; Marchetti, F.; Paoletti, M. Synthesis of Palladium Sulfonium Ylides and the Structures of trans-$[PdCl(CH_2SR_2)(PBut_2H)_2]X$ (X = CF_3SO_3, SR_2) Tetrahydrothiophene; X= PF_6, R = Et). *Organometallics* **1997**, *16*, 2146−2151. (d) Kilbourn, B. T.; Felix, D. The Crystal Structure of Methyldineopentylsulphonium Tri-iododineopentylsulphoniummethylzincate, $[(C_5H_{11})_2SMe]^+$ $[(C_5H_{11})_2SCH_2ZnI_3]$ −. *J. Chem. Soc. A* **1969**, 163−168. (e) Fackler, J. P., Jr.; Paparizos, C. Trimethylgold- (III) Complexes of Reactive Sulfoxonium and Sulfonium Ylides. *J. Am. Chem. Soc.* **1977**, *99*, 2363−2364. (f) Vicente, J.; Chicote, M.-T.; Abrisqueta, M. D.; Alvarez-Falcon, M. M.; Ramírez de Arellano, M. C.; Jones, P. G. New Carbenegold(I) Complexes Synthesized by the "Acac Method". *Organometallics* **2003**, *22*, 4327−4333.

6. (a) Lappas, D.; Hoffman, D. M.; Folting, K.; Huffman, J. C. Synthesis and Structure of a Resonance Stabilized (Trimethylphosphonio)metallapropenide. *Angew. Chem., Int. Ed. Engl.* **1988**, *27*, 587−589. (b) Hoffman, D. M.; Huffman, J. C.; Lappas, D.; Wierda, D. A. Alkyne Reactions with Rhenium(V) Oxo Alkyl Phosphine Complexes□Phosphine Displacement versus Apparent Re-P Insertion. *Organometallics* **1993**, *12*, 4312−4320. (c) Rogers, R. D.; Alt, H. G.; Maisel, H. E. Die Molekülstruktur des carbenartigen Ylidkomplexes $(C_5H_4Me)(CO)_2Mn[CHCH(PEt_3)]$. *J. Organomet. Chem.* **1990**, *381*, 233−238. (d) Chin, C. S.; Lee, S.; Oh, M.; Won, G.; Kim, M.; Park, Y. J. cis-Bis(alkenyl)iridium(III) Compounds by Apparent Insertion of Two Acetylenes into Two IrP Bonds: Crystal Structures of cis, trans-$[IrCl(-CH = CH^+ PPh_3)_2(CO)(PPh_3)_2]_2^+$ and $[Ir(OClO_3)(CH_3)(H_2O)(CO)-(PPh_3)_2]^+$. *Organometallics* **2000**, *19*, 1572−1577. (e) Chin, C. S.; Park, Y.; Kim, J.; Lee, B. Facile Insertion of Alkynes into Ir-P (Phosphine) and Ir-As (Arsine) Bonds: Second and Third Alkyne Addition to Mononuclear Iridium Complexes. J. Chem. Soc., *Chem. Commun.* **1995**, 1495−1496. (f) Takats, J.;

Washington, J.; Santarsiero, B. D. Condensation of $Os(CO)_4\eta^2$-HCCH) with $CpRh(CO)(PR_3)$. Unexpected Phosphine Dependence in the Formation of Dimetallacycles: Reverse Regiochemistry and a Zwitterionic Compound. *Organometallics* **1994**, *13*, 1078−1080. (g) Yang, K.; Bott, S. G.; Richmond, M. G. Regioselective phosphine attack on the coordinated alkyne in $Co_2\mu$-alkyne) complexes Reactivity studies and X-ray diffraction structures of $Co_2(CO)_4$(bma)- μ-HC≡Ct Bu) and the zwitterionic hydrocarbyl complexes $Co_2(CO)_4[\mu_2$::2::1::1:-RC = C(R')PPh_2C = C(PPh_2)C(O)C(O)]. *J. Organomet. Chem.* **1996**, *516*, 65−80. (h) Bott, S. G.; Shen, H.; Senter, R. A.; Richmond, M. G. Acetylide Participation in Ligand Substitution and P-C Bond Cleavage in the Reaction between $HRu_3(CO)_9([\mu_2$::2::1-C≡CPh) and 4,5-Bis(diphenylphosphino)-4-cyclopenten-1,3-dione (bpcd). Syntheses and X-ray Structures of $HRu_3(CO)_7[[\mu_2$::2::1::1::1 –Ph_2PC = CC(O)CH_2C(O)PPh_2C = CPh] and $Ru_3(CO)_7\mu_2$ ::1 :-PhC = CHPh)[μ_2::1:-PPhC = CC(O)CH_2C-(O)PPh_2]. *Organometallics* **2003**, *22*, 1953−1959.

7. (a) Boland-Lussier, B. F.; Churchill, M. R.; Hughes, R. P.; Rheingold, A. L. Synthesis and characterization of cationic iron vinylidene compounds: formation of carbon-hydrogen, carbonnitrogen and carbon-phosphorus bonds and the x-ray crystal structure of $[Fe((-C_5H_5)(CO)(PPh_3)\{C(PPh_3)=CH_2\}]^+BF_4$ −. *Organometallics* **1982**, *1*, 628−634. (b) Hogarth, G.; Knox, S. A. R.; Lloyd, B. R.; Macpherson, K. A.; Morton, D. A. V.; Orpen, A. G. Structural Observation of Bis(diphenyphosphino)methane Reactivity at a Diiron Centre: Crystal Structures of Isomeric $[Fe_2(CO)_5$((- CHCHCO){{-P(Ph_2)CH_2PPh_2}], $[Fe_2(CO)_6$((-C(CH_2)P(Ph_2)- CH_2PPh_2}] and [$Fe_2(CO)_2$}{{-C(CH_2Ph)P(Ph_2)CH_2PPh}]. *J. Chem. Soc., Chem. Commun.* **1988**, 360−362. (c) Bamber, M.; Froom, S. F. T.; Green, M.; Schulz, M.; Werner, H. Nucleophilic attack by isocyanides, phosphines and cyclohexenesulphide on the -carbon of "side-on" bonded 2 -(4e)-vinylidenes; formation of thioketene and thioaldehyde dimolybdenum complexes. *J. Organomet. Chem.* **1992**, *434*, C19−C25.

8. Henrick, K.; McPartlin, M.; Deeming, A. J.; Hasso, S.; Manning, P. Addition of dimethylphenylphosphine to μ- and μ_3-alkynyl and μ_3- allenyl ligands in triosmium clusters: X-ray crystal structures of three zwitterionic adducts. *J. Chem. Soc., Dalton Trans.* **1982**, 899−906.

9. (a) Chin, C. S.; Lee, H.; Oh, M. Reactions of Iridium(III) Compounds with Alkynes in the Presence of Triethylamine: The First Example of M-CH = CH-$^+NR_3$. *Organometallics* **1997**, *16*, 816−818. (b) Chin, C. S.; Cho, H.; Won, G.; Oh, M.; Ok, K. M. Reaction of an (Alkyl)(alkenyl)(alkynyl)iridium(III) Complex with HCl: Intramolecular C-C Bond Formation from Alkyl, Alkenyl, and Alkynyl Groups Coordinated to "Ir(CO)(PPh_3)$_2$". H/D Exchange between CH_3 and DCl. *Organometallics* **1999**, *18*, 4810−4816.

10. Xu, S.; He, Z. *RSC Adv.*, **2013**, *3*, 16885–16904

11. Meng, W.; Zhao H.; Nie, J.; Zheng, Y.; Fu, A.; Ma, J. *Chem. Sci*., **2012**, *3*, 3053–3057

12. Xu, Z.; Lu. X. Tetrahedron Letters, **1999**, *40*, 549-552 (b) Zhang, C.; Lu, X. *J. Org. Chem.* **1995**, *60*, 2906-2908 (c) Xu, Z.; Lu, X. *J. Org. Chem.* **1998**, *63*, 5031-5041

13. (a) Saito, S.; Yamamoto, Y. Recent Advances in the Transition-Metal-Catalyzed Regioselective Approaches to Polysubstituted Benzene Derivatives. *Chem. Rev.* **2000,** *100*, 2901−2915. (b) Walton, J. C. A Valuable Upgrade to the Portfolio of Cycloaddition Reactions. *Angew. Chem., Int. Ed.* **2016**, *55*, 7034−7036. (c) Galan, B. R.; Rovis, T. Beyond Reppe: Building Substituted Arenes by [2+2+2] Cycloadditions of Alkynes. *Angew. Chem., Int. Ed.* **2009,** *48*, 2830−2834. (d) Roglans, A.; Pla-Quintana, A.; Sola, M. *Chem Rev*, **2021**, *121*, 1894-1979. (e) Lindner, E.; Jansen, R. M.; Mayer, H. A.; Hiller, W.; Fawzi, R. *Organometallics* **1989**, *8*, 2355−2360. (f) Ernst, C.; Walter, O.; Dinjus, E. *J. Prakt. Chem.* **1999**, *341*, 801−804.

14. (a) Kotha, S.; Brahmachary, E.; Lahiri, K. Transition Metal Catalyzed [2 + 2 + 2] Cycloaddition and Application in Organic Synthesis. *Eur. J. Org. Chem.* **2005**, 4741−4767. (b) Kotha, S.; Goyal, D.; Chavan, A. S. Diversity-Oriented Approaches to Unusual α-Amino Acids and Peptides: Step Economy, Atom Economy, Redox Economy, and Beyond. *J. Org. Chem.* **2013**, *78*, 12288−12313. (c) Yamamoto, Y. Recent Advances in Intramolecular Alkyne Cyclotrimerization and Its Applications. *Curr. Org. Chem.* **2005**, *9*, 503−519. (d) Albano, G.; Aronica, L. A. Cyclization Reactions for the Synthesis of Phthalans and Isoindolines. *Synthesis*, **2018**, *50*, 1209−1227.

15. Johnson, B. F. G.; Johnston, R. D.; Lewis, J., *Inorg. Phys. Theor*. **1968**, 0, 2865-2868.

16. Johnson, B. F. G.; Lewis, J.; Sankey, S. W.; Wong, K.; McPartlin, M.; Nelson, W. J. H., *J. Organomet. Chem*. **1980**, *191*, C3-C7.

17. Mingos, D. M. P. *Acc. Chem. Res.* **1984**, *17*, 311 – 319.

18. Dyson, P. J. *Advances in Organometallic* Chemistry, **1999**, *43*, 43-124

19. Salter, I.D., Cluster Complexes with Bonds Between Transition Elements and Copper, Silver and Gold. In *Comprehensive Organometallic Chemistry II*; Abel, E.W; Stone, F.G.A; Wilkinson, G. Eds; Pergamon: Oxford, **1995**, 10, 256-259

20. Sinfelt, J. H.; Heights, B.; Barnett, A. E., U.S. Patent 3,835,034 (**1974**).

21. Rice, R.W.; Lu, K. *J. Catal*. **1982**, *77*, 104-117

22. Sinfelt, J.H. Acc. Chem. Res., **1977**, *10* (1), 15–20

23. Robinson, A.M.; Hensley, J.E.; Medlin, J.W. *ACS Catal*. **2016**, *6*, 5026−5043

24. a) Buchwalter, P.; Rosé, J.; Braunstein, P. Multimetallic Catalysis Based on Heterometallic Complexes and Clusters, *Chem. Rev*., **2015**, *115*, 28−126. b) Thomas, J. M.; Johnson, B. F. G.; Raja, R.; Sankar, G.; Midgley, P. A. High-Performance Nanocatalysts for Single-Step Hydrogenations, *Acc. Chem. Res*., **2003**, *35*, 20 - 30. c) P. Braunstein, J. Rosé, Heterometallic Clusters in Catalysis, in *Metal Clusters in Chemistry*, P Braunstein, L. A. Oro, P. R. Raithby, Eds. Wiley-VCH, Weinheim, **1999**, Vol. 2, Sec. 2.2, 616 – 677. d) P. Braunstein, J. Rosé, Heterometallic Clusters for Heterogeneous

Catalysis, in *Catalysis by Di- and Polynuclear Metal Complexes*, R. D. Adams and F. A. Cotton, Eds. Wiley-VCH, New York, **1998**, Ch. 13, 443 – 508. e) R. D. Adams and E. Trufan, Ruthenium-Tin Cluster Complexes and their Applications as Bimetallic Nanoscale Heterogeneous Hydrogenation Catalysts, *Phil. Trans Royal. Soc.* **2010**, *368*, 1473-1493. f) A. B. Hungria, R. Raja, R. D. Adams, B. Captain, J. M. Thomas, P. A. Midgley, V. Golvenko and B. F. G. Johnson, Single-Step Conversion of Dimethyl Terephthalate to Cyclohexanedimethanol with A Trimetallic Nanoparticle Catalyst: Ru_5PtSn, *Angew. Chem. int. Ed.* **2006**, *45*, 4782-4785. g) R. D. Adams, D. A. Blom, B. Captain, R. Raja, J. M. Thomas, and E. Trufan, Toward Less Dependence on Platinum Group Metal Catalysts: The Merits of Utilizing Tin, *Langmuir*, **2008**, *24*, 9223-9226.

25. (a) H.-L. Jiang, Q. Xu, Recent progress in synergistic catalysis over heterometallic nanoparticles, *J. Mater. Chem*., **2011**, *21*, 13705 - 13725. (b) G. Kyriakou, A. M. Marquez, J. P. Holgado, M. J. Taylor, A. E. H. Wheatley, J. P. Mehta, J. F. Sanz, S. K. Beaumont, Comprehensive Experimental and Theoretical Study of the CO + NO Reaction Catalyzed by Au/Ni Nanoparticles, *ACS Catal.*, **2019**, *9*, 4919−4929. (c) F. Gao, D. W. Goodman, Pd–Au bimetallic catalysts: understanding alloy effects from planar models and (supported) nanoparticles, *Chem. Soc. Rev.*, **2012**, *41*, 8009–8020. (d) M. Chen, D. Kumar, C.-W. Yi, D.W. Goodman, The Promotional Effect of Gold in Catalysis by Palladium-Gold, *Science*, **2005**, *310*, 291 – 293. (e) G. J. Hutchings, Selective oxidation using supported gold bimetallic and trimetallic nanoparticles, *Catalysis Today*, **2014**, *238*, 69–73. (f) Y. Zhang, X. Cui, F. Shi, Y. Deng, Nano-Gold Catalysis in Fine Chemical Synthesis, *Chem. Rev.*, **2012**, *112*, 2467–2505. (g) G. J. Hutchings, Nanocrystalline gold and gold palladium alloy catalysts for chemical Synthesis, *Chem. Commun*., **2008**, 1148 – 1164. (h) J. A. Lopez-Sanchez, N. Dimitratos, N. Glanvilla, L. Kesavan, C. Hammond, J. K. Edwards, A. F. Carley, C. J. Kiely, G. J. Hutchings, Reactivity studies of Au–Pd supported nanoparticles for catalytic applications, *Applied Catalysis A: General*, **2011**, *391*, 400 – 406. (i) M. Sharma, B. Das, M. J. Baruah, S. Biswas, S. Roy, A. Hazarika, S. K. Bhargavad, K. K. Baniaa, Pd-Au-Y as Efficient Catalyst for C-C Coupling Reactions, Benzylic C-H Bond Activation and Oxidation of Ethanol for Synthesis of Cinnamaldehydes, *ACS Catal.* **2019**, *9*, 5860−5875. (j) M. Hasbi Ab Rahim, R. D. Armstrong, C. Hammond, N. Dimitratos, S. J. Freakley, M. M. Forde, D. J. Morgan, G. Lalev, R. L. Jenkins, J. A. Lopez-Sanchez, S. H. Taylor, G. J. Hutchings, Low temperature selective oxidation of methane to methanol using titania supported gold palladium copper catalysts, *Catal. Sci. Technol.*, **2016**, *9*, 3410-3418. (k) P. Buchwalter, J. Rosé, P. Braunstein, Multimetallic Catalysis Based on Heterometallic Complexes and Clusters, *Chem. Rev.*, **2015**, *115*, 28–126. (l) M. Böhmer, F. Kampert, T. T. Y. Tan, G. Guisado-Barrios, E. Peris, F. E. Hahn, IrIII/AuI and RhIII/AuI Heterobimetallic Complexes as Catalysts for the Coupling of Nitrobenzene and Benzylic Alcohol, *Organometallics*, **2018**, *37*, 4092 - 4099. (m) J. Wisniewska, C.-M. Yang, M, Ziolek, Changes in bimetallic silver–platinum catalysts during activation and oxidation of methanol and propene, *Catalysis Today*, **2019**, *333*, 89–96. (n) M. Zhu, X.-L. Du, Y. Zhao, B. Mei, Q. Zhang, F. Sun, Z. Jiang, Y.-M. Liu, H.-Y. He, and Y. Cao, Ring-Opening Transformation of 5-Hydroxymethylfurfural Using a Golden Single-Atomic-Site Palladium Catalyst, *ACS Catal.* **2019**, *9*, 6212−6222.

26. (a) D. S. Shephard, T. Maschmeyer, G. Sankar, J. M. Thomas, D. Ozkaya, B. F. G. Johnson, R. Raja, R. D. Oldroyd, R. G. Bell, Preparation, Characterisation and Performance of Encapsulated Copper - Ruthenium Bimetallic Catalysts Derived from Molecular Cluster Carbonyl Precursors, *Chem. Eur. J.*, **1998**, *4*, 1214 – 1224. (b) J. F. Sinfelt, Catalysis by Alloys and Bimetallic Clusters, *Accts. Chem. Res.*, **1977**, *10*, 15 - 20. (c) J. F. Sinfelt, Supported "Bimetallic Cluster" Catalysts, *J. Catal.*, **1973**, *29*, 308-315. (d) J. F. Sinfelt, Catalysis by Alloys and Bimetallic Clusters, Acc. Chem. Res., **1977**, *10*, 15 (e) J. F. Sinfelt, Y. L. Lam, J. A. Cusumano, A. E. Barnett, Nature of Ruthenium-Copper Catalysts, *J. Catal*., **1976**, *42*, 227- 237.

27. (a) C. Ciabatti, M. Femoni, S. Carmela Iapalucci, S. Ruggieri, S. Zacchini**,** The role of gold in transition metal carbonyl clusters, *Coord. Chem. Rev.*, **2018**, *355*, 27–38. (b) I. D. Salter, Cluster Complexes with Bonds Between Transition Element and Copper, Silver and Gold, in "Comprehensive Organometallic Chemistry II" E. W. Abel, F. G. A. Stone, G. Wilkinson, Eds., Pergamon, Oxford, **1995**, Vol. 10, Ch. 5, 255 – 322. (c) D.M.P. Mingos, M.J. Watson, Heteronuclear Gold Cluster Compounds, *Adv. Inorg. Chem.*, **1992**, *39*, 327–399. (d) I.D. Salter, Heteronuclear Cluster Chemistry of Copper, Silver and Gold, *Adv. Organomet. Chem.*, **1989**, *29*, 249–343. (e) T. Nakajimaa, H. Konomotob, H. Ogawab, Y. Wakatsuki, Synthesis of three-component high nuclearity cluster complexes with ruthenium carbido carbonyl clusters as a building block, *J. Organomet. Chem.*, **2007**, *692*, 5071–5080 (f) P. Braunstein, J. Rose, Gold in Bimetallic Molecular Clusters, *Gold Bull.*, **1985,** *18*, 17–30. (g) M. A. Beswick, J. Lewis, P. R. Raithby, M. C. Ramirez de Arellano, The High Nuclearity Mixed-Metal Cluster Dianions $[Ru_8H_2Cu_7Cl_3(CO)_{24}]^{2-}$ and $[Ru_{12}H_2Cu_6Cl_2(CO)_{34}]^{2-}$ *Angew. Chem. Int. Ed. Engl.*, **1997**, *36*, 291 – 293.

28. C. E. Coffey, J. Lewis, R. S. Nyholm, *J. Chem. Soc.* **1964,** 1741 – 1749.

29. a) D. S. Shephard, T. Maschmeyer, G. Sankar, J. M. Thomas, D. Ozkaya, B. F. G. Johnson, R. Raja, R. D. Oldroyd, R. G. Bell, Preparation, Characterisation and Performance of Encapsulated Copper - Ruthenium Bimetallic Catalysts Derived from Molecular Cluster Carbonyl Precursors, *Chem. Eur. J*. **1998**, *4*, 1214 – 1224. (b) C. L. Bracey, P. R. Ellis, G. J. Hutchings, Application of copper–gold alloys in catalysis: current status and future perspectives, *Chem. Soc. Rev*. **2009**, *28*, 2231–2243. c) C. Rhodes, G. J. Hutchings, A. M. Ward, Water-gas shift reaction: finding the mechanistic boundary, *Catal. Today* **1995,** *23*, 43-58. d) H. Iwai, T. Umeki, M. Yokomatsu and C. Egawa , Methanol partial oxidation on Cu–Zn thin films grown on Ni(1 0 0) surface**,** Surf. Sci. **2008**, *602*, 2541 - 2546. e) J.-D. Grunwaldt, A. M. Molenbroek, N.-Y. Topsøe, H. Topsøe, and B. S. Clausen, Investigations of Structural Changes in Cu/ZnO Catalysts, *J. Catal*. **2000,** *194*, 452–460, doi:10.1006/jcat.2000.2930 f) B H. Lipshutz, D. M. Nihan, E. Vinogradova, B. R. Taft, Z. V. Boskovic, Copper + Nickel-in-Charcoal (Cu-Ni/C): A Bimetallic, Heterogeneous Catalyst for Cross-Couplings, *Org. Lett*. **2008**, *10*, 4279 – 4282. g) J. H. Sinfelt, Catalysis by Alloys and Bimetallic Clusters, *Acc. Chem. Res*. **1977**, *10*, 15 – 20. h) A. B. Boricha, H. C. Bajaj, T. H. Kim, S. H. R. Abdi, R. V. Jasra, Preparation of Highly Dispersed Pd–Cu on Silica for the Aerobic Hydroxylation of Benzene to Phenol Under Ambient Conditions, *Catal. Lett*. **2010**, *137*, 202–209.

30. A. M. Echavarren, N. Jiao, V. Gevorgyan, Coinage metals in organic synthesis, *Chem. Soc. Rev.* **2016**, *45*, 4445 – 4447.

31. (a) J. Hassan, M. Sevignon, C. Gozzi, E. Schulz, M. Lemaire, Aryl-Aryl Bond Formation One Century after the Discovery of the Ullmann Reaction, *Chem. Rev.* **2002**, *102*, 1359–1470. (b) I. P. Beletskaya, A. V. Cheprakov, Copper in cross-coupling reactions. The post-Ullmann chemistry, *Coord. Chem. Rev*. **2004**, *248*, 2337–2364. (c) F. Monnier, M. Taillefer, Catalytic C-C, C-N, and C-O Ullmann-Type Coupling Reactions, *Angew. Chem. Int. Ed*. **2009,** *48*, 6954 – 6971. (d) *M. V. Kirillova, Y N. Kozlov, L. S. Shul'pina, O. Y. Lyakin, A. M. Kirillov, E. P. Talsi, A. J. L. Pombeiro, G. B. Shul'pin,* Remarkably fast oxidation of alkanes by hydrogen peroxide catalyzed by a tetracopper(II) triethanolaminate complex: Promoting effects of acid co-catalysts and water, kinetic and mechanistic features, *J. Catal*. **2009**, *268*, 26-38. (e) M. Yamada, K. D. Karlin, S. Fukuzumi, One-step selective hydroxylation of benzene to phenol with hydrogen peroxide catalysed by copper complexes incorporated into mesoporous silica–alumina, *Chem. Sci*., **2016**, *7*, 2856–2863. (f) C.-J. Li, Cross-Dehydrogenative Coupling (CDC): Exploring C-C Bond Formations beyond Functional Group Transformations, *Acc. Chem. Res*. **2009**, *42*, 335 – 344. (g) L. S. Shul'pina, M. M. Vinogradov, Y. N. Kozlov, Y. V. Nelyubina, N. S. Ikonnikov, G. B. Shul'pin, Copper complexes with 1,10-phenanthrolines as efficient catalysts for oxidation of alkanes by hydrogen peroxide, *Inorg. Chim. Acta*, **2020**, *512*, 119889. (h) M. Meldal, C. W. Tornøe, Cu-Catalyzed Azide−Alkyne Cycloaddition, *Chem. Rev.* **2008**, *108*, 2952–3015. (i) X. Zhu, S. Chiba, Copper-catalyzed oxidative carbon–heteroatom bond formation: a recent update, *Chem. Soc. Rev*. **2016**, *45*, 4504 – 4523. (j) S. D. McCann, S. S. Stahl, Copper-Catalyzed Aerobic Oxidations of Organic Molecules: Pathways for Two-Electron Oxidation with a Four-Electron Oxidant and a One-Electron Redox-Active Catalyst, *Acc. Chem. Res*. **2015**, *48*, 1756−1766.

32. (a) S. C. Allen, R. R. Walvoord, R. Padilla-Salinas, M. C. Kozlowski, Aerobic Copper-Catalyzed Organic Reactions. *Chem. Rev*. **2013**, *113*, 6234−6458. (b) X. X. Guo, D.-W. Gu, Z. X. Wu, W. B. Zhang, Copper-Catalyzed C−H Functionalization Reactions: Efficient Synthesis of Heterocycles, *Chem. Rev*. **2015**, *115*, 1622−1651. (c) X. Tang, W. Wu, W. Zeng, H. Jiang, Copper-Catalyzed Oxidative Carbon−Carbon and/or Carbon−Heteroatom Bond Formation with O_2 or Internal Oxidants, *Acc. Chem. Res*. **2018**, *51*, 1092−1105. (d) R. Trammell, K. Rajabimoghadam, I. Garcia-Bosch, Copper-Promoted Functionalization of Organic Molecules: from Biologically Relevant Cu/O_2 Model Systems to Organometallic Transformations, *Chem. Rev*. **2019**, *119*, 2954−3031.

33. a) C. Fliedel, A. Labande, E. Manoury, R. Poli, Chiral N-heterocyclic carbene ligands with additional chelating group(s) applied to homogeneous metal-mediated asymmetric catalysis, *Coord. Chem. Rev*. **2019**, *394*, 65 – 103. b) F. Lazreg, F. Nahra, C. S. J. Cazin, Copper–NHC complexes in catalysis, *Coord. Chem. Rev*. **2015**, *293–294*, 48 - 79. c) J. D. Egbert, C. S. J. Cazin, S. P. Nolan, Copper N-heterocyclic carbene complexes in catalysis, *Catal. Sci. Technol*. **2013**, *3*, 912 – 926. d) R. Jazzar, M. Soleilhavoup, G. Bertrand, Cyclic (Alkyl)- and (Aryl)-(amino)carbene Coinage Metal Complexes and Their Applications, I. **2020**, *120*, 4141−4168. e) J. C. Y. Lin, R. T. W. Huang, C. S. Lee,

A. Bhattacharyya, W. S. Hwang, I. J. B. Lin, Coinage Metal-N-Heterocyclic Carbene Complexes, *Chem. Rev*. **2009**, *109*, 3561–3598. f) A. A. Danopoulos, T. Simler, P. Braunstein, N-Heterocyclic Carbene Complexes of Copper, Nickel, and Cobalt, *Chem. Rev*. **2019**, *119*, 3730−3961. g) S. Díez-González, E. D. Stevens, N. M. Scott, J. L. Petersen, S. P. Nolan, Synthesis and Characterization of $[Cu(NHC)_2]X$ Complexes: Catalytic and Mechanistic Studies of Hydrosilylation Reactions, *Chem. Eur. J*. **2008**, *14*, 158 – 168.

34. (a) R. D. Adams, Synthesis of Compounds Containing Heteronuclear Metal-Metal Bonds, in "Comprehensive Organometallic Chemistry II" G. Wilkinson, F. G. A. Stone, E. W. Abel, Eds. Pergamon, Oxford, **1995**, Vol. 10, Ch. 1, 1-22. (b) D. A. Roberts, G. L. Geoffroy, Synthesis of Compounds Containing Heteronuclear Metal-Metal Bonds, in "Comprehensive Organometallic Chemistry I" E. W. Abel, F. G. A. Stone, G. Wilkinson, Pergamon, Eds., Oxford, **1982**, Vol. 6, Ch. 40, 763 - 877.

35. (a) M. Tachikawa, A. C. Sievert, E. L. Muetterties, M. R. Thompson, C. S. Day, V. W. Day, Metal Clusters. 24.1 Synthesis and Structure of Heteronuclear Metal Carbide Clusters, *J. Am. Chem. Soc.* **1980**, *102*, 1725 – 1727. (b) M. Bortoluzzi, I. Ciabatti, C. Femoni, T. Funaioli, M. Hayatifar, M. C. Iapalucci, G. Longoni, S. Zacchini, Homoleptic and heteroleptic Au(I) complexes containing the new $[Co_5C(CO)_{12}]^-$ cluster as Ligand, *Dalton Trans.* **2014**, *43*, 9633 - 9646. (c) I. Ciabatti, C. Femoni, M. Hayatifar, M. C. Iapalucci, S. Zacchini, Co_5C and Co_4C carbido carbonyl clusters stabilized by $[AuPPh_3]^+$ fragments, *Inorg. Chim. Acta* **2015**, *428*, 203 – 211. (d) B. F. G. Johnson, J. Lewis, W. J. H. Nelson, J. N. Nicholls, M. D. Vargas, *J. Organomet. Chem.* **1983**, *249*, 255 – 272.

36. (a) *C. E. Housecroft*, Transition metal boride clusters at the molecular level, *Coord. Chem. Rev.* **1995**, *143*, 297 – 330. (b) *C. E. Housecroft*, Boron atoms in transition metal clusters, *Adv. Organomet. Chem.* **1991**, *33*, 1 – 50.

37. (a) C. K. Schauer, E. J. Voss, M. Sabat, D. F. Shriver, Synthesis and structure of a capped square-pyramidal five-metal oxo cluster, $[Fe_2Ru_3(CO)_{14}(\mu_4\text{-}O)]^{2-}$, *J. Am. Chem. Soc.* **1989**, *111*, 7662-7664. (b) C. K. Schauer, D. F. Shriver, Synthesis and Structure of $[(PPh_3)_2N][Fe_3Mn(CO)_{12}(\mu_4\text{-}O)]$: A Butterfly Oxo Cluster, *Angew. Chem., Int. Ed.* **1987**, *26*, 255 - 256.

38. R. Della Pergola, A. Fumagalli, F. Fabrizi de Biani, L. Garlaschelli, F. Laschi, M. Carlotta Malatesta, M. Manassero, E. Roda, M. Sansoni, and P. Zanello, Carbonyl-Nitrido Mixed-Metal Clusters: Synthesis, Reactivity, Electrochemical Behavior and Solid-State Structure of $[Co_5MoN(CO)_{14}]^{2-}$ and $[Co_5MoN(CO)_{14}AuPPh_3]^-$, *Eur. J. Inorg. Chem*. **2004**, 3901-3906.

39. Blohm, M.L.; Gladfelter, W.L. *Inorg. Synth*. **1989**, *26*, 286

40. C. R. Eady, B. F. G. Johnson, J. Lewis, *J. Chem. Soc., Dalton Trans*, **1978**, 1358 – 1363.

41. Malatesta, L.; Naldini, L.; Simonetta, G.; Cariati, F. *Coord. Chem. Rev*. **1966**, *1*, 255−262.

42. Kauffman, G.B.; Teter, L.A. *Inorg. Synth*. **1963**, *7*, 9

43. Adams, R. D.; Pellechia, P. J.; Smith, M. D.; Tedder, J. D.; Wakdikar, N. D.; *J. Organomet. Chem.* **2019**, *898*, 120872

CHAPTER 2

ZWITTERIONIC AMMONIUMALKENYL LIGANDS IN METAL CLUSTER COMPLEXES. SYNTHESIS, STRUCTURES AND TRANSFORMATION OF ZWITTERIONIC TRIMETHYLAMMONIUMALKENYL LIGANDS IN HEXARUTHENIUM CARBIDO CARBONYL COMPLEXES[1]

[1]Adams, R. D.; Smith, M. D.; Wakdikar, N. D. *Inorganic Chemistry* **2020**, *59*, 2, 1513–1521

Reprinted here with permission from publisher

2.1 Introduction

Hydrocarbylonium zwitterions have been of great interest ever since the first reports of the phosphorus ylides by Wittig in the 1950s.[1] Zwitterions are neutral molecules that formally have positively and negatively charged groups within the same molecule.[2] Phosphorus ylides **A** and their sulfur analogs **B** are an important family of zwitterions that are valuable reagents in organic synthesis.[3, 4]

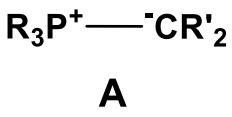

A

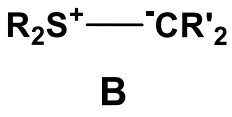

B

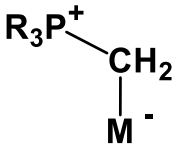

C

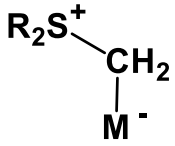

D

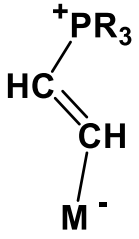

E

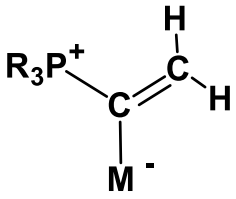

F

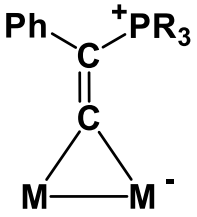

G

There are a number of examples in which these zwitterions are complexed to metal atoms, e. g. **C** and **D**. Almost all are coordinated exclusively through the carbon atom, and the negative charge is formally transferred to the metal atom.[5, 6] There are also a variety of more extended zwitterionic hydrocarbylonium species. Most examples of these species contain the phosphonium grouping. Some examples of these are **E**, **F,** and **G,** and

all of these have been isolated only as ligands in complexes containing one or more metal atoms.[7-9] Complexes containing the zwitterionic phosphoniumalkenyl ligands **E** are the most abundant.[7] Metal complexes containing zwitterionic ammoniumalkenyl ligands, such as **H**, are quite rare.[10]

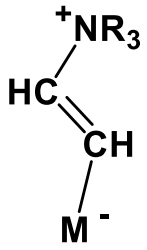

H

In recent studies, we have been investigating the reactions of organic ligands with ethyne,[11] alkenes,[12] aldehydes,[13] and gold-phenyl compounds[14] with ruthenium carbonyl cluster complexes. We have now discovered some interesting new polynuclear ruthenium carbonyl complexes containing ammoniumethenyl ligands formed by the combination of ethyne and methyl propiolate with NMe_3 in reactions with the Ru_6 carbido carbonyl cluster complex $Ru_6(\mu_6\text{-}C)(CO)_{17}$, **2.1** in the presence of Me_3NO. These results are reported herein.

2.2 Experimental Section

General Data

All reactions were performed under an atmosphere of nitrogen. Reagent grade solvents were dried by the standard procedures and were freshly distilled prior to use. Infrared spectra were recorded on a Thermo Scientific Nicolet IS10. ^1H NMR spectra

were recorded on a Varian Mercury 300 spectrometer operating at 300.1 MHz. Mass spectrometric (MS) measurements were performed by a direct-exposure probe by using electron impact (EI) ionization. $Ru_3(CO)_{12}$ was obtained from STREM and was used without further purification. $Ru_6(\mu_6\text{-}C)(CO)_{17}$, **2.1,** was prepared from $Ru_3(CO)_{12}$ according to a previously reported procedure.[20] Ethyne gas (HC_2H) (industrial grade) was obtained from National Welders and was used without further purification. Ethyne and carbon monoxide are hazardous gases and should be used only in a well-ventilated fume hood. Methyl propiolate and trimethylamine-N-oxide (Me_3NO) were obtained from Sigma-Aldrich and were used without further purification. Product separations were performed by TLC in the open air on Analtech 0.25 mm and 0.50 mm silica gel 60 Å F254 or alumina on glass plates.

Reaction of 2.1 with C_2H_2 and Me_3NO.

A 37.0 mg (0.034 mmol) amount of **2.1** was added to 50 mL three-neck flask in 15 mL of degassed dichloromethane. A slow purge of C_2H_2 was then allowed to pass through the solution for 30 min at room temperature. This was followed by addition of 7.0 mg (0.093 mmol) of Me_3NO. After stirring for 20 min, solvent was removed *in vacuo*. The products were then separated by TLC by using a solvent mixture of hexane/methylene chloride/acetone to yield two bands in the order of elution: 15.0 mg (39% yield) of dark red $Ru_6C(CO)_{15}(\mu\text{–}\eta^2\text{–}C_2H_2NMe_3)$, **2.2** and 6.3 mg (17% yield) of brown $Ru_6C(CO)_{14}(\mu_3\text{–}\eta^4\text{–}C_4H_4NMe_3)$, **2.3**. Spectral data for **2.2**: IR, ν_{CO} (cm^{-1} in CH_2Cl_2): 2073.0 (m), 2025.9 (s), 1964.3 (w). ^1H NMR (in CD_2Cl_2, δ in ppm): 8.85 (d, C**H**, $^3J_{H\text{-}H}$ = 7.5 Hz), 4.28 (d, C**H,** $^3J_{H\text{-}H}$ = 7.5 Hz), 3.19 (s, N(C**H**$_3$)$_3$). Elemental analysis: Calculated for $Ru_6NO_{15}C_{21}H_{11}$: C, 22.45%; H, 0.99%; N, 1.25%. Found: C, 21.80%; H,

0.97%; N, 1.13%. Spectral data for **2.3**: IR, ν_{CO} (cm^{-1} in CH_2Cl_2): 2065.2(m), 2022.7(vs), 2016.7(s), 1995.1(sh), 1964.0(w), 1804.5(w,br). ^1H NMR (in CD_2Cl_2, δ in ppm): 9.53 (d, C**H,** $^3J_{H-H}$ = 6.0 Hz), 6.40 (dd, C**H,** $^3J_{H-H}$ = 6.0 Hz, $^3J_{H-H}$ = 6.3 Hz), 4.21 (d, C**H,** $^3J_{H-H}$ = 7.5 Hz), 2.44 (dd, C**H,** J= 7.5Hz, $^3J_{H-H}$ = 6.3 Hz), 3.38 (s, N(C**H**$_3$)$_3$). Elemental analysis: Calculated for $Ru_6NO_{14}C_{22}H_{13}$: C, 23.56%; H, 1.17%; N, 1.25%. Found: C, 24.55%; H, 1.46%; N, 1.39%.

Reaction of 2.2 with Me_3NO and C_2H_2.

A 10.0 mg (0.009 mmol) amount of **2.2** was added to 10 mL of CH_2Cl_2 in a 50 mL three-neck flask. A slow purge of C_2H_2 was then passed through the solution for 15 min at room temperature. This was followed by addition of 1.5 mg of Me_3NO with stirring for 30 min. The solvent was removed *in vacuo*. The product was then separated by TLC by using hexane/methylene chloride solvent mixtures to yield the following in the order of elution: 0.7 mg of unreacted **2.2**, 1.0 mg of compound **2.3** (10% yield).

Reaction of 2.2 with CO.

A 4.2 mg (0.003 mmol) amount of **2.2** was dissolved in 2.5 mL of d_2-dichloromethane in an NMR tube. CO gas was allowed to purge through this solution for 1 min and the NMR tube was then closed. The solution was then allowed to stand at room temperature for 24 h. After this period, CO was again purged through the solution for 1 min. The NMR tube was closed and was kept at room temperature for another 24 h. After this period, resonances for the new products were observed by ^1H NMR spectroscopy. Workup of the reaction mixture by TLC by using a hexane/methylene chloride solvent mixture yielded the following products in the order of elution: 1.7 mg of $Ru_3(CO)_{12}$ and 1.7 mg (40% yield) of bright orange compound $Ru_6C(CO)_{16}(\eta^1\text{–}E\text{–}C_2H_2NMe_3)$, **2.4**.

Spectral data of **2.4**: IR ν_{CO} (cm^{-1} in CH_2Cl_2): 2074.9(w), 2023.3 (s), 1967.4(m). ^1H NMR (in CD_2Cl_2, δ in ppm): 7.58 (d, C**H,** $^3J_{H-H}$ = 14.4 Hz), 5.83 (d, C**H,** $^3J_{H-H}$ = 14.4 Hz), 3.13 (s, NMe_3). Mass Spectrum (ES^+): M^+ = 1148.0, M^+- $C_2H_2NMe_3$ = 1066.0.

Thermal Transformation of 2.2.

A 19.0 mg (0.017 mmol) amount of **2.2** was dissolved in 10 mL of 1,2-dichloroethane in a 50 mL three-neck flask. This reaction mixture was then heated to reflux for 20 min. The solvent was removed *in vacuo*. The product $Ru_6C(CO)_{15}(\mu_3\text{-}C_2H_2)$, **2.5** was isolated by TLC yield 10.0 mg (55% yield). Spectral data of **2.5**: IR, ν_{CO} (cm^{-1} in CH_2Cl_2): 2091.1(w), 2044.7 (s), 2024.2(m), 2016.3(m). ^1H NMR (CD_2Cl_2, δ in ppm): 10.39 (s, C**H**). Mass Spectrum (ES^+): M^+ = 1065.0. The isotope distribution pattern is consistent with the presence of six ruthenium atoms.

Thermal Decarbonylation of 2.4.

A 8.0 mg (0.0070 mmol) amount of **2.4** was dissolved in 10 mL of dichloroethane in an 50 mL three-neck flask. This reaction mixture was then heated to reflux for 3h. The solvent was removed *in vacuo*. Workup by using TLC, yielded 6.4 mg (86% yield) of compound $Ru_6C(CO)_{15}(\mu_3\text{-}C_2H_2)$, **2.5**.

Thermal Transformation of 2.3.

6.7 mg (0.006 mmol) of **2.3** was dissolved in 10 mL of 1,2-dichloroethane in a 50 mL three-neck flask. This reaction mixture was then heated to reflux for 20 min. The solvent was removed *in vacuo*. Workup by using TLC, yielded 4.0 mg (64% yield) of compound $Ru_6C(CO)_{14}(\mu_3\text{–}\eta^4\text{–}C_4H_4)$, **2.6**. Spectral data of **2.6**: IR, ν_{CO} (cm^{-1} in CH_2Cl_2): 2083.6 (m), 2045.9 (s), 2034.8 (vs), 1983.6 (w), 1852 (w,br). ^1H NMR (in CD_2Cl_2, δ in ppm): 10.31 (dd, C**H,** $^3J_{H-H}$ = 3.3 Hz, $^4J_{H-H}$ = 3.3 Hz), 5.27 (dd, C**H,** $^3J_{H-H}$ = 3.3 Hz, $^4J_{H-H}$

= 3.3 Hz). Mass Spectrum (ES^+): M^+ = 1063.0. The isotope distribution pattern is consistent with the presence of six ruthenium atoms.

Addition of NMe_3 to 2.5.

A 10.0 mg (0.009 mmol) amount of **2.5** was dissolved in 2.5 mL of d_2-CH_2Cl_2 in an NMR tube. NMe_3 gas was then purged slowly through this solution for 1 min at room temperature. The formation of compound **2.2** was observed by ^1H NMR spectroscopy. Workup of the reaction mixture after 15 min by TLC yielded 3.0 mg of compound **2.2** (30% yield)**.**

Addition of NMe_3 to 2.6.

A 5.0 mg (0.005 mmol) amount of **2.6** was dissolved in 2.5 mL of d_2-CH_2Cl_2 in an NMR tube. NMe_3 gas was purged through this solution for 1 min at room temperature and the NMR tube was then sealed. The formation of compound **2.3** was observed by ^1H NMR spectroscopy. Workup of the reaction mixture after 15 min by using TLC yielded 1.0 mg of compound **2.3** (18% yield).

Synthesis of $Ru_6C(CO)_{16}[\eta^1$-*E*-$(CO_2Me)=C(H)NMe_3]$, 2.7.

A 45.0 mg (0.041 mmol) amount of **2.1** was added to 50 mL three-neck flask in 15 mL of degassed dichloromethane. To this solution, 40 µL of methyl propiolate was added and was followed by addition of 8.0 mg of Me_3NO. After stirring for 15 min, the solvent was removed *in vacuo*. The products were then separated by TLC by using a solvent mixture of hexane/methylene chloride to yield the band of 5.0 mg (10% yield) of orange $Ru_6C(CO)_{16}[\eta^1$-*E*-$C(CO_2Me)=C(H)NMe_3]$, **2.7**. Spectral data of **2.7**: IR spectra, ν_{CO} (cm^{-1} in CH_2Cl_2): 2077.1(m), 2026.3 (s). ^1H NMR (in CD_2Cl_2, δ in ppm): 3.72 (s,

C**H**), 3.12 (s, OC**H**$_3$), 1.33 (s, br N(C**H**$_3$)$_3$). Mass Spectrum (ES$^+$): M$^+$ = 1211.0. The isotope distribution pattern is consistent with the presence of six ruthenium atoms.

Synthesis of Ru$_6$C(CO)$_{15}$[μ$_3$-HC$_2$(CO$_2$Me)], 2.8.

20.0 mg (0.017 mmol) of **2.7** was dissolved in 10 mL of 1,2-dichloroethane in an 50 mL three-neck flask. This reaction mixture was then heated to reflux (83ºC) for 30 min. The solvent was removed *in vacuo*. Workup by using TLC provided 12.5 mg (66% yield) of compound Ru$_6$C(CO)$_{15}$[μ$_3$-HC$_2$(CO$_2$Me)], **2.8** (66% yield) and 1.8 mg of unreacted **2.7**. Spectral data of **2.8**: IR, ν_{CO} (cm^{-1} in CH_2Cl_2): 2093.6 (m), 2048.4 (vs), 2022.8 (s), 1996.4(w). ^{1}H NMR (in CD_2Cl_2, δ in ppm): 10.50 (s, C**H**), 3.89 (s, OC**H**$_3$). Mass Spectrum (EI$^+$): M$^+$ = 1124.0. The isotope distribution pattern is consistent with the presence of six ruthenium atoms.

Crystallographic Analyses.

Crystals of each product suitable for single-crystal X-ray diffraction analyses were grown by slow evaporation of solvent from solutions of the pure compound in the open air. Dark red crystals of compound **2.2** were obtained from a CH_2Cl_2/hexane solvent mixture at -25˚C. Brown orange crystals of compound **2.3** were obtained from a CH_2Cl_2/benzene/octane solvent mixture. Dark red crystals of compound **2.4** were obtained from a solution in a CH_2Cl_2/benzene/octane solvent mixture. Dark red crystals of compound **2.5** were obtained from a CH_2Cl_2/benzene/octane solvent mixture. Red crystals of compound **2.6** were obtained from a CH_2Cl_2/benzene/octane solvent mixture. Red crystals of compound **2.7** were obtained from a solution in a CH_2Cl_2/octane solvent mixture. Dark red crystals of **2.8** were obtained from a solution in a CH_2Cl_2/benzene/octane solvent mixture.

X-ray intensity data were measured by using a Bruker D8 QUEST diffractometer equipped with a PHOTON-100 CMOS area detector and an Incoatec microfocus source (Mo Kα radiation, λ = 0.71073 Å).[21] The structures were solved with SHELXT.[22] Subsequent difference Fourier calculations and full-matrix least-squares refinement against F^2 were performed by using SHELXL-2018[22] or by using OLEX2.[23]

For compound **2.2**, the pattern of systematic absences in the intensity data was uniquely consistent with the space group $P4_2/n$. The asymmetric unit consists of one molecule. The C_2 group of the C_2NMe_3 substituent is disordered, scrambled over two conformations across the Ru1-Ru2 bond. Free refinement of the atomic site occupation factors (*sof*) for the four affected atoms (C1-C4) resulted in occupancies near 50% for each atom. After location and anisotropic refinement of atoms of the primary molecular orientation, a pattern of large residual electron density peaks of magnitude ca. 6 e^- /Å^3 was observed. The largest were located near ruthenium atoms Ru2, Ru3, Ru4 and Ru6 of the cluster. Trial refinements of atomic site occupancies were consistent with disorder of most of the entire cluster. Atoms Ru2, Ru3, Ru4 and Ru6 refined to near 80% occupancy, while the four largest residual peaks located near these atoms refined to near 20% Ru occupancy. Smaller peaks were observed in positions consistent with some carbonyl groups of the minor component. However reliable positions for the complete set of minor carbonyl group atoms could be located, and a complete whole-molecule disorder model could not be refined. To achieve reasonable refinement statistics and more reliable derived parameters for the major disorder component, the four ruthenium atoms of the minor disorder component were included in the final structural model (Ru2B, Ru3B, Ru4B, Ru6B). Omitting the minor component Ru atoms results in final residuals of

R1/wR2 = 0.069/0.139 and difference map extrema of +5.7/-4.5 e-/Å^3. The major disorder occupancy refined to 0.784(5). The cluster disorder takes the form of a slight (ca. 15°) rotation about the vector defined by atoms Ru1 and Ru5. The C_2NMe_3 disorder is apparently independent of the cluster disorder, as the carbon atom C1/C2 and C3/C4 occupancies all refined independently to near 50% each, distinct from the 78/22 % Ru atom disorder. For the final model, C1-C4 occupancies were fixed at 0.50. No reliable hydrogen atom positions could be located, and none were calculated for atoms C1-C4 of the C_2NMe_3 group. All non-hydrogen atoms were refined with anisotropic displacement parameters except for minor disorder component atoms Ru2B, Ru3B, Ru4B, Ru6B (isotropic). Methyl hydrogen atoms were placed in geometrically idealized positions and included as riding atoms with d(C-H) = 0.98 Å and Uiso(H) = 1.5Ueq(C) for methyl hydrogens. They were allowed to rotate as a rigid group to the orientation of maximum observed electron density. The largest residual electron density peak in the final difference map is 1.69 e- /Å^3, located 2.20 Å from C61. This, together with several other peaks of similar magnitude, represents minor disorder component carbonyl C and O atoms which could not be successfully modeled.

For compound **2.5**, the systematic absences in the intensity data were consistent with the space groups $P2_1$ and $P2_1/m$; $P2_1$ was confirmed by structure solution and by examination of the finished structure. The asymmetric unit consists of two crystallographically independent molecules. Three-fold disorder of the C_2H_2 grouping bonded to one of the two independent Ru6 clusters (atoms C3-C4 A/B/C bonded to Ru7-Ru12) was observed. Three superimposed atomic positions were refined corresponding to the three orientations. Occupancies of the three components refined to A/B/C =

0.477(4)/0.250(4)/0.273(4). The occupancy sum was constrained to 1.0. The anisotropic displacement parameters for the C3C/C4B site were restrained to approximate a spherical shape (SHELX ISOR). Hydrogen atoms were not observable in the difference Fourier map but were placed in approximate idealized positions and included as riding atoms with d(C-H) = 1.0 Å and Uiso(H) = 1.2Ueq(C). The absolute structure (Flack) parameter after the final refinement cycle was -0.004(8).

Compound **2.6** crystallized in the monoclinic system. The pattern of systematic absences in the intensity data was consistent with the space group $P2_1/c$, which was confirmed by structure solution. The asymmetric unit consists of one molecule. After normal location and anisotropic refinement of the main molecule, residual factors were high (R1 > 9%), and several large electron density remained in a pattern which could be fit to the same molecule in a different orientation, apparently disordered on the same site as the primary occupant. Six large residual peaks observed near the ruthenium atoms were most prominent, but smaller peaks corresponding to C and O atoms were also observed. This was interpreted as whole-molecule disorder. From trial disorder modeling, the minor disorder component (atom label suffixes "B") is structurally identical to the major (atom label suffixes "A"). The geometry of the entire minor component was therefore restrained to be similar to that of the major using a SHELX SAME instruction. This resulted in a stable refinement with reasonable displacement parameters for most atoms. The two components disorder via an approximate non-crystallographic mirror plane passing near to Ru3A/B, Ru5A/B and C0A/B. In the reported refinement model, the minor component is therefore the mirror-related isomer of the major. The total occupancy of the two components was constrained to sum to one, and refined to A/B =

0.813(3)/0.187(3). All non-hydrogen atoms of the major component were refined with anisotropic displacement parameters. Those of the minor were refined isotropically with the exception of the ruthenium atoms and some carbon and oxygen atoms which appeared nearly superimposed on major component atoms; these were given equal anisotropic displacement parameters as the overlapped atoms of component "A". Hydrogen atoms bonded to the C_4H_4 group of the major component were located in difference Fourier maps before being placed in geometrically idealized positions and included as riding atoms with d(C-H) = 1.00 Å and Uiso(H) = 1.2Ueq(C); those of the minor component were simply idealized before being treated the same way. The largest residual electron density peak in the final difference map is 1.17 e- /$Å^3$, located 0.78 Å from Ru2A.The observed disorder is not imposed by incorrect space group symmetry, as trial refinements in lower space groups ($P2_1$, Pc) also showed whole-molecule disorder. Datasets collected from two additional crystals at 100 K and one at room temperature likewise gave identical results. Because of the small minor component population fraction and the requirement for refinement restraints to achieve a reasonable molecular geometry, derived parameters for component "B" are approximate. Atomic parameters, bond distances and angles of the minor component should be considered unreliable and only those of the major component are discussed.

Compound **2.7** crystallized in the space group $P2_1/n$ of the monoclinic system. The asymmetric unit consists of one molecule. There is two-fold crystallographic disorder affecting only the -$C(O)OCH_3$ part of the -$CCH(NMe_3)C(O)OCH_3$ ligand (atoms O1, O2, C3, C4). The major disorder component (O1A-C4A) occupancy refined to 0.700(9). Like C-C and C-O distances between the components were restrained to be

similar (SHELX SADI). The anisotropic displacement parameters of nearly superimposed atoms were held equal. All non-hydrogen atoms were refined with anisotropic displacement parameters. An additional spherical restraint was necessary for the displacement parameters of atom O2A. Methyl hydrogen atoms were placed in geometrically idealized positions and included as riding atoms with d(C-H) = 0.98 Å and Uiso(H) = 1.5Ueq(C). The methyl hydrogen atoms were allowed to rotate as a rigid group to the orientation of maximum observed electron density. Hydrogen atom H1 was located in a difference Fourier map. Its atomic coordinates were refined freely with Uiso(H) = 1.2Ueq(C). The largest residual electron density peak in the final difference map is 1.02 e- /Å3, located 0.81 Å from Ru3. Crystal data, data collection parameters, and results for each analysis are summarized in Table 2.1 and 2.2.

2.3 Results and Discussion

Two products, $Ru_6(\mu_6\text{-}C)(CO)_{15}(\mu\text{–}\eta^2\text{–}C_2H_2NMe_3)$, **2.2** and $Ru_6(\mu_6\text{-}C)(CO)_{14}(\mu_3\text{–}\eta^4\text{–}C_4H_4NMe_3)$, **2.3**, were obtained from the reaction of compound **2.1** with C_2H_2 in the presence of Me_3NO at room temperature for 20 min. Both products were characterized by single-crystal X-ray diffraction analyses. An ORTEP diagram of the molecular structure of compound **2.2** is shown in Figure 2.1. Compound **2.2** contains an octahedral-shaped Ru_6 cluster with 15 carbonyl ligands. The most interesting ligand in **2.2** is a 2-trimethylammoniumethenyl ligand, $CH{=}CHNMe_3$, that bridges the Ru1 – Ru2 edge of the cluster. The $CH{=}CHNMe_3$ ligand is coordinated in the $\sigma{+}\pi$ fashion that is well established for bridging alkenyl ligands.[15] The two CH groups exhibit a 50/50 disorder in the crystal as shown in the figure. The disordered ethenyl carbon atoms C1/C3 are σ-bonded to both Ru1, Ru1-C1 = 2.057(14) Å, Ru1-C3 = 2.112(12) Å while C(1) and

C(2) / C(3 and C(4) are bonded to Ru2, Ru2-C1 = 2.084(12) Å, Ru2-C2 = 2.155(12) Å and Ru2-C3 = 2.269(12) Å, Ru2-C4 = 2.253(13) Å. The C – C distance is short, C1-C2 = 1.427(19) Å and C3-C4 = 1.419(18) Å, and indicative of a π-coordinated C-C double bond. Takats et al. reported the synthesis of the complex $Os(CO)_3RhCp(\mu–\eta^2$-$CHCHPMe_3)$-(μ-CO) a number of years ago which contains a similarly coordinated σ+π ethenyl(trimethylphosphonium) ligand bridging two metal atoms.[7e] There is a NMe_3 group in **2.2** (not disordered) that is bonded to the disordered carbon atoms C2/C4 at a normal C – N single bond length, N1-C2 = 1.565(11) Å / N1-C4 = 1.553(11) Å. There is a single hydrogen atom (not shown) attached to each ethenyl carbon atom. They are observed at δ = 8.85 (d, $^3J_{H-H}$ = 7.5 Hz) and 4.29 (d, $^3J_{H-H}$ = 7.5 Hz) in the H NMR spectrum, and there is a singlet at 3.19 ppm for the NMe_3 group. Formally, there is a positive charge on the nitrogen atom N1. A negative charge could be formally assigned to the metal atom Ru1, but this charge is certainly distributed through the delocalized bonding molecular orbitals of the entire Ru_6 cluster. The bridging $CH=CHNMe_3$ ligand in **2.2** serves formally as a four-electron donor, the complex overall obtains a total of 86 cluster valence electrons which is in complete accord with the observation of an octahedral cluster of six metal atoms.[16]

An ORTEP diagram of the molecular structure of compound **2.3** is shown in Figure 2.2. Compound **2.3** contains an octahedral-shaped Ru_6 cluster with 14 carbonyl ligands. The most interesting ligand in **2.3** is a monometallated-η^4–4-trimethylammoniumbutadienyl, $Me_3N^+CHCHCHCH$, ligand that bridges the Ru1 – Ru2 – Ru3 face of the cluster. This novel ligand was formed by the coupling of two equivalents of HC_2H and addition of one molecule of NMe_3 to one of the terminal carbon

atoms of the C_4-chain. Carbon atoms C1 and C2 are π-bonded to Ru2, Ru2-C1 = 2.108(8) Å, Ru2-C2 = 2.288(8) Å. Carbon atoms C3 and C4 are π-bonded to Ru1, Ru1-C3 = 2.227(8) Å, Ru1-C4 = 2.194(7) Å and C4 is also σ-bonded to Ru3, Ru3-C4 = 2.063(8) Å. The π–coordinated C – C double bonds are significantly shorter, C1-C2 = 1.437(11) Å and C3-C4 = 1.401(11) Å, than the C2 – C3 bond which is formally a C – C single bond, C2-C3 = 1.462(12) Å. The C1 – N1 bond is also a single bond, N1 - C1 = 1.540(10) Å. Formally, there is a positive charge on the nitrogen atom N1 and a negative charge on the Ru_6 cluster. Each carbon atom in the C_4-chain contains one hydrogen atom. Accordingly, there are four proton resonances with appropriate H – H couplings in the ^{1}H NMR spectrum, δ = 9.53 (d, C**H,** $^3J_{H-H}$ = 6.0 Hz), 6.40 (dd, C**H,** $^3J_{H-H}$ = 6.0 Hz, $^3J_{H-H}$ = 6.3 Hz), 4.21 (d, C**H,** $^3J_{H-H}$ = 7.5 Hz), 2.44 (dd, C**H,** J= 7.5Hz, $^3J_{H-H}$ = 6.3 Hz) and a singlet at δ = 3.38 for the NMe_3 group. Compound **2.3** contains one less CO ligand than **2.2**. Formally, $Me_3N^+CHCHCHCH$ ligand serves as a six-electron donor to the cluster. Thus, the six ruthenium atoms contain a total of 86 electrons which is in accord with the observed octahedral-shaped Ru_6 cluster.[16] It was possible to obtain compound **2.3** from **2.2** in a low yield (10%) from the reaction of **2.2** with an additional quantity of C_2H_2 in the presence of Me_3NO which was used to aid in the removal of a CO ligand.

When compound **2.2** was placed under an atmosphere of CO (1 atm) at 25 °C for 24 h, the new compound $Ru_6C(CO)_{16}(\eta^1–E–C_2H_2NMe_3)$, **2.4,** was obtained in 40% yield. An ORTEP diagram of the molecular structure of compound **2.4** is shown in Figure 2.3. Compound **2.4** contains an octahedral-shaped Ru_6 cluster with 16 carbonyl ligands. The most interesting ligand is a 2-trimethylammoniumethenyl, $HC=CH(NMe_3)$, ligand that is terminally coordinated to the metal atom Ru1 by the carbon atom C1, Ru1-C1 = 2.097(2)

Å. There is a C – C double bond between the atoms C1 and C2, C1-C2 = 1.306(3) Å and a NMe_3 group bonded to atom C2, N1-C2 = 1.508(3) Å. The CH groups exhibit an *E*-stereochemistry, and this is confirmed by the large coupling, $^3J_{H-H}$ = 14.4 Hz, between the two CH resonances, δ = 7.58 and 5.83, observed in the ^1H NMR spectrum. The methyl resonance of the NMe_3 group occurs at 3.13 ppm. Compound **2.4** was formed by the addition of one CO ligand to the Ru_6 cluster. This addition induces the conversion of the $C_2H_2NMe_3$ ligand from a bridging four electron donating ligand to a terminally coordinated two electron donating ligand by release of the coordinated C – C double bond. The terminally coordinated $C_2H_2NMe_3$ ligand is a two-electron donor, and compound **2.4** thus contains a total of 86 cluster valence electrons which is in accord with the observation of an octahedral cluster of six metal atoms.[16] Similar terminally coordinated C(H)=CH(NEt_3) ligands were found in the complexes, [Ir(H)(-C≡CPh)(-CH=CHNEt_3)L_3]$^+$ and [Ir-CH=CHCH=CH)(-CH=CH-NEt_3)L_3]$^+$.[10]

When a solution of **2.2** was heated to reflux in 1,2-dichloroethane solvent (83 °C) for 20 min., the NMe_3 group was eliminated from the molecule to yield the ethyne complex $Ru_6C(CO)_{15}(\mu_3\text{-}C_2H_2)$, **2.5** in 55% yield. Similarly, when a solution of **2.4** in 1,2-dichloroethane was heated to reflux (83°C) for 3h, compound **2.5** was obtained in 86% yield by loss of one CO ligand and the NMe_3 group. Compound **2.5** was also characterized structurally by a single-crystal X-ray diffraction analysis. An ORTEP diagram of the molecular structure of **2.5** is shown in Figure 2.4. Compound **2.5** contains two independent molecules in the asymmetric crystal unit. One of the two molecules exhibits a 3-fold disorder of the C_2H_2 ligand in the solid state. An ORTEP diagram of the structure of the undisordered molecule of **2.5** in the crystal is shown in Figure 2.4.

Compound **2.5** contains 15 linear terminal carbonyl ligands on an octahedral Ru_6C cluster of metal atoms with a triply bridging ethyne ligand on one of the Ru_3 faces (Ru1-Ru2-Ru3) of the cluster. The C1 – C2 distance of 1.352(9) Å is consistent with that of a coordinated triple bond. The structure of **2.5** is similar to the structures of $Ru_6C(CO)_{15}(\mu_3\text{-}HC_2Ph)$ and $Ru_6C(CO)_{15}(\mu_3\text{-}PhC_2Me)$ both of which contain triply bridging alkyne ligands on Ru_6 cluster complexes.[17] Compound **2.5** was first obtained a number of years ago by reaction of the anion $[Ru_6C(CO)_{16}]^{2-}$ with ethyne and treatment by $[FeCp_2][BF_4]$, but it was not structurally characterized.[17]

Interestingly, the NMe_3 elimination from **2.2** is reversible. When NMe_3 gas was passed through a solution of **2.5** in an NMR tube in CD_2Cl_2 solvent, the immediate formation of compound **2.2** was observed at room temperature. It subsequently isolated in 30% yield.

When a solution of **2.3** was heated to reflux in 1,2-dichloroethane solvent (83 ^oC) for 20 min, the NMe_3 group was eliminated from the molecule to yield the dimetallated butadiendiyl complex $Ru_6C(CO)_{14}(\mu_3\text{–}\eta^4\text{–}C_4H_4)$, **2.6** in 64% yield. Compound **2.6** was also characterized structurally by single-crystal X-ray diffraction analysis. Compound **2.6** exhibits a 2-fold disorder in a 80/20 ratio in the solid state. An ORTEP diagram of its molecular structure of the major component from the disorder model is shown in Figure 2.5. Compound **2.6** contains 14 carbonyl ligands on an octahedral Ru_6C cluster. There is a η^4–triply bridging C_4H_4 butadiendiyl ligand on the Ru1-Ru2-Ru3 triangular face of the cluster. The coordinated C1a-C2a = 1.418(11) Å and C3a-C4a = 1.421(11) Å distances which are formally double bonds are slightly shorter than the C2a-C3a = 1.442(11) Å, which is formally a single bond. Two resonances with appropriate couplings were

observed for the CH protons in the ^{1}H NMR spectrum: δ = 10.31 (dd, $^3J_{H-H}$ = 3.3 Hz, $^4J_{H-H}$ = 3.3 Hz) and 5.27 (dd, $^3J_{H-H}$ = 3.3 Hz, $^4J_{H-H}$ = 3.3 Hz). The bridging η^4–C_4H_4 ligand in **2.6** serves formally as a six electron donor, thus compound **2.6** contains a total of 86 cluster valence electrons which is in accord with the observation of an octahedral cluster of six metal atoms.[16] Compound **2.6** is structurally similar to the diphenyl-substituted dimetallabutadienyl compound $[Ru_6C(CO)_{14}\{(\mu_5\text{-}\eta^4\text{-}1,4\text{-}C(Ph)CHCHC(Ph)\}]$.[18]

Interestingly, the elimination of NMe_3 from **2.3** is reversible, and when a solution of **2.6** in CD_2Cl_2 was treated with NMe_3 gas at 25^{o}C, compound **2.3** was regenerated and subsequently isolated in 18% yield.

In order to investigate the scope of the alkyne-tertiary amine zwitterion formation reaction further, we performed the reaction of **2.1** with methyl propiolate, $HC{\equiv}C(CO_2Me)$, and Me_3NO in CH_2Cl_2 at room temperature. After 15 min, the compound $Ru_6C(CO)_{16}[\eta^1\text{-}E\text{-}C(CO_2Me)=C(H)NMe_3]$, **2.7** was formed and subsequently isolated in 10% yield. Compound **2.7** was characterized structurally by single-crystal X-ray diffraction analysis. An ORTEP diagram of the molecular structure of compound **2.7** is shown in Figure 2.6. Compound **2.7** contains an octahedral-shaped Ru_6 cluster with 16 carbonyl ligands similar to that of **2.4**. There is a 2-trimethylammonium-1-(methoxycarbonyl)ethenyl ligand, E-$C(CO_2M)=C(H)NMe_3$, having an E-conformation at the C1 and C2 double bond that is terminally coordinated to the metal atom Ru1 at the carbon atom C2, Ru1-C2 = 2.120(5), Å. The C – C double bond distance, C1-C2 = 1.304(3) Å is virtually the same as that found in **2.4**. The C – N bond distance to the NMe_3 group N1-C1 is 1.477(7) Å. There is a formal positive charge on the nitrogen atom

N1 and a negative charge on the Ru_6 cluster. It is believed that the bulky NMe_3 group is bonded to the carbon atom C1 that contains the hydrogen atom for steric reasons. The single ethenyl CH resonance was observed at $\delta = 5.21$ (t, $^2J_{N-H} = 4.8$ Hz) in the ^1H NMR spectrum. The methyl resonance of the NMe_3 group occurs at $\delta = 3.13$. The $C(CO_2Me)=C(H)NMe_3$ ligand serves as a two electron donor to the Ru_6 cluster which thus achieves a total cluster valence electron count of 86 electrons that is in accord with the observation of an octahedral-shaped cluster.[16]

When a solution of **2.7** in 1,2-dichloroethane solvent was heated to reflux (83 ^oC) for 30 min., it was transformed into the new compound $Ru_6C(CO)_{15}[\mu_3\text{-}HC_2(CO_2Me)]$, **2.8** in 66% yield by loss of two CO ligands and the NMe_3 group on $C(CO_2CH_3)=C(H)NMe_3$ ligand. Compound **2.8** was characterized structurally by single-crystal X-ray diffraction analysis. An ORTEP diagram of the molecular structure of compound **2.8** is shown in Figure 2.7. Compound **2.8** is a homologue of **2.5**. It contains an octahedral-shaped Ru_6 cluster with 15 linear terminal carbonyl ligands and a triply bridging methyl propiolate ligand. The alkyne C – C bond distance, C1-C2 = 1.392(5) Å, is slightly longer than that in **2.5**. The alkyne CH resonance occurs at $\delta = 10.50$ and the methoxy methyl resonance at $\delta = 3.89$, as expected. Compound **2.8** contains a total of 86 cluster valence electrons which is in accord with the observation of an octahedral-shaped cluster.[16]

A number of years ago, Johnson and Lewis et al. reported the synthesis of the complex $Ru_6C(CO)_{15}(\mu_3\text{-}HC_2Ph)$, **2.9,** from the reaction of **2.1** with HC_2Ph in the presence of Me_3NO.[18] The Me_3NO was added to assist in the removal of CO ligands by

transferring its O atom to a CO ligand to form CO_2 which was then eliminated from the complex. The HC_2Ph molecule was then added to the Ru_6 cluster to become a bridging ligand similar to that found in compound **2.5**. Compound **2.9** was found to react with an additional quantity of HC_2Ph in the presence of Me_3NO to yield the complex $Ru_6C(CO)_{14}(\mu_3{-}\eta^4{-}C_4H_2Ph_2)$, **2.10,** that exists as two isomers formed by the head-to-tail and head-to-head coupling of the two molecules of HC_2Ph to form disubstituted, bridging dimetalated butadienediyl ligands that are coordinated to the cluster in a fashion similar to that observed in compound **2.6**. No evidence for the formation of products containing NMe_3 groups was provided in this report.

A summary of our studies of the reactions of **2.1** with ethyne in the presence of Me_3NO are shown in Scheme 2.1. Compounds **2.2** and **2.3** were the only products isolated from the original reaction mixture. Two additional new products, **2.5** and **2.6**, were formed by elimination of the NMe_3 group when solutions of **2.2** and **2.3** were heated to 83^{o}C, respectively. Most interestingly, it was found that when the reaction of **2.1** with HC_2H and Me_3NO was examined at room temperature, in situ, by following by ^1H NMR spectroscopy, the formation of compound **2.5** was observed as the major product in solution within the first 5 minutes. Compound **2.5** subsequently disappeared with the formation of compound **2.2**, presumably via the direct addition of NMe_3 to **2.5** as we later confirmed independently. It was also found that compound **2.3** can be obtained from **2.2** by reaction with additional quantities of HC_2H and Me_3NO, but no **2.6** was observed in this reaction. Compound **2.6** was obtained by heating solutions of **2.3** at 83 ^{o}C, but it could not be obtained from **2.5** with the use of additional HC_2H and Me_3NO at room temperature. We have been able to obtain **2.6** only through the **2.2** → **2.3** → **2.6**

sequence. It thus appears that the low temperature C – C coupling that leads to the formation of C_4H_4 groupings in both **2.3** and **2.6** proceeds via **2.2** as an intermediate and not from **2.5**. This in turn suggests that the NMe_3 group may be serving as an "activator" for the HC_2H ligand in **2.5** for the HC_2H - HC_2H coupling process. A number of years ago, Chin et al. demonstrated an example of C – C bond formation between a triethylammoniumethenyl ligand and an alkenyl ligand in an iridium complex by what appears to be a C – C reductive elimination process.[19]

Compound **2.4** containing the terminally coordinated $C(H)=CH(NMe_3)$ ligand was obtained by the addition of CO to **2.2**. Compound **2.7** containing the terminally-coordinated $C(CO_2Me)=CH(NMe_3)$ ligand was obtained directly by the reaction of **2.1** with $HC\equiv C(CO_2Me)$ in presence of Me_3NO, see Scheme 2.2.

2.4 Conclusions

In this work it has been shown that zwitterionic complexes containing novel bridging trimethylammoniumethenyl ligands can be formed in Ru_6 cluster complexes by reactions of ethyne and NMe_3 generated *in situ* from reactions of Me_3NO with the CO ligands of **2.1** or by direct NMe_3 addition to the bridging ethyne ligand in complex **2.5** and the bridging butadiendiyl ligand in **2.6** to yield the complexes **2.2** and **2.3**, respectively, by formation of a C – N bond. The C – N bond formation steps can be reversed by mild heating. Compound **2.3** was also obtained by the addition of ethyne to compound **2.2** in the presence of Me_3NO by loss of CO and a C – C coupling to the trimethylammoniumethenyl ligand. It is worth noting that we were not able to obtain any ammoniumethenyl zwitterionic ligands from disubstituted alkynes. This may be due to

destabilizations caused by the increased steric interactions that would occur as a consequence of having the bulky NMe_3 group and a substituent located on the same carbon atom of such disubstituted ammoniumethenyl ligands.

Table 2.1. Crystal Data for the X-Ray Structural Analyses for Compounds **2.2** – **2.4**.

Compound	**2.2**	**2.3**	**2.4**
Empirical formula	$C_{21}H_9NO_{15}Ru_6$	$C_{22}H_{13}NO_{14}Ru_6$	$C_{22}H_{11}NO_{16}Ru_6$
Formula weight	1121.71	1121.75	1151.74
Crystal system	Tetragonal	trigonal	Triclinic
Lattice parameters			
a (Å)	20.8204(11)	40.5292(12)	9.3876(3)
b (Å)	20.8204(11)	40.5292(12)	10.8470(4)
c (Å)	13.5235(7)	12.4689(4)	15.1324(5)
α (deg)	90.00	90	87.990(2)
β (deg)	90.00	90	79.119(2)
γ (deg)	90.00	120	82.674(2)
V ($Å^3$)	5862.3(7)	17737.6(12)	1500.74(9)
Space group	$P4_2/n$	*R*-3	*P*-1
Z value	8	18	2
ρ_{calc} (g/cm^3)	2.542	1.890	2.549
μ (Mo Kα) (mm^{-1})	3.083	2.291	3.017
Temperature (K)	100(2)	100(2)	100(2)
$2\theta_{max}$ (°)	52.828	52.738	60.00
No. Obs. ($I>2\sigma(I)$)	6015	8052	8718
No. of parameters	426	407	418
Goodness of fit (GOF)	1.110	1.029	1.051
Max. shift/error on final cycle	0.001	0.001	0.002
Residuals $2\sigma(I)$*: R1; wR2	0.0429/0.0816	0.0526;0.1156	0.0225;0.0388
Absorption Corr,	Semi-empirical	Semi-empirical	Semi-empirical
Max/min	0.5624/0.4895	0.4912/0.4052	0.8638/0.5566
Largest peak in Final Diff. Map (e^- / $Å^3$)	1.69	2.50	0.713

[a] $R1 = \Sigma_{hkl}(\,|\,|F_{obs}|-|F_{calc}|\,|)/\Sigma_{hkl}|F_{obs}|$; $wR2 = [\Sigma_{hkl}w(|F_{obs}|-|F_{calc}|)^2/\Sigma_{hkl}wF^2_{obs}]^{1/2}$; $w = 1/\sigma^2(F_{obs})$; $GOF = [\Sigma_{hkl}w(|F_{obs}|-|F_{calc}|)^2/(n_{data} - n_{vari})]^{1/2}$

Table 2.2. Crystal Data for the X-Ray Structural Analyses for Compounds **2.5** – **2.8**

Compound	**2.5**	**2.6**	**2.7**	**2.8**
Empirical formula	$C_{18}H_2O_{15}Ru_6$	$C_{19}H_4O_{14}Ru_6$	$C_{24}H_{13}NO_{18}Ru_6$	$C_{20}H_4O_{17}Ru_6$
Formula weight	1064.62	1062.64	1209.77	1122.65
Crystal system	Monoclinic	Monoclinic	Monoclinic	Triclinic
Lattice parameters				
a (Å)	9.4653(4)	17.6818(8)	9.7490(14)	9.5104(4)
b (Å)	31.6224(14)	9.0814(4)	24.118(3)	9.6762(4)
c (Å)	9.5914(4)	17.4537(8)	13.2505(18)	14.7081(6)
α (deg)	90.00	90.00	90.00	83.416(2)
β (deg)	119.1210(10)	116.458(2)	94.341(4)	86.599(2)
γ (deg)	90.00	90.00	90.00	85.219(2)
V (Å^3)	2507.96(19)	2509.1(2)	3106.6(8)	1338.21(10)
Space group	$P2_1$	$P2_1$ /c	$P2_1/n$	P-1
Z value	4	4	4	2
ρ_{calc} (g/cm^3)	2.820	2.813	2.587	2.786
μ (Mo Kα) (mm^{-1})	3.594	3.590	2.927	3.381
Temperature (K)	100(2)	294(2)	100(2)	100(2)
$2\theta_{max}$ (°)	65.274	56.784	53.46	56.90
No. Obs. (I>2σ(I))	18308	6227	6449	6696
No. of parameters	716	511	476	394
Goodness of fit(GOF)	1.030	1.273	1.063	1.065
Max. shift/error on final cycle	0.002	0.001	0.005	0.001
Residuals*:R1; wR2	0.0252;0.0478	0.0397; 0.0876	0.0330; 0.0565	0.0244;0.0544
Absorption Corr., Max/min	Semi-empirical 0.5655/0.5243	Semi-empirical 0.5633/0.4380	Semi-empirical 0.9438/ 0.7996	Semi-empirical 0.8766/0.5512
Largest peak in Final Diff. Map (e$^-$/Å^3)	2.50	1.17	1.342	1.615

[a] $R1 = \Sigma_{hkl}(\,|\,|F_{obs}|-|F_{calc}|\,|)/\Sigma_{hkl}|F_{obs}|$; $wR2 = [\Sigma_{hkl}w(|F_{obs}|-|F_{calc}|)^2/\Sigma_{hkl}wF^2_{obs}]^{1/2}$; $w = 1/\sigma^2(F_{obs})$; $GOF = [\Sigma_{hkl}w(|F_{obs}|-|F_{calc}|)^2/(n_{data} - n_{vari})]^{1/2}$

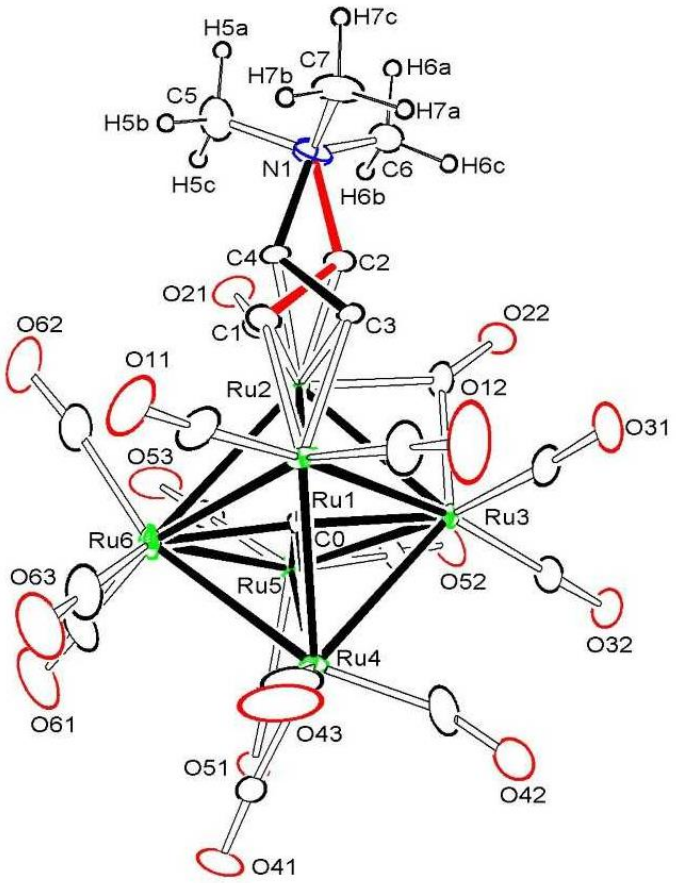

Figure 2.1. An ORTEP diagram of the molecular structure of the compound $Ru_6(\mu_6\text{-}C)(CO)_{15}(\mu\text{–}\eta^2\text{–}CHCHNMe_3)$, **2.2** showing the disorder in the $CH{=}CHNMe_3$ ligand. Thermal ellipsoidal probabilities are shown at 25%. Selected interatomic distances (Å) are as follows: Ru1-C1 = 2.057(14), Ru1-C3 = 2.112(12), Ru2-C1 = 2.084(12), Ru2-C2 = 2.155(12), Ru2-C3 = 2.269(12), Ru2-C4 = 2.253(13), C1-C2 = 1.427(19), C3-C4 = 1.419(18), N1-C2 = 1.565(11), N1-C4 = 1.553(11), N1-C5 = 1.475(10), N1-C6 = 1.481(11), N1-C7 = 1.516(9).

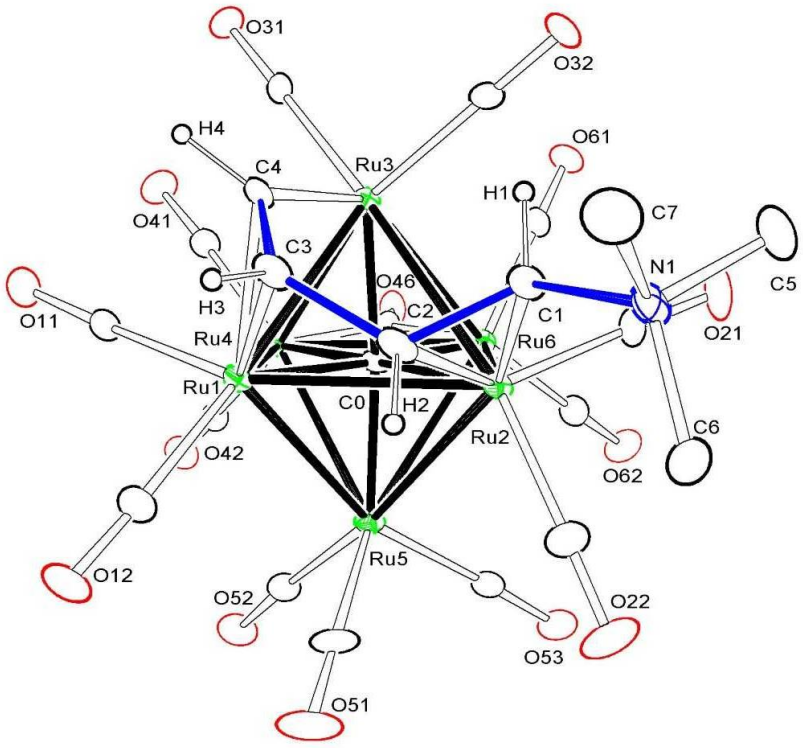

Figure 2.2. An ORTEP diagram of the molecular structure of the compound $Ru_6(\mu_6\text{-}C)(CO)_{14}(\mu_3{-}\eta^4{-}C_4H_4NMe_3)$, **2.3** showing the 20% thermal ellipsoidal probability. Selected interatomic distances (Å) are as follows: Ru1-C3 = 2.227(8), Ru1-C4 = 2.194(7), Ru2-C1 = 2.108(8), Ru2-C2 = 2.288(8), Ru3-C4 = 2.063(8), N1-C1 = 1.540(10), C1-C2 = 1.437(11), C2-C3 = 1.462(12), C3-C4 = 1.401(11), N1-C1 = 1.540(10) N1-C5 = 1.484(11), N1-C6 = 1.480(11), N1-C7 = 1.518(11).

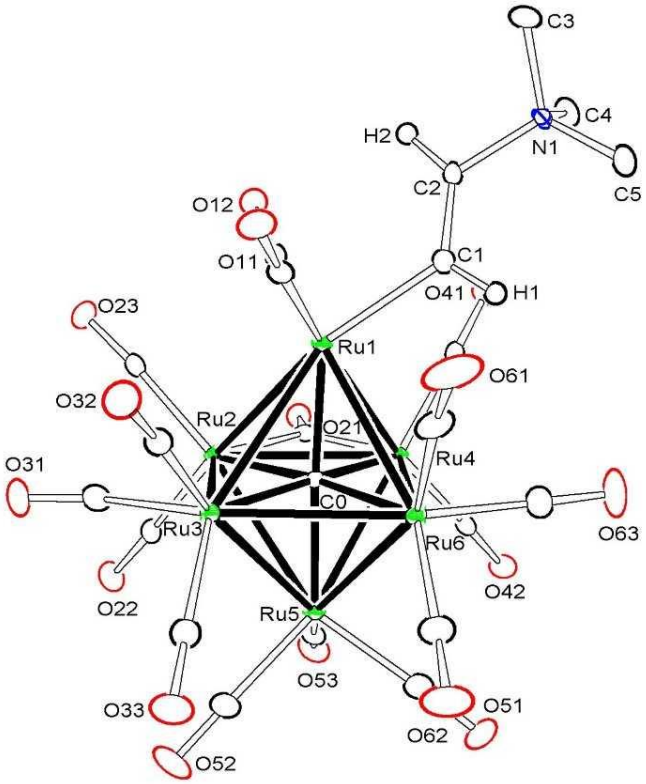

Figure 2.3. An ORTEP diagram of the molecular structure of the compound $Ru_6C(CO)_{16}(\eta^1\text{–}E\text{–}C_2H_2NMe_3)$, **2.4** showing the 40% thermal ellipsoidal probability. Selected interatomic distances (Å) are as follows: Ru1-C1 = 2.097(2), C1-C2 = 1.306(3), C1-H1 = 0.90(4), C2-H2 = 0.93(3), N1-C2 = 1.508(3), N1-C5 = 1.494(3), N1-C3 = 1.499(3), N1-C4 = 1.502(3).

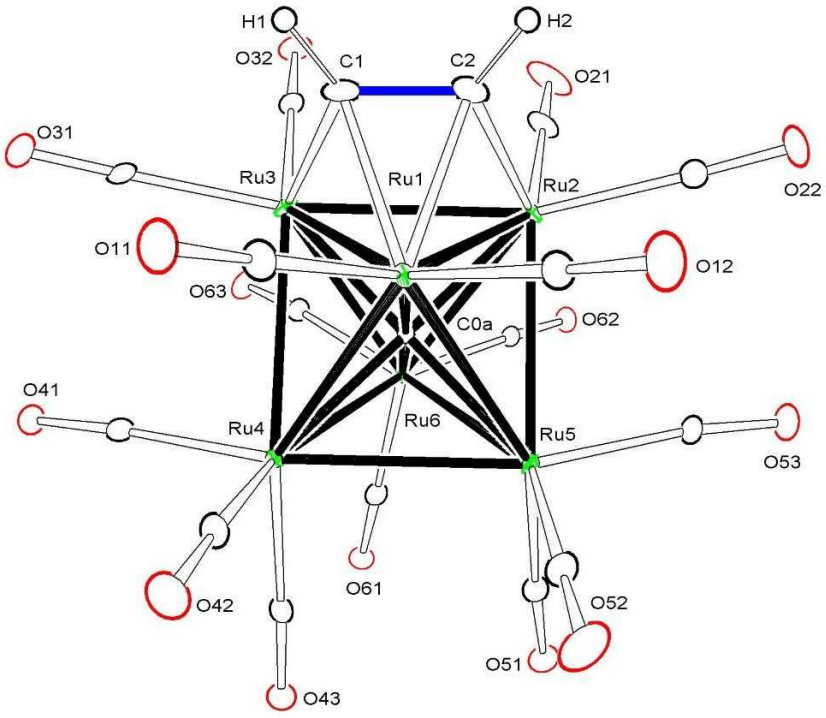

Figure 2.4. An ORTEP diagram of the molecular structure of the compound $Ru_6C(CO)_{15}(\mu_3\text{-}C_2H_2)$, **2.5** showing the 25% thermal ellipsoidal probability. Selected interatomic distances (Å) are as follows: Ru1-C1 = 2.172(6), Ru1-C2 = 2.215(6), Ru2-C2 = 2.052(6), Ru3-C1 = 2.055(6), C1-C2 = 1.352(9).

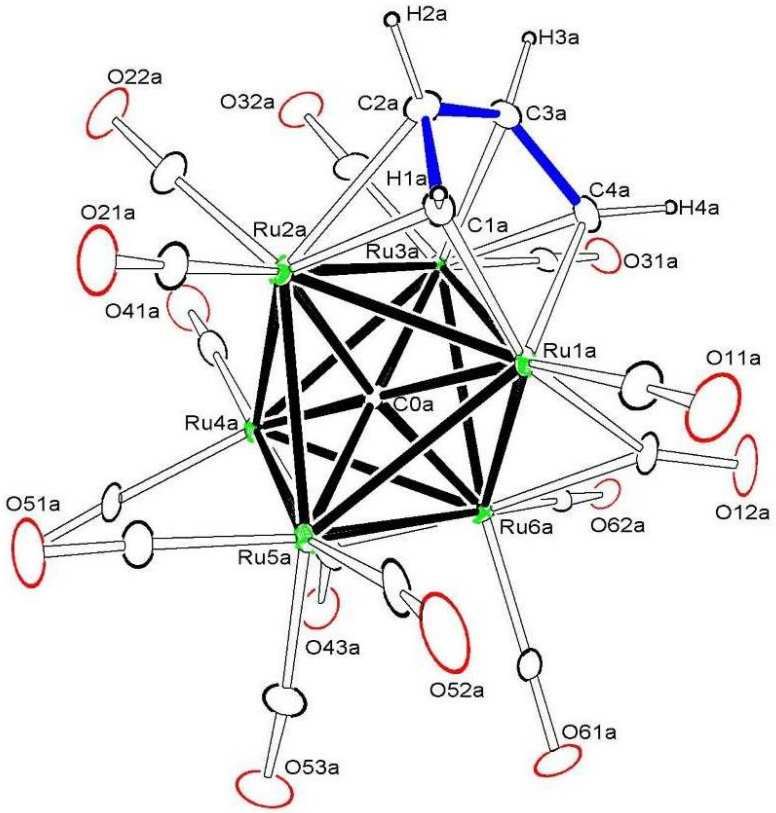

Figure 2.5. An ORTEP diagram of the molecular structure of compound $Ru_6C(CO)_{14}(\mu_3{-}\eta^4{-}C_4H_4)$, **2.6** showing the 20% thermal ellipsoidal probability. Selected interatomic distances (Å) for the major disorder component are as follows: Ru1a-C1a = 2.108(8), Ru1a-C4a = 2.048(8), Ru2a-C1a = 2.106(8), Ru2a-C2a = 2.301(8), Ru3a-C3a = 2.253(7), Ru3a-C4a = 2.161(7), C1a-C2a = 1.418(11), C2a-C3a = 1.442(11), C3a-C4a = 1.421(11).

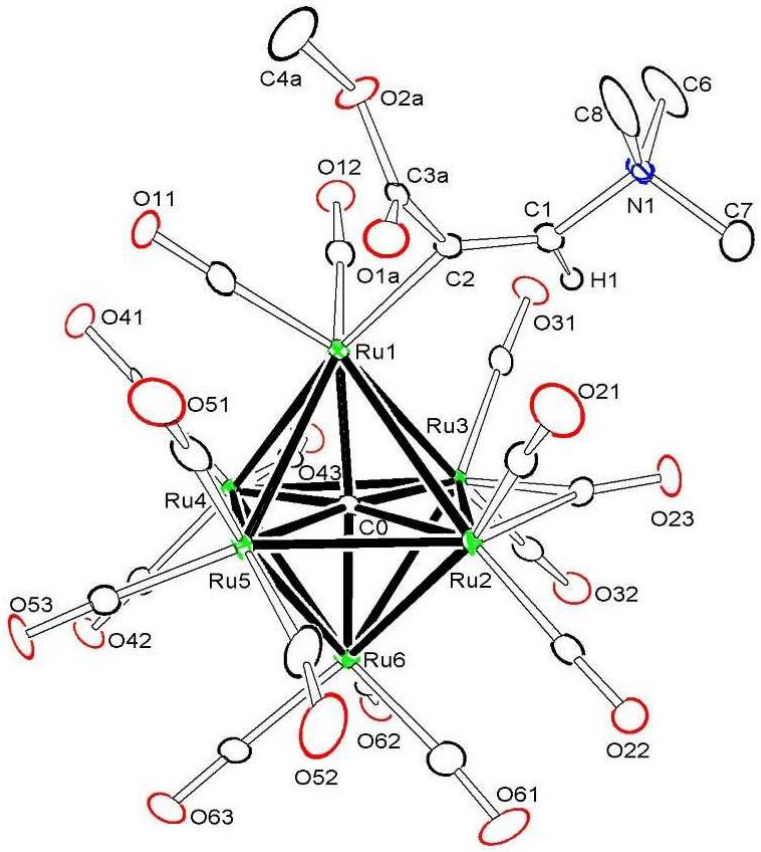

Figure 2.6. An ORTEP diagram of the molecular structure of the compound $Ru_6C(CO)_{16}[\eta^1$-*E*-$C(CO_2Me)=C(H)NMe_3]$, **2.7** showing the 30% thermal ellipsoidal probability. Selected interatomic distances (Å) are as follows: Ru1-C2 = 2.120(5), C1-C2 = 1.304(7), N1-C1 = 1.477(7), N1-C6 = 1.450(7), N1-C8 = 1.459(7), N1-C7 = 1.462(7), C2-C3a = 1.522(9), C3a-O1a = 1.182(10), C3a-O2a = 1.325(9), C4a-O2a = 1.440(9).

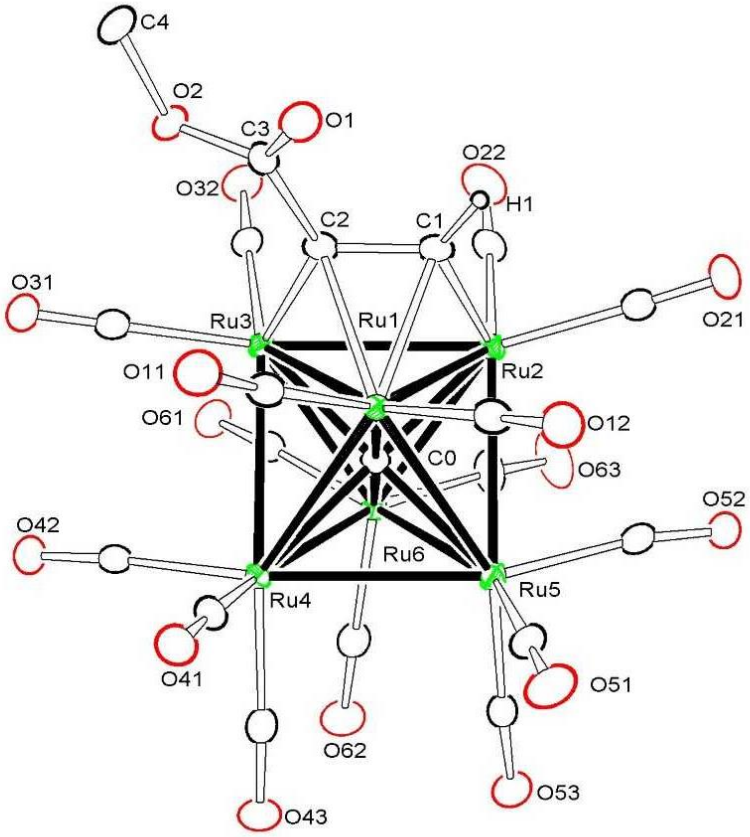

Figure 2.7. An ORTEP diagram of the molecular structure of the compound $Ru_6C(CO)_{15}[\mu_3–HC_2(CO_2CH_3)]$, **2.8** showing the 30% thermal ellipsoidal probability. Selected interatomic distances (Å) are as follows: Ru1-C1 = 2.186(3), Ru1-C2 = 2.184(3), Ru2-C1 = 2.034(3), Ru3-C2 = 2.049(3), C1-C2 = 1.392(5), C2-C3 = 1.504(5), C3-O1 = 1.206(4), C3-O2 = 1.331(4), C4-O2 = 1.446(4).

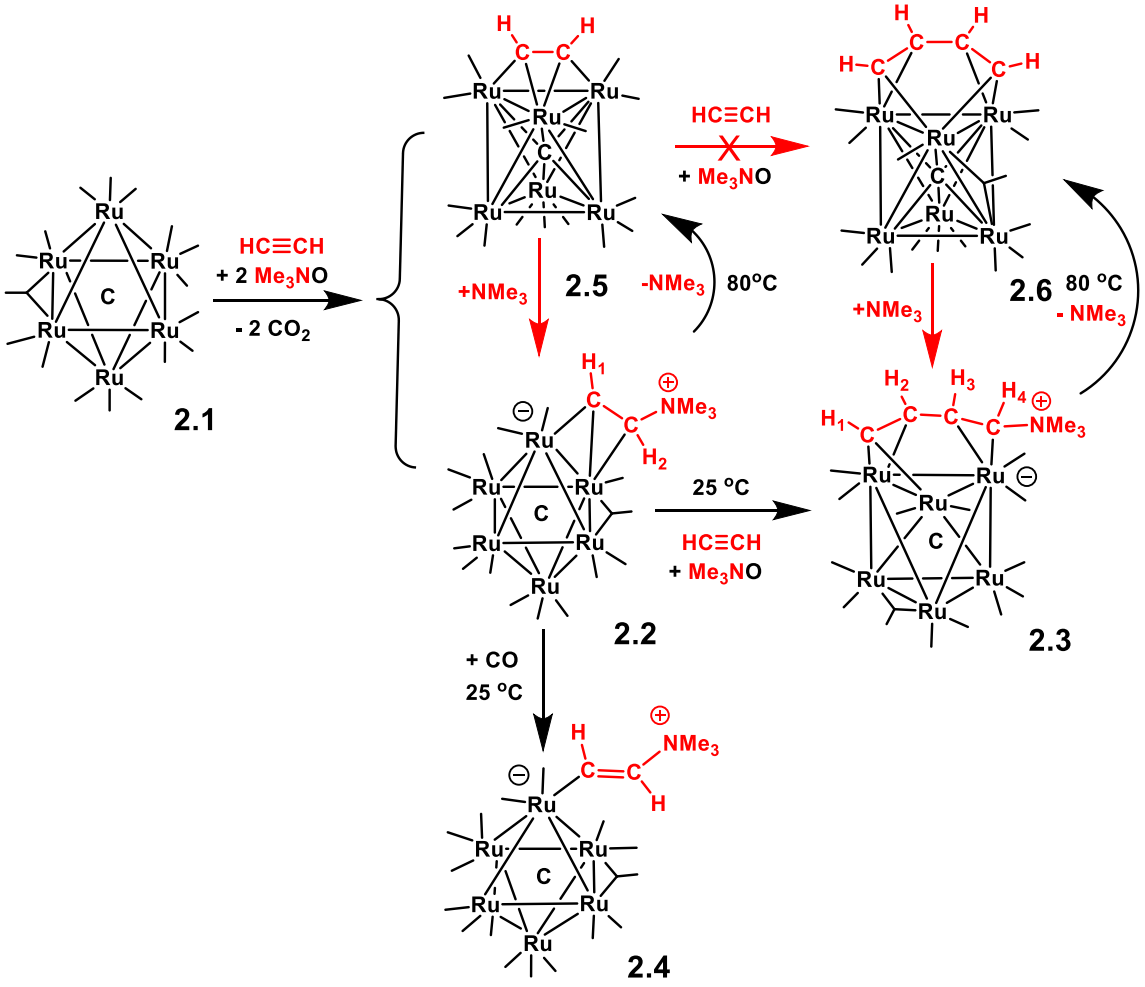
HC≡CH
+ 2 Me3NO
- 2 CO2
2.1
2.5
+NMe3
-NMe3
80°C
HC≡CH
+ Me3NO
2.6
80 °C
- NMe3
+NMe3
2.2
25 °C
HC≡CH
+ Me3NO
2.3
+ CO
25 °C
2.4

Scheme 2.1

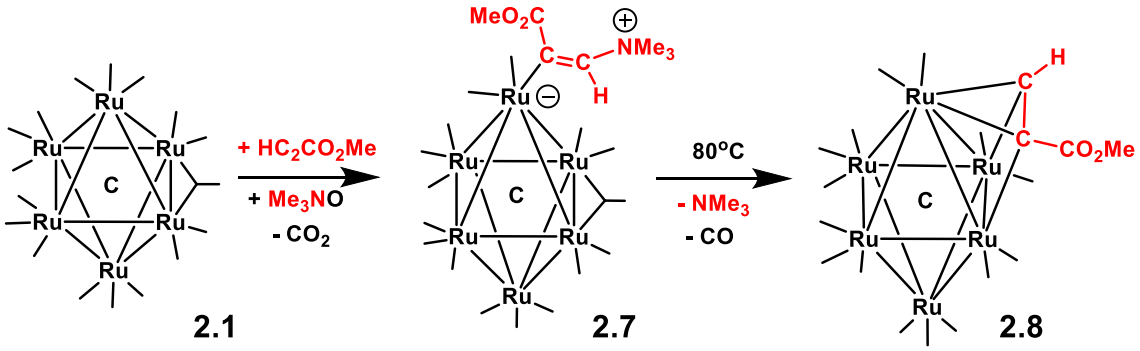

Scheme 2.2

2.5 References

1) (a) Wittig, G; Schollkope, U., Über Triphenyl-phosphin-methylene als olefinbildende Reagenzien I., *Chem. Ber.-Rec.* **1954**, *87*, 1318 - 1330. (b) Wittig, G; Haag, Über Triphenyl-phosphinmethylene als olefinbildende Reagenzien II., *Chem. Ber.-Rec* **1955**, *88*, 1654 - 1666.

2) IUPAC. Compendium of Chemical Terminology, 2nd ed. (the "Gold Book"). Compiled by A. D. McNaught and A. Wilkinson. Blackwell Scientific Publications, Oxford (**1997**); Online version (**2019-**) created by S. J. Chalk. ISBN 0-9678550-9-8. https://doi.org/10.1351/goldbook.

3) (a) Maryanoff, B. E.; Reitz, A. B., The Wittig Olefination Reaction and Modifications Involving Phosphoryl-Stabilized Carbanions. Stereochemistry, Mechanism, and Selected Synthetic Aspects, *Chem. Rev*. **1989**, *89*, 863 - 927. (b) Johnson, A. W.; Kaska, W. C.; Starzewski, K. A. O.; Dixon, D. *Ylides and Imines of Phosphorus*; Wiley: New York, **1993**.

4) (a) Trost, B. M.; Melvin, L. S., "Sulfur Ylides. Emerging Synthetic Intermediates", Academic Press, New York, **1975**. (b) Neuhaus, J. D.; Oost, R.; Merad, J.; Maulide, N. Sulfur-Based Ylides in Transition-Metal-Catalysed Processes. *Top. Curr. Chem*. **2018**, *376*, 15. (c) Lu, L.-Q.; Li, T.-R.; Wang, Q.; Xiao, W.-J. Beyond Sulfide-Centric Catalysis: Recent Advances in the Catalytic Cyclization Reactions of Sulfur Ylides. *Chem. Soc. Rev*. **2017**, *46*, 4135−4149. (d) Zhang, Y.; Wang, J. Catalytic [2,3]-Sigmatropic Rearrangement of Sulfur Ylide Derived from Metal Carbene, *Coord.* I. A. Sulfoxonium and Sulfonium Ylides as Diazocarbonyl Equivalents in Metal-Catalyzed Insertion Reactions, *Eur. J. Org. Chem*. **2013**, 5005−5016. (f) Li, A.-H.; Dai, L.-X.; Aggarwal, V. K. Asymmetric Ylide Reactions: Epoxidation, Cyclopropanation, Aziridination, Olefination, and Rearrangement, *Chem. Rev*. **1997**, *97*, 2341−2372.

5) Selected examples include: (a) Pattacini, R., Jiez, S. Braunstein, P., Facile dichloromethane activation and phosphine methylation. Isolation of unprecedented zwitterionic organozinc and organocobalt Intermediates. *Chem. Commun*. **2009**, 890 – 892. (b) Engelter, C.; Moss, J.R.; Niven, M.L.; Nassimbeni, L.R.; Reid, G., A cationic ylide complex of platinum (II): its structure and formation from a chloromethyl-platinum complex. *J. Organomet. Chem*. **1982**, *232*, C78 – C80. (c) *Kermode*, N, J,; *Lappert*, M.F.; *Skelton*, B. W.; *White*, A. H.; *Holton*, J., Synthesis of ylideplatinum(II) complexes via α-functionalised alkylplatinum(II) intermediates and some comparative data on palladium(II) complexes; X-ray structure of trans-[Pt(CH_2PEt_3)I(PEt_3)$_2$]I. *J. Organomet. Chem*. **1982**, *228*, C71 - C75. (d) Azam, K.A.; Frew, A.A.; Lloyd, B.R.; Manojlovic-Muir, L.; Muir, K.W.; Puddephatt, R.J., (μ-Methylene) diplatinum complexes: their syntheses, structures, and properties. *Organometallics* **1985**, *4*, 1400 – 1406. (e) Churchill, M. R.; Wasserman, H. J., Crystal and molecular structure of [W(CH_2PMe_3)$(CO)_2$Cl(PMe_3)$_3$][CF_3SO_3], a seven-coordinate tungsten(II) complex produced by transfer of a trimethylphosphine to the W:CH_2 system. *Inorg. Chem.* **1982**, *21*, 3913-3916. (f)

Toupet, L. Weinberger, B.; Abbayes, H. D.; Gross, U., Structure du Complexe Tetracarbonyle(methylenetriphenylphosphorane-C)fer(II), $[Fe(C_{19}H_{17}P)(CO)_4]$. *Acta Crystallogr. Sect.C: Cryst.Struct.Commun*. **1984**, *40*, 2056 – 2058. (g) *Moss*, J. R.; *Niven*, M. L.; *Stretch*, P. M., Haloalkyl complexes of the transition metals. Part 5. The synthesis and reactions of some new pentamethylcyclopentadienyl halomethyl and methoxymethyl complexes of molybdenum (II) and tungsten (II) and the X-ray crystal structure of the cationic ylide complex $[\eta\text{-}C_5Me_5W(CO)_3CH_2PPh_3]I$. *Inorg. Chim. Acta*, **1986**, *119*, 177 – 186. h) Porter, L. C.; Knachel H.; Fackler, Jr., J. P., A Mononuelear Gold(l) Complex Containing a Covalently Bound Ylide Ligand. The Structure of Chloro[methyl(methylene)diphenylphosphoranyI-C]gold(I). *Acta Cryst.* **1987,** *C43*, 1833-1835. i) Uson, R.; Laguna, A.; Uson, A.; Jones, P. G.; Meyer-Base, K., Synthesis of Pentafluorophenyl(ylide)silver(l) Complexes: X-Ray Structures of two Modifications of $[Ag(C_6F_5)(CH_2PPh_3)]$, *J. Chem. Soc., Dalton Trans*. **1988**, 341 – 345. j) Uson, R.; Laguna, A.; Laguna, Gimeno, M. C.; de Pablo, A.; Jones, P. G.; Meyer-Base, K., Erdbrugger, C. F., Synthesis and reactivity of neutral complexes of the types $[AuX_3(ylide)]$ and trans-$[Au(C_6F_5)X_2(ylide)]$ (X = halide or pseudohalide). X-ray structure of $[Au(SCN)_3(CH_2PPh_3)]$. *J. Organomet. Chem*., **1987**, *336*, 461 – 468. k) Hoover J. F.; Stryker, J. M., Synthesis of Platinum Bis(phosphonium ylide) Complexes from -Halomethyl Precursors, *Organometallics* **1988**, *7*, 2082 – 2084. l) Cerrada, E.; Concepcion Gimeno, M. Laguna, A.; Laguna, M.; Orera, V.; Jones, P. G.**,** Charge-transfer salts with mononuclear and dinuclear ylide gold(I) complexes: x-ray structure of [Au(CH2PPh 3) 2](TCNQ) (TCNQ = 7,7',8,8'-tetracyanoquinodimethane). *J. Organomet. Chem*., **1996**, *506*, 203 – 210.

6) Selected examples include: (a) O'Connor, E. J.; Helquist, P., Stable precursors of transition-metal carbene complexes. Simplified preparation and crystal structure of (η^5-cyclopentadienyl)[(dimethylsulfonium)methyl]dicarbonyliron(II) fluorosulfonate. *J. Am. Chem. Soc.* **1982**, *104*, 1869 - 1874. (b) Hevia, E., Perez, J., Riera, V.; Miguel, D., Manganese(I) and Rhenium(I) Tricarbonyl(Alkylthio)methyl and Alkylidenesulfonium Complexes. *Organometallics* **2002**, *21*, 5312 - 5319. (c) Leoni, P.; Marchetti, F.; Paoletti, M., Synthesis of Palladium Sulfonium Ylides and the Structures of *trans*-$[PdCl(CH_2SR_2)(PBu^t_2H)_2]X$ ($X=CF_3SO_3$, SR_2) Tetrahydrothiophene; X= PF_6, R = Et). *Organometallics* **1997**, *16*, 2146 - 2151. (d) Kilbourn, B. T., Felix, D., The Crystal Structure of Methylidineopentylsulphonium Tri-iododineopentylsulphonium-methylzincate, $(C_5H_{11})_2SMe]^+[(C_5H_{11})_2SCH_2ZnI_3]^-$. *J. Chem. Soc. A*, **1969, 163 - 168. (e)** Fackler, Jr., J. P., Paparizos, C., Trimethylgold(III) Complexes of Reactive Sulfoxonium and Sulfoniium Ylides. *J. Am. Chem. Soc*. **1977**, *99*, 2363 - 2364. (f) Vicente, J., Chicote, M.-T., Abrisqueta, M.D., Alvarez-Falcon, M.M.; de Arellano, M.C.R., Jones, P.G., New Carbenegold(I) Complexes Synthesized by the "Acac Method". *Organometallics* **2003**, *22*, 4327 – 4333.

7) (a) Lappas, D.; Hoffman, D. M.; Folting, K.; Huffman, J. C., Synthesis and Structure of a Resonance Stabilized (Trimethylphosphonio)metallapropenide, *Angew. Chem., Int. Ed. Engl*. **1988**, *27*, 587 – 589. (b) Hoffman, D. M.; Huffman, J. C.; Lappas, D.; Wierda, D. A. Alkyne Reactions with Rhenium(V) Oxo Alkyl

Phosphine Complexes—Phosphine Displacement versus Apparent Re-P Insertion. *Organometallics* **1993**, *12*, 4312 – 4320. (c) Chin, C. S.; Lee, S.; Oh, M.; Won, G.; Kim, M.; Park, Y. J., *cis*-Bis(alkenyl)iridium(III) Compounds by Apparent Insertion of Two Acetylenes into Two Ir-P Bonds: Crystal Structures of *cis,trans*-$[IrCl(-CH=CH^{+}PPh_3)_2(CO)(PPh_3)_2]^{2+}$ and $[Ir(OClO_3)(CH_3)(H_2O)(CO)(PPh_3)_2]^{+}$. *Organometallics* **2000,** *19*, 1572 - 1577. (d) Chin, C. S.; Park, Y.; Kim, J.; Byeongno Lee, B., Facile Insertion of Alkynes into Ir-P (Phosphine) and Ir-As (Arsine) Bonds: Second and Third Alkyne Addition to Mononuclear Iridium Complexes. *J. Chem. Soc., Chem. Commun*. **1995**, 1495 – 1496. (e) Takats, J.; Washington, J.; Santarsiero, B. D., Condensation of $Os(CO)_4(\eta^2\text{-HCCH})$ with $CpRh(CO)(PR_3)$. Unexpected Phosphine Dependence in the Formation of Dimetallacycles: Reverse Regiochemistry and a Zwitterionic Compound. *Organometallics* **1994**, *13*, 1078 - 1080. (f) Yang, K.; Bott, S. G. Richmond, M. G., Regioselective phosphine attack on the coordinated alkyne in $Co_2(\mu\text{-alkyne})$ complexes Reactivity studies and X-ray diffraction structures of $Co_2(CO)_4(bma)(\mu\text{-}HC{\equiv}C^{t}Bu)$ and the zwitterionic hydrocarbyl complexes $Co_2(CO)_4[(\mu\text{-}\eta^2{:}\eta^2{:}\eta^1{:}\eta^1\text{:-}RC{=}C(R')PPh_2C{=}C(PPh_2)C(O)C(O)]$. *J. Organomet. Chem.* **1996**, *516*, 65 – 80. (g) Bott, S. G.; Shen, H.; Senter, R. A.; Richmond, M. G., Acetylide Participation in Ligand Substitution and P-C Bond Cleavage in the Reaction between and 4,5-Bis(diphenylphosphino)-4-cyclopenten-1,3-dione (bpcd). Syntheses and X-ray Structures of $HRu_3(CO)_7[[(\mu_3\text{-}\eta^2{:}\eta^2{:}\eta^1{:}\eta^1{:}\eta^1\text{-}Ph_2PC{=}CC(O)CH_2C(O)PPh_2C{=}CPh]$ and $Ru_3(CO)_7((\mu\text{-}\eta^2{:}\eta^1\text{:-}PhC{=}CHPh)[(\mu\text{-}\eta^2{:}\eta^1\text{:-}PPhC{=}CC(O)CH_2C(O)PPh_2]$. *Organometallics* **2003,** *22*, 1953 - 1959.

8) (a) Boland-Lussier, B. F.; Churchill, M. R.; Hughes, R. P.; Rheingold, A. L., Synthesis and characterization of cationic iron vinylidene compounds: formation of carbon-hydrogen, carbon-nitrogen and carbon-phosphorus bonds and the x-ray crystal structure of $[Fe(\eta\text{-}C_5H_5)(CO)(PPh_3)\{C(PPh_3){=}CH_2\}]^{+}BF_4^{-}$, *Organometallics* **1982**, *1*, 628 – 634. (b) Hogarth, G.; Knox, S. A. R., Lloyd, B. R.; Macpherson, K. A.; Morton, D. A. V.; Orpen, A. G., Structural Observation of Bis(diphenyphosphino)methane Reactivity at a Di-iron Centre: Crystal Structures of Isomeric $[Fe_2(CO)_5(\mu\text{-}CHCHCO)\{\mu\text{-}P(Ph_2)CH_2PPh_2\}]$, $[Fe_2(CO)_6(\mu\text{-}C(CH_2)P(Ph_2)CH_2PPh_2\}]$ and $[Fe_2(CO)_2\{\mu\text{-}C(CH_2Ph)P(Ph_2)CH_2PPh\}]$, *J. Chem. Soc., Chem. Commun*. **1988**, 360 – 362. (c) Bamber, M.; Froom, S. F. T.; Green, M.; Schulz, M., Werner, H. Nucleophilic attack by isocyanides, phosphines and cyclohexenesulphide on the α-carbon of "side-on" bonded $\mu\text{–}\sigma\text{:}\eta^2\text{-(4e)-}$ vinylidenes; formation of thioketene and thioaldehyde dimolybdenum complexes. *J. Organomet. Chem.*, **1992**, *434*, C19-C25.

9) Henrick K.; McPartlin, M.; Deeming, A. J.; Hasso, S.; Manning, P., Addition of dimethylphenylphosphine to μ- and μ_3-alkynyl and μ_3-allenyl ligands in triosmium clusters: X-ray crystal structures of three zwitterionic adducts, *J. Chem Soc., Chem. Commum.* 1**982**, 899 – 906.

10) Chin, C. S.; Lee, H.; Oh, M., Reactions of Iridium (III) Compounds with Alkynes in the Presence of Triethylamine: The First Example of $M\text{-}CH{=}CH\text{-}^{+}NR_3$. *Organometallics* **1997**, *16*, 816 – 818.

11) Adams, R. D.; Tedder, J. D., Formation of N,N-Dimethylacrylamide by a Multicenter Hydrocarbamoylation of C_2H_2 with N,N-Dimethylformamide Activated by $Ru_5(\mu_5\text{-}C)(CO)_{15}$, *Inorg. Chem.* **2018**, *57*, 5707 – 5710.

12) (a) Adams, R. D.; Smith, M. D.; Tedder, J. D.; Wakdikar, N. Selective Activation of CH Bonds in Polar Vinyl Olefins and Coupling of Ethylene to the Activated Carbon Atoms in Pentaruthenium Complexes. *Inorg. Chem.* **2019**, *58*, 8357−8368. (b) Adams, R. D.; Prince, C.; Smith, M. D.; Tedder, J. D.; Wakdikar, N. C - C Coupling of CH Activated Polar Vinyl Monomers by a Pentaruthenium Cluster Complex. *J. Organomet. Chem.* **2019**, *901*, 120938.

13) Adams, R. D.; Akter, H.; Tedder, J. D. CH Activations in Aldehydes in Reactions with $Ru_5(\mu_5\text{-}C)(CO)_{15}$. *J. Organomet. Chem*. **2018**, *871*, 159−166.

14) Adams, R. D.; Tedder, J. D.; Wong, Y. O. Phenyl - Gold Complexes of Ru6 and Ru5 Carbonyl Clusters. *J. Organomet. Chem.* **2015**, *795*, 2−10.

15) (a) Orpen, A. G.; Pippard, D.; Sheldrick, G. M.; Rouse, K. D. Decacarbonyl-μ-hydrido-μ-vinyl-triangulo-triosmium: A Combined X-ray and Neutron Diffraction Study. *Acta Cryst.* **1978**, *B34*, 2466-2472. (b) Adams, R. D.; Wong, Y. O. New rhenium carbonyl cluster complexes containing bridging hydrocarbyl and bridging mercury groups. *J. Organomet. Chem*. **2015**, *784*, 109−113. (c) Adams, R. D.; Dhull, P.; Kaushal, M.; Smith, M. D., The Activation and Transformations of Vinyl Acetate at a Dirhenium Carbonyl Center. *J. Organomet. Chem.* **2019**, *902*, 120969.

16) Mingos, D. M. P.; May, A. S., in *The Chemistry of Metal Cluster Complexes*. Shriver, D. F.; Kaesz, H. D.; Adams, R. D., VCH Publishers, New York, **1990**, Ch. 2.

17) Drake, S. R.; Johnson, B. F. G.; Lewis, J.; Conole, G.; McPartlin, M., Synthesis of a series of hexanuclear ruthenium carbido cluster alkynes under mild conditions: X-ray structure analyses of the complexes $[Ru_6C(CO)_{15}(\mu_3\text{-}\eta^2\text{-}PhCCH)]$ and $[Ru_6C(CO)_{15}(\mu_3\text{-}\eta^2\text{-}PhCCMe)]$. *J. Chem. Soc., Dalton Trans.*, **1990**, 995 - 1000.

18) Blake, A. J.; Haggitt, J. L.; Johnson, B. F. G.; Parsons, S., Alkyne-based derivatives of $[Ru_6C(CO)_{17}]$ and the stepwise synthesis of $[Ru_6C(CO)_{13}(\eta^5\text{-}C_5H_5Ph_2)(\mu_3\text{-}CPh)]$. *J. Chem. Soc., Dalton Trans.*, **1997**, 991–994.

19) Chin, C. S.; Cho, H.; Won, G.; Oh, M.; Ok, K. M., Reaction of an (Alkyl)(alkenyl)(alkynyl)iridium(III) Complex with HCl: Intramolecular C-C Bond Formation from Alkyl, Alkenyl, and Alkynyl Groups Coordinated to "$Ir(CO)(PPh_3)_2$". H/D Exchange between CH_3 and DCl, *Organometallics* **1999**, *18*, 4810 - 4816.

20) Johnson, B. F. G.; Lewis, J.; Sankey, S. W.; Wong, K.; McPartlin, M.; Nelson, W. J. H., An Improved Synthesis of the hexaruthenium carbido Cluster $Ru_6(C)(CO)_{17}$. X-

ray structure of the Salt $[Ph_4As]_2[Ru_6(C)(CO)_{16}]$, *J. Organomet. Chem*., **1980**, *191*, C3-C7.

21) *APEX3*, Version 2018.1-0 and *SAINT+*, Version 8.38A. Bruker *AXS*, Inc., Madison, Wisconsin, USA, **2016**.

22) Sheldrick, G. M. SHELXT – Integrated space-group and crystal-structure determination. *Acta Crystallogr*., *Sect. A.: Found. Adv.* **2015**, *A71*, 3-8.

23) Dolomanov, O. V., Bourhis, L. J., Gildea, R. J., Howard J. A. K.; Puschmann, H. OLEX2: a complete structure solution, refinement and analysis program. *J. Appl. Cryst.* **2009**, *42*, 339 - 341.

CHAPTER 3

ALKYNE CYCLIZATION IN METAL CLUSTER COMPLEXES. THE ADDITION AND COUPLING OF DIMETHYL ACETYLENE DICARBOXYLATE TO THE DIENYL LIGAND IN $Ru_6(\mu_6\text{-}C)(CO)_{14}(\mu_3\text{-}\eta^4\text{-}C_4H_4)$[2]

[2]Adams, R. D.; Smith, M. D.; Wakdikar, N. D.; *Manuscript in preparation,* **2021**

3.1 Introduction

Compounds containing 6-membered aromatic rings have attracted the attention of chemists since their discovery.[1] They are widespread in nature and range from fragrances to solvents, octane boosters in fuels and most importantly to a wide range of pharmaceuticals. Aromatic compounds can be synthesized by a variety of methods.[2,3,4] Notably, the [2+2+2] cyclization of alkynes by using transition metal catalysts is known to yield a variety of aromatic compounds in all of their isomeric forms.[4] The metal-catalyzed coupling of alkynes occurs in a series of steps. To begin two alkynes are added to a metal complex and are then oxidatively coupled to form a metallacycle. If only one metal atom is involved a metallacyclopentadienyl group, such as **A** Scheme 3.1, is typically formed.[5] If two or more metal atoms are involved, then diendiyl ligands can form that form bridges across the metal atoms by using the π–bonds to coordinate to the carbon atoms, e. g. **B**[4a-b,e,6] or **C**,[7] see Scheme 3.1.

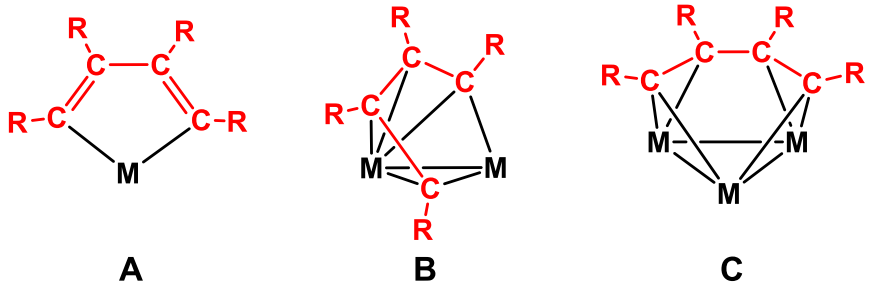

Scheme 3.1

Mechanisms for the addition of a third alkyne to form aromatic rings from diendiyl ligands in the species **A** and **B** are still being investigated. The two most widely discussed mechanisms are shown, in part, in Scheme 3.2 below. One involves insertion of a third alkyne into a metal – carbon bond of the diendiyl ligand, e. g. **A**, to yield a metallacycloheptatriene intermediate such as **D** that subsequently cyclizes by a C – C

reductive-elimination to yield an arene ligand in a complex **F** and ultimately a free arene.[8] An alternative mechanism involves a 4 +2 cycloaddition to yield coordinated carbocyclic C_6 rings, such as **E**, that leads to an arene ligand and ultimately a free arene, Scheme 3.2. Support for the latter mechanism has been increasing in recent years.[8a-b,9]

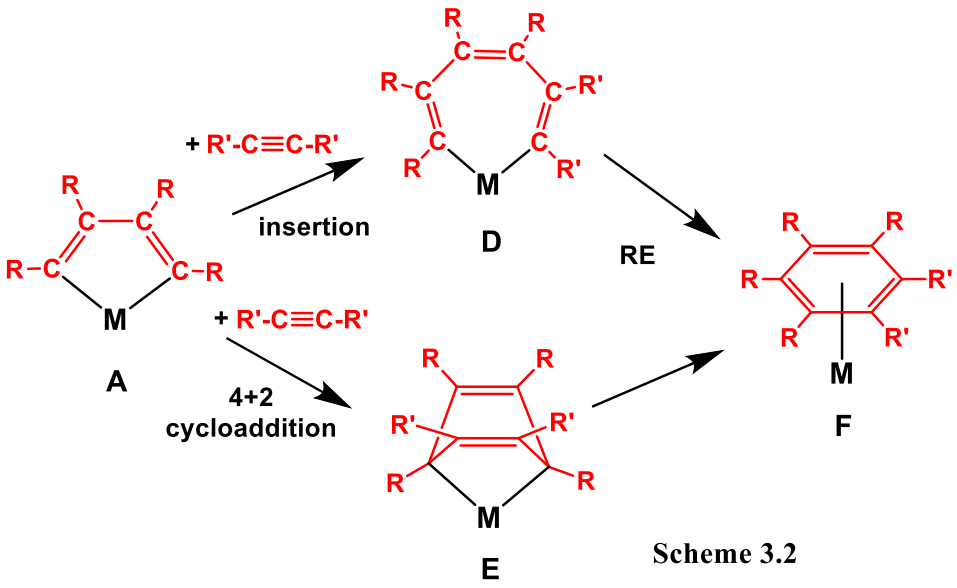

Scheme 3.2

In recent studies, we have synthesized the hexaruthenium carbonyl complex $Ru_6(\mu_6\text{-}C)(CO)_{14}(\mu_3{-}\eta^4\text{-}C_4H_4)$, **3.2** that contains the triply-bridging η^4 -butadiendiyl ligand **C**, R = H by elimination of NMe_3 from the $\mu_3\text{-}\eta^4\text{-}CHCHCHCH^+NMe_3$ ligand in the zwitterionic hexaruthenium complex $Ru_6(\mu_6\text{-}C)(CO)_{14}[\mu_3\text{-}\eta^4\text{-}C_4H_4(NMe_3)]$, **3.1**, eq. (3.1).[7a]

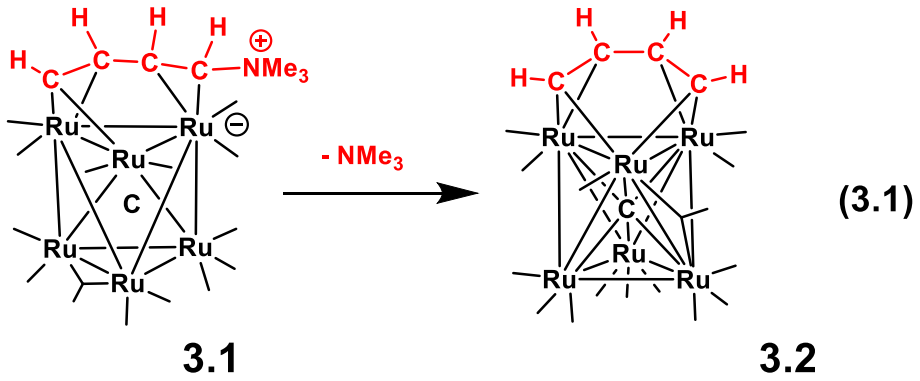

(3.1)

We have now investigated the reactions of **3.2** with the electron deficient acetylene dimethyl acetylenedicarboxylate, $(MeO_2C)C{\equiv}C(CO_2Me)$, **DMAD**. The synthesis, structures and the chemistry of these new complexes which includes complexes containing the coordinated 1,2-$C_6H_4(CO_2Me)_2$ arene ring are reported herein.

3.2 Experimental Section

General Data

All reactions were performed under an atmosphere of nitrogen. Reagent grade solvents were dried by the standard procedures and were freshly distilled prior to use. Infrared spectra were recorded on a Thermo Scientific Nicolet IS10. ^{1}H NMR spectra were recorded on a Varian Mercury 300 spectrometer operating at 300.1 MHz. Mass spectrometric (MS) measurements were performed by a direct-exposure probe by using electron impact (EI) ionization or positive ion electrospray (ES+). $Ru_6(\mu_6\text{-}C)(CO)_{14}(\mu_3{-}\eta^4{-}C_4H_4)$, **3.2** was prepared according to a previously reported procedure.[7a] Dimethyl acetylenedicarboxylate (DMAD) and Trimethylamine-N-oxide (Me_3NO) were purchased from Sigma-Aldrich and were used without further purification. Product separations were performed by TLC in the open air on Analtech 0.25 mm and 0.50 mm silica gel 60 Å F254 or alumina on glass plates.

Reaction of $Ru_6(\mu_6\text{-}C)(CO)_{14}(\mu_3{-}\eta^4\text{-}C_4H_4)$, 3.2 with DMAD.

18 mg (0.017 mmol) of **3.2** was dissolved in 2.5 mL of dichloromethane-d_2 in an NMR tube. 6.0 µL of dimethyl acetylene dicarboxylate (DMAD) was added and the NMR tube was then sealed. The reaction mixture was kept at 25^{o}C for 3 days. After this period, resonances for the products were observed by ^{1}H NMR spectroscopy. Workup of the reaction mixture by TLC by using a hexane/methylene chloride solvent mixture

yielded the following products in the order of elution: 1.2 mg (6.4% yield) of $Ru_6(\mu_6\text{-}C)(CO)_{16}(\mu\text{–}\eta^4\text{–}C_4H_4)$, **3.3**, 1.0 mg (4.7% yield) of $Ru_6(\mu_6\text{-}C)(CO)_{14}[\eta^6\text{-}C_6H_4(CO_2Me)_2]$, **3.4**, 1.0 mg (4.8% yield) of $Ru_6(\mu_6\text{-}C)(CO)_{14}(\mu\text{–}\eta^4\text{–}C_4H_4)[\mu_3\text{–}C_2(CO_2Me)_2]$, **3.5**, 4.0 mg of (19.5% yield) of $Ru_6(\mu_6\text{-}C)(CO)_{14}(\mu\text{–}\eta^4\text{–}C_4H_4)[\mu_3\text{–}C_2(CO_2Me)_2]$, **3.6** and 8.0 mg (39% yield) of $Ru_6(\mu_6\text{-}C)(CO)_{14}[\mu_3\text{–}\eta^6\text{-}C_6H_4(CO_2Me)_2]$, **3.7**. Spectral data for **3.3**: IR, ν_{CO} (cm^{-1} in CH_2Cl_2): 2104.6 (w), 2081.4 (vs), 2049.5 (s), 2033.3 (vs), 2010.9 (m), 1968.0 (vw). ^1H NMR (in CD_2Cl_2, δ in ppm): 5.81 (m, br, C**H),** 5.65 (m, br, C**H**). Mass Spectrum (ES^+): M^+ = 1119.5. Spectral data for **3.4**: IR, ν_{CO} (cm^{-1} in CH_2Cl_2): 2080.2 (s), 2029.7 (vs), 1988.8 (m), 1828.5 (w, br). ^1H NMR (in CD_2Cl_2, δ in ppm): 6.03 (dd, C**H,** $^3J_{H3\text{-}H4}$ = 6.2 Hz), 5.69 (dd, C**H,** $^3J_{H3\text{-}H5}$ = 1.2 Hz), 3.83 (s, OC**H**$_3$). Mass Spectrum (ES^+): M^+ -CO = 1176.0. Spectral data for **3.5**: IR, ν_{CO} (cm^{-1} in CH_2Cl_2): 2094.4 (m), 2058.1 (vs), 2042.4 (s), 2032.5 (s), 1993.9 (w), 1927.4 (vw,br). ^1H NMR at 25 °C (δ in CD_2Cl_2) δ = 6.20 (m, 2H, C**H)** and 3.95 (s, (OC**H**$_3$)$_2$); at -90 °C (in CD_2Cl_2, δ): 7.32 (m, 1H, C**H)**, 6.14 (m, 2H, C**H)**, 3.94 (s, 3H, O(C**H**$_3$)), 3.87 (s, 3H, O(C**H**$_3$)) and 2.80 (m, 1H, C**H)**. Mass Spectrum (ES^+): $M^+ + Na^+$ = 1228.0, M^+ -CO = 1174.0, M^+ -2CO = 1146.0. Spectral data for **3.6**: IR, ν_{CO} (cm^{-1} in CH_2Cl_2): 2094.0 (m), 2062.1 (vs), 2053.8 (vs, sh), 2038.8 (s), 2032.9 (s, sh), 2014.4 (w), 1978.2 (vw), 1938.0 (vw,br), 1892.3 (vw, br). ^1H NMR (in CD_2Cl_2, δ in ppm, 25 °C: 7.53 (br, 2H, C**H)**, 6.94 (m, 2H, C**H)**, 3.94 (s, 6H, OC**H**$_3$); at -90C): 8.58 (m, 1H, C**H)**, 7.14 (m, 1H, C**H)**, 6.85 (m, 1H, C**H)**, 6.39 (m, 1H, C**H)**, 3.95 (s, OC**H**$_3$), 3.78 (s, OC**H**$_3$). Mass Spectrum (ES^+): M^+ = 1205.0. Spectral data for **3.7**: IR, ν_{CO} (cm^{-1} in CH_2Cl_2): 2085.3 (m), 2048.3 (s), 2034.1 (vs), 1981.3 (w), 1816.6 (vw,br). ^1H NMR (in CD_2Cl_2, δ in ppm): 4.63 (dd, C**H,** $^3J_{H3\text{-}H4}$ = 6.2 Hz), 4.41 (dd, C**H,** $^3J_{H3\text{-}H5}$ = 1.2 Hz), 3.76 (s, O(C**H**$_3$)). Mass Spectrum (ES^+): M^+ -CO = 1177.0.

Reaction of 3.2 with CO

A 4.0 mg (0.0037 mmol) amount of **3.2** was dissolved in 2.5 mL of dichloromethane-d_2 in an NMR tube. CO gas was allowed to purge through this solution for 2 min and the NMR tube was then closed. The solution was then allowed to stand at room temperature for 24 h. After this period, resonance for compound **3.3** was observed by ^{1}H NMR spectroscopy. Workup of the reaction mixture by TLC by using a hexane/methylene chloride solvent mixture yielded 3.0 mg (72% conversion) of compound $Ru_6(\mu_6\text{-}C)(CO)_{16}(\mu\text{–}\eta^4\text{–}C_4H_4)$, **3.3**.

Synthesis of 3.8 by Reaction of 3.3 with DMAD.

A 5.0 mg (0.0045 mmol) amount of **3.3** was dissolved in 2.5 mL of toluene-d_8 in an NMR tube. To this, 3.0 μL of dimethyl acetylenedicarboxylate (**DMAD**) was added and the NMR tube was then closed. The reaction mixture was heated to 85 ^{o}C in a mineral oil bath for 48 h. After this period, resonances for compound **3.8** was observed by ^{1}H NMR spectroscopy. Workup of the reaction mixture by TLC by using a hexane/methylene chloride solvent mixture yielded 2.0 mg (36% yield) of compound $Ru_6C(CO)_{15}(\mu\text{–}\eta^4\text{–}C_4H_4)[\mu\text{–}C_2(CO_2Me)_2]$, **3.8**. Spectral data for **3.8**: IR, ν_{CO} (cm^{-1} in CH_2Cl_2): 2103.8 (vw), 2084.5 (vs), 2058.1 (s), 2043.1 (m), 2026.2 (w), 2010.0 (w,sh), 1982.1 (vw), 1947.8 (vw), 1914.0 (vw). ^{1}H NMR (in CD_2Cl_2, δ in ppm): 5.95 (dd, 2H, C**H,** $^3J_{H1\text{-}H2}$ = 5.8 Hz), 5.60 (dd, 2H, C**H,** $^3J_{H1\text{-}H3}$ = 2.7 Hz), 3.82 (s, 6H, OC**H**$_3$).

Thermal Transformation of 3.7.

A 3.0 mg (0.0025 mmol) amount of **3.7** was dissolved in 2.5 mL of dichloromethane-d_2 in an NMR tube. This reaction mixture in this tube was then heated to 50 ^{o}C in a constant temperature mineral oil bath for 5 days. After this period, the

resonances for compounds **3.4** and **3.5** were observed by ^{1}H NMR spectroscopy. Workup of the reaction mixture by TLC by using a hexane/methylene chloride solvent mixture yielded 1.5 mg (~50% conversion) of compound $Ru_6(\mu_6\text{-}C)(CO)_{14}(\eta^6\text{-}C_6H_4[CO_2Me]_2)$, **3.4** and 0.3 mg of unreacted **3.7**.

Reaction of 3.4 with CO

A 1.0 mg amount of **3.4** was dissolved in 2.5 mL of dichloromethane-d_2 in an NMR tube. CO gas was allowed to purge through this solution for 2 min and the NMR tube was then closed. The solution was then allowed to stand at room temperature for 24 h. After this period, new resonances attributed to $C_6H_4(CO_2Me)_2$, **3.11** were observed by ^{1}H NMR spectroscopy. Workup of the reaction mixture by TLC by using a hexane/methylene chloride solvent mixture yielded 0.4 mg of $Ru_6(\mu_6\text{-}C)(CO)_{17}$ and 0.1 mg of colorless band of **3.11** (62% yield) was obtained. Spectral Analysis of **3.11:** ^{1}H NMR (in CD_2Cl_2, δ in ppm): 7.71 (m, C**H**), 7.56(m, C**H**), 3.87 (s, O(C**H**$_3$)$_3$). Mass Spectrum (EI$^+$): 194.0, M^+; 163.0, M^+ -OCH_3; 135.0, M^+ -CO_2CH_3; 104.0, M^+ -CO_2CH_3 + OCH_3.

Thermal transformation of 3.5 to 3.9.

A 2.0 mg amount of **3.5** was dissolved in 2.5 mL of dichloromethane-d_2 in a high-pressure NMR tube. The tube was sealed, and the solution was heated at 65 ^{O}C for 4 days. The reaction was followed by NMR spectroscopy. Workup of the reaction was performed by TLC using hexane/methylene chloride mixture yielded 0.5 mg of $Ru_6C(CO)_{14}[\mu_4\text{–}\eta^6\text{–}CHCHCHCC(CO_2Me)C(CO_2Me)](\mu\text{-}H)$, **3.9**, 25% yield. Spectral Analysis of **3.9**: IR, ν_{CO} (cm^{-1} in hexane): 2095.2(w), 2078.6(vs), 2055.7(s), 2046.7(s), 2032.1(w), 2020.3(m). ^{1}H NMR (in CD_2Cl_2, δ in ppm): 6.69 (m, C**H,** $^3J_{H\text{-}H}$ = 6.0 Hz, $^4J_{H\text{-}}$

$_H$ = 3.0 Hz), 5.94 (dd, C**H,** $^3J_{H-H}$ = 3.0 Hz, $^3J_{H-H}$ = 3.0 Hz), 5.71 (m, C**H,** $^3J_{H-H}$ = 6.3Hz, $^4J_{H-H}$ = 3.0 Hz**),** 3.95 (s, O(C**H**$_3$)$_3$), 3.87 (s, O(C**H**$_3$)$_3$), -21.9 (s, H). Mass Spectrum (ES$^+$): M^+ = 1205.0

Reaction of 3.7 with CO.

A 2.0 mg amount of **3.7** was dissolved in 2.5 mL of dichloromethane-d_2 in an NMR tube. CO gas was allowed to purge through this solution for 2 min and the NMR tube was then closed. The solution was then allowed to stand at room temperature for 24 h. After this period, the resonances of the product **3.11** were observed by ^{1}H NMR spectroscopy. Workup of the reaction mixture by TLC by using a hexane/methylene chloride solvent mixture yielded 0.7 mg of $Ru_6(\mu_6\text{-}C)(CO)_{17}$ and 0.2 mg of a colorless band of **3.11** (62% yield).

Reaction of 3.3 with Me_3NO

A 9.0 mg (0.0084mmol) amount of **3.3** was dissolved in 2.5 mL of toluene-d_8 in an NMR tube. To this solution 1.5 mg of Me_3NO was added and the mixture was then heated at 50 ^{o}C for 3 d. The reaction was monitored by ^{1}H NMR spectroscopy. Workup of the reaction mixture by TLC by using a hexane/methylene chloride solvent mixture yielded 1.0 mg (10.5% yield) of $Ru_6C(CO)_{15}(\mu\text{–}\eta^4\text{–}C_4H_4)(NMe_3)$, **3.10** and 1.0 mg of unreacted **3.3.** Spectral Analysis of **3.10**: IR, ν_{CO} (cm^{-1} in hexane): 2081.8(m), 2045.5(s), 2031.3(vs), 2009.3(w), 2001.4(w), 1982.1(vw), 1967.9(vw). ^{1}H NMR (in CD_2Cl_2, δ in ppm): 5.71 (dd, C**H,** $^3J_{H-H}$ = 3.9 Hz), 5.23 (dd, C**H,** $^3J_{H-H}$ = 3.9 Hz), 2.73 (s, N(C**H**$_3$)$_3$). Mass Spectrum (ESI$^+$): M^+ = 1150.0.

Isomerization of 3.6 to 3.5.

A 1.0 mg amount of **3.6** was dissolved in 2.5 mL of dichloromethane-d_2 in an NMR tube. The solution was heated at 50C for 48 h. The reaction was monitored by ^{1}H NMR spectroscopy. Workup of the reaction mixture by TLC using a hexane/methylene chloride solvent mixture yielded 0.5 mg (50% yield) of **3.5**.

Crystallographic Analyses.

Single crystals of compounds **3.3** – **3.10** suitable for X-ray diffraction analyses were obtained by slow evaporation of solvent from solutions of the pure compounds at room temperature. X-ray intensity data were measured by using a Bruker D8 QUEST diffractometer equipped with a PHOTON-100 CMOS area detector and an Incoatec microfocus source (Mo K_α radiation, $\lambda = 0.71073$ Å).[10] The raw area detector data frames were reduced, scaled, and corrected for absorption effects using the SAINT[10] and SADABS[11] programs. All structures were solved with SHELXT.[12] Subsequent difference Fourier calculations and full-matrix least-squares refinement against F^2 were performed by using SHELXL-2018[12] or by using OLEX2.[13] Full details for these analyses are available in the Supporting Information. Crystal data, data collection parameters, and results for each analysis are summarized in Table 3.1.

Results and Discussion

Reaction of the butadiendiyl hexaruthenium cluster complex **3.2** with dimethyl acetylenedicarboxylate (DMAD) at 25 ^{o}C for 3d yielded five new compounds, two of which contain a six-membered arene ring as a ligand. These compounds have been identified as $Ru_6(\mu_6\text{-}C)(CO)_{16}(\mu\text{–}\eta^4\text{–}C_4H_4)$, **3.3**, (6.4% yield); $Ru_6(\mu_6\text{-}C)(CO)_{14}[\eta^6\text{-}1,2\text{-}C_6H_4(CO_2Me)_2]$, **3.4** (4.7% yield); $Ru_6(\mu_6\text{-}C)(CO)_{14}(\mu\text{–}\eta^4\text{–}C_4H_4)[\mu_3\text{–}C_2(CO_2Me)_2]$, **3.5**,

(4.8% yield); $Ru_6(\mu_6\text{-}C)(CO)_{14}(\mu\text{–}\eta^4\text{–}C_4H_4)[\mu_3\text{–}C_2(CO_2Me)_2]$, **3.6** (19.5% yield) and $Ru_6(\mu_6\text{-}C)(CO)_{14}[\mu_3\text{–}\eta^6\text{–}1,2\text{–}C_6H_4(CO_2Me)_2]$, **3.7** (39% yield). All of the new compounds were characterized by IR, ^{1}H NMR, single-crystal X-ray diffraction analysis and mass spectrometry.

An ORTEP diagram of molecular structure of **3.3** is shown in Figure 3.1. Compound **3.3** contains a cluster of six ruthenium metal atoms that may be described as 'spiked' square pyramid. One of the ruthenium carbonyl groups, Ru(6), has been dislodged from the octahedral Ru_6 cluster of found in **3.2**, but it remains attached to the apical ruthenium atom Ru(1) of the pentaruthenium carbide carbonyl cluster core by a Ru – Ru single bond. The Ru1-Ru6 distance, 2.74975(19) Å, is a little short due to the presence of the bridging η^4-C_4H_4 butadiendiyl ligand, see below. The Ru – Ru distances in the square-pyramidal Ru_5 portion of the cluster, 2.80862(19) - 2.96963(19) Å, are similar to those in the related square-pyramidal Ru_5 cluster complexes, $Ru_5C(CO)_{15}$ and $Ru_5C(CO)_{14}PPh_3$.[16] Compound **3.3** contains a total of sixteen carbonyl ligands distributed as shown in Figure 3.1. There is a bridging CO ligand across the Ru4 – Ru5 bond and semi-bridging CO ligands across the Ru1 – Ru2 and Ru1 – Ru3 metal – metal bonds in **3.3**. There is also a η^4-C_4H_4 butadiendiyl ligand that bridges Ru1-Ru6 bond to the spiked-ruthenium atom Ru6 of the cluster. All four carbon atoms are π-bonded to Ru(6), Ru6-C1 = 2.3026(15) Å, Ru6-C2 = 2.1971(16) Å, Ru6-C3 = 2.2053(16) Å and Ru6-C4 = 2.3006(16) Å. The terminal carbon atoms C1 and C4 are σ-bonded to the apical ruthenium atom of the square pyramid, Ru(1), Ru1-C1 = 2.0897(16) Å and Ru1-C4 = 2.0978(16) Å. The C – C bond distances within the butadiendiyl ligand are equal, C1−C2 = 1.422(2) Å, C2−C3 = 1.430(2) Å and C3−C4 = 1.422(2) Å within experimental error,

indicating the C – C bonding is fully delocalized across these four carbon atoms. ^{1}H NMR spectrum of **3.3** shows two broad deshielded resonances that can be assigned to the CH protons of the C_4H_4 ligand, δ = 5.81 (br, CH), 5.65 (br, CH).

The bridging η^4–C_4H_4 ligand in **3.3** serves formally as a six-electron donor and with a total of sixteen CO ligands, compound **3.3** obtains a total of 90 cluster valence electrons which is in accord with both the effective atomic number rule and the polyhedral skeletal electron pair (PSEP) counting method for an apex-spiked square pyramidal cluster core of six transition metal atoms.[15] Compound **3.3** contains two more CO ligands than its precursor complex **3.2**, and as expected, when compound **3.2** was exposed to an atmosphere of CO at room temperature for 24 h, compound **3.3** was formed in a good yield (72%) by the addition of two equivalents CO.

Compounds **3.4** and **3.7** are similar in that they both contain a coordinated 1,2-$C_6H_4(CO_2Me)_2$ arene ring as a ligand. ORTEP diagrams of the molecular structures of **3.4** and **3.7** are shown in Figures 3.2 and 3.3, respectively. Both compounds contain an octahedral cluster of six ruthenium atom with a carbide ligand in the center like the parent **3.2**. In **3.7**, the 1,2-$C_6H_4(CO_2Me)_2$ ligand is coordinated in a triply-bridging, η^6-fashion to one of the triangular faces of the Ru_6 cluster. In **3.4** the 1,2-$C_6H_4(CO_2Me)_2$ ligand is coordinated in a terminal η^6-fashion to only one of the ruthenium atoms of the cluster.

Interestingly, when a solution of **3.7** was heated at 50 ^{o}C for 5 days, it was converted to compound **3.4** in 50% yield. The reverse transformation does not occur which suggests that compound **3.7** is an intermediate and precursor to compound **3.4** in the series of reactions. The transformation of triply-bridging arene ligands to terminally-

coordinated arene ligands in ruthenium cluster complexes has been observed previously.[17] In both complexes the $C_6H_4(CO_2Me)_2$ ligand serves as a six-electron donor to the cluster. Each cluster contains fourteen carbonyl ligands and both complexes contain a total of 86 cluster valence electrons and are in accord with the PSEP electron counting method.[15]

An ORTEP diagram of molecular structure of **3.5** is shown in Figure 3.4. The metal cluster compound **3.5** is best described as an open square-pyramid, i.e. one of the apical-basal metal-metal bonds, Ru1···Ru4 = 3.3627(2) Å, is missing. One of the edge bonds of the Ru_5 cluster, Ru1 –Ru5, is bridged by another ruthenium atom Ru6, Ru1-Ru6 = 2.8643(2) Å and Ru5-Ru6 = 3.0992(2) Å. There is a bridging η^4–C_4H_4 ligand across the Ru1-Ru6 bond. As in **3.3**, it is π–bonded to Ru6, Ru6-C1 = 2.229(2) Å, Ru6-C2 = 2.239(2) Å, Ru6-C3 = 2.251(2) Å, Ru6-C4 = 2.273(2) Å and σ-bonded to Ru1, Ru1-C1 = 2.086(2) Å, Ru1-C4 = 2.106(2) Å. The C – C bond distances, C1-C2 = 1.395(3) Å and C3-C4 = 1.397(3) Å, are shorter than the C2-C3 bond, 1.434(3) Å, and may have more double character than the C2-C3 bond. There is a triply-bridging **DMAD** ligand across the three ruthenium atoms, Ru4, Ru5 and Ru6, with Ru6-C8 = 2.099(2) Å, Ru5-C7 = 2.191(2) Å, Ru5-C8 = 2.216(2) Å, Ru4-C7 = 2.072(2) Å, but there is no metal – metal bond between Ru4 and Ru6, Ru4···Ru6 = 3.750(1) Å.

The ^{1}H NMR spectrum of **3.5** varies with temperature that is indicative of dynamical exchange activity, see Figure 3.5. At 25 ^{o}C, the ^{1}H NMR spectrum exhibits only two resonances: one at δ = 6.20 (m, 2H) for two of the four C_4H_4 protons and a singlet at δ = 3.95 (s, 6H) for the two OMe groups of the **DMAD** ligand. At -90 ^{o}C, the H NMR spectrum of **3.5** exhibits five resonances at δ = 7.32 (m, 1H, CH**)**, 6.14 (m, 2H,

CH**)**, 3.94 (s, 3H, OCH_3), 3.87 (s, 3H, OCH_3) and 2.80 (m, 1H, CH**)**. The OCH_3 resonances broaden as the temperature is raised and coalesce at -15 ^oC. The multiplets at 7.32 and 2.80 broaden equally and reversibly, and collapse into the baseline at 25 ^oC, but because of the large shift difference between them, the averaged resonance was not observed even temperatures moderately above 25 ^oC. It is apparent from these spectral changes that **3.5** is engaging in dynamical exchange processes involving both the inequivalent methoxyl groups on the DMAD ligand and the inequivalent CH protons of the C_4H_4 ligand, although averaging of one pair of the CH protons, presumably the protons on the inner CH groups, C2 and C3, was still not slowed to resolution even at -90 ^oC presumably due to a much smaller shift difference between them.

We have been able to explain these averaging dynamics by the exchange process shown in Scheme 3.3. It is proposed that **3.5** is reversibly exchanged with its enantiomer **3.5*** via an intermediate such as **3.I**. In the process the methoxy groups of the DMAD ligand are exchanged and the alkenyl hydrogen atoms on C1 and C4, and C2 and C3 are exchanged in pairs, but those on C1 and C4 are not exchanged with those on C2 and C3. In the process the Ru5 – Ru6 bond in **3.5** is cleaved and a new Ru – Ru bond is formed to Ru4, which is Ru5 in the enantiomer **3.5***. Note: both enantiomers are present in the solid-state structure of the complex. The proposed intermediate **I** exhibits a mirror like symmetry along the Ru1 – Ru6 bond.

With fourteen carbonyl ligands, a μ–η^4–C_4H_4 ligand and one triply-bridging, DMAD ligand, compound **3.5** contains a total of 90 cluster valence electrons for the six metal atoms which is in accord with both the effective atomic number rule and the PSEP theory for an edge-bridged, open, square-pyramidal cluster.[15]

There are two structurally similar independent molecules of **3.6** in the asymmetric crystal unit. An ORTEP diagram of molecular structure of one of these two molecules is shown in Figure 3.6. Compound **3.6** is an isomer of **3.5**, and there are structural similarities. For example, both compounds contain a bridging η^4–C_4H_4 ligand, a triply-bridging **DMAD** ligand and fourteen carbonyl ligands. However, the Ru_6 metal cluster of **3.6** has a slightly but significantly different structure from that of **3.5**. The metal cluster in **3.6** could be described as a capped, square-pyramid, except that one of the apex – basal metal - metal bonds, namely Ru1 – Ru5 is missing, Ru1A···Ru5A = 3.604(4) Å, so the Ru_5 portion of the cluster has an open, square pyramidal shape.

Unlike **3.5**, Ru6 in **3.6** is bonded to three other metal atoms instead of two, e. g. Ru1A-Ru6A = 2.8523(14) Å, Ru4A-Ru6A = 3.0388(14) Å, Ru5A-Ru6A = 2.8396(14) Å. In addition, although the η^4–C_4H_4 ligand in **3.6** bridges the metal – metal bond, Ru1 – Ru6, as that in **3.5**, but in **3.6** it is π–bonded to Ru1 instead of Ru6, Ru1A-C1A = 2.216(11) Å, Ru1A-C2A = 2.237(12) Å, Ru1A-C3A = 2.261(12) Å, Ru1A- C4A = 2.377(12) Å and di-σ-bonded to Ru6, Ru6A-C1A = 2.041(12) Å, Ru6A-C4A = 2.095(12) Å. The C – C bond distances in the C_4H_4 ligand in **3.6** are equivalent within experimental error, C1A-C2A = 1.415(17) Å, C2A-C3A = 1.411(19) Å and C3A-C4A = 1.431(17) Å. The **DMAD** ligand in **3.6** is a triply-bridging ligand across the closed triangular Ru_3 group, Ru4, Ru5 and Ru6.

The ^{1}H NMR spectra of **3.6** indicate that like **3.5**, it is also dynamically active in solution, see Figure 3.**7.** At -90 ^{o}C, the ^{1}H NMR of **3.6** in CD_2Cl_2 exhibits six resonances: four for the four inequivalent CH protons of the C_4H_4 ligand at 8.58 (br, 1H**)**, 7.14 (br, 1H**)**, 6.85 (br, 1H), 6.39 (br, 1H**)** and two for the two inequivalent methyl groups of the

DMAD ligand at 3.95 (s, 3H), 3.78 (s, 3H). This spectrum is consistent with the structure observed in the solid state. As the temperature is raised, all of the resonances begin to broaden and average in pairs: 7.14 with 6.85, coalescence at ~ -65 ^{o}C; 8.58 with 6.39, coalescence at -35 ^{o}C; and OCH_3 3.95 with 3.78, coalescence at ~ -65 ^{o}C. At 25 ^{o}C the spectrum shows only three resonances for the averaged protons at 7.53 (br, 2H, C**H)**, 6.94 (m, 2H, C**H)** and 3.94 (s, 6H, OC$\mathbf{H}_3$). The resonance averaging can be explained by the metal shifting, dynamical exchange process shown in Scheme 3.4. In this simple process, the Ru1-Ru4 bond in **3.6** is reversibly cleaved and reformed between the atoms Ru1 and Ru5 to yield the enantiomer **3.6*** of **3.6**. The CH groups C1 and C4 and C2 and C3 exchange in pairs as well as the methoxy groups C7 and C8 on the DMAD ligands as observed experimentally.

When a sample **3.3** was placed in an NMR tube with DMAD in toluene-d_8 and heated to 85 ^{o}C for 48 h, it lost one equivalent of CO and added one equivalent of DMAD and was converted to the new compound $Ru_6C(CO)_{15}(\mu–\eta^4–C_4H_4)[\mu–C_2(CO_2Me)_2]$, **3.8** in 36% yield. Compound **3.8** was characterized structurally by a single-crystal X-ray diffraction analysis and an ORTEP diagram of its molecular structure is shown in Figure 3.8. Compound **3.8** contains a spiked, square pyramidal cluster of six ruthenium atoms similar to that observed in **3.3**. The Ru – Ru bonding in **3.8** is also very similar to that in **3.3**. As in **3.3**, the Ru1 – Ru6 bond to the "spike" is the shortest metal – metal bond in the cluster, Ru1-Ru6 = 2.7436(3) Å. The C_4H_4 ligand bridges the Ru1 – Ru6 bond as in **3.3**. The C – C bonds within the C_4H_4 ligand are similar to those in **3.3**, C1-C2 = 1.426(4) Å, C2-C3 = 1.426(4) Å, C3-C4 = 1.410(4) Å. There is a DMAD ligand bridging a basal edge of the square pyramidal cluster at the Ru4 – Ru5 bond in a di-σ coordination

fashion. It has replaced the bridging CO ligand in **3.3** and as a result the Ru4 –Ru5 bond increased in length by approx. 0.05 Å, Ru4-Ru5 = 2.8080(3) Å.

The ^{1}H NMR spectrum for **3.8** shows three resonances: two for the two inequivalent pairs of C_4H_4 protons δ = 5.95 (dd, 2H, $^{3}J_{H1\text{-}H2}$ = 5.8 Hz, $^{3}J_{H1\text{-}H3}$ = 2.7 Hz) and 5.60 (dd, 2H, $^{3}J_{H1\text{-}H2}$ = 5.8 Hz, $^{3}J_{H1\text{-}H3}$ = 2.7 Hz) and one for the equivalent methoxy group on the DMAD ligand, δ = 3.82 (s, 6H, OC**H**$_3$). Compound **3.8** contains a total of 90 cluster valence electrons as found in **3.3** which is consistent with the EAN and PSEP electron counting rules.

When a solution of compound **3.5** was heated to 65 ^{o}C for 4 days, it was converted to the new compound $Ru_6C(CO)_{14}[\mu_4\text{–}\eta^6\text{–}CHCHCHCC(CO_2Me)C(CO_2Me)](\mu\text{-}H)$, **3.9**, 25% yield. Compound **3.9** was characterized by IR, ^{1}H NMR, single-crystal X-ray diffraction analysis and mass spectrometry. The crystal of **3.9** contains two independent molecules in the asymmetric unit. Both molecules are structurally similar. An ORTEP diagram of the molecular structure of molecule A of **3.9** is shown in Figure 3.9. The cluster contains six ruthenium atoms in the arrangement of a spiked, square pyramid similar to those found in compounds **3.3** and **3.8**. As in **3.3** and **3.8**, the C_4-bridged Ru1 – Ru6 bond to the spike Ru6 is one of the shortest Ru – Ru bonds in the molecule, Ru1a-Ru6a = 2.7517(6) Å. The most interesting ligand in the complex is a $\mu_4\text{-}\eta^6$-1,2-$(MeO_2C)_2$CCHCHCH ligand that bridges the Ru1-Ru2-Ru3 triangular face of the Ru_5 square pyramid and extends to the metal spike Ru6. The 1,2-$(MeO_2C)_2$CCHCHCH ligand was formed by a C – C coupling of one of the carbon atoms of the DMAD ligand of **3.5** and one of the terminal CH groups of the C_4H_4 ligand of **3.5**. A C – C bond was formed C4a and C5a, C4a-C5a =

1.454(5) Å, followed by a cleavage of the CH bond on atom C4a. Atom C4a became a bridge across the metal atoms Ru1a and Ru2a, Ru1a-C4a = 2.142(3) Å and Ru2a-C4a = 2.309(3) Å, and the hydrogen atom became a bridging ligand across the Ru1a and Ru3a bond in the cluster and it was located and refined in the structural analysis. Its resonance is shown in the ^{1}H NMR spectrum at δ = -21.9 as expected. The three CH protons on the C_6 chain exhibit resonances at δ = 6.69 (m, $^3J_{H-H}$ = 6.0 Hz, $^4J_{H-H}$ = 3.0 Hz), 5.94 (dd, $^3J_{H-H}$ = 3.0 Hz, $^3J_{H-H}$ = 3.0 Hz) and 5.71 (m, $^3J_{H-H}$ = 6.3Hz, $^4J_{H-H}$ = 3.0 Hz) as expected and the methoxyl methyl groups appear as singlets at δ = 3.95 and 3.87. The bridging 1,2-$(MeO_2C)_2CCHCHCH$ ligand serves as a 9-electron donor, the hydride as a one electron donor and with fourteen CO ligands, complex **3.9** achieves a total of 90 cluster valence electrons which is consistent with the observed spiked, square-pyramidal Ru_6 structure according to both the EAN rule and the PSEP theories of electron counting.[15]

When compound **3.3** was allowed to react with Me_3NO in a toluene-d_8 solution at 50 ^{o}C for 3 d it was converted to the new compound $Ru_6C(CO)_{15}(\mu–\eta^4–C_4H_4)(NMe_3)$, **3.10** in 10.5% yield. Compound **3.10** is a simple NMe_3 derivative of **3.3** formed by a Me_3NO induced decarbonylation of **3.3** and the addition of the resultant NMe_3 to one of the metal atoms of the Ru_6 cluster. Compound **3.10** was characterized by a single-crystal, X-ray diffraction analysis and An ORTEP diagram of the molecular structure of **3.10** is shown in Figure 3.10. As expected, the metal cluster of **3.10** also contains a spiked, square-pyramidal Ru_6 structure similar to **3.3** and **3.8**. It contains a bridging $\eta^4–C_4H_4$ ligand across the Ru5 – Ru6 bond to the Ru6 spike. As expected, the bond distance Ru5-Ru6 = 2.7422(3) Å, is contracted due to the presence of the bridging C_4H_4 ligand. The NMe_3 ligand is located on the Ru6 spike *trans* to the Ru5 – Ru6 bond, Ru6-N =

2.2241(19) Å. The ^{1}H NMR spectrum of **3.10** exhibits two resonances for the two pairs of CH protons on the C_4H_4 ligand at δ = 5.71 (dd, $^{3}J_{H-H}$ = 3.9 Hz, $^{3}J_{H-H}$ = 3.9 Hz), 5.23 (dd, $^{3}J_{H-H}$ = 3.9 Hz, $^{3}J_{H-H}$ = 3.9 Hz) and one resonance δ = 2.73 for the methyl groups on NMe_3 ligand.

Discussion

Studies have shown that alkyne ligands undergo C-C bond coupling at mono- and dinuclear metal centers.[5,6,18] A number of metallacycles have been structurally characterized that have been formed by C – C coupling of two, three and four alkyne molecules at dinuclear metal centers.[18] Arenes are a common product in many of these reactions. A variety of mechanisms have been proposed for their formation.[9]

In this work, we have investigated the reactions of the Ru_6 cluster complex **3.2** with disubstituted alkyne DMAD and a triply-bridging C_4H_4 ligand in the complex **3.2**. A summary of these reactions is shown in Scheme 3.5. Two isomeric complexes, **3.4** and **3.7**, were each found to contain an octahedral-shaped cluster of six ruthenium atoms with a π-coordinated 1,2-$C_6H_4(CO_2Me)_2$ arene ring as a ligand that was formed by a coupling of the DMAD to the bridging C_4H_4 ligand. The mechanism of the formation of this arene ligand has not been determined yet. The triply-bridging 1,2-$C_6H_4(CO_2Me)_2$ ligand in **3.7** was converted to a terminal, π-coordinated 1,2-$C_6H_4(CO_2Me)_2$ ligand in **3.4** simply by heating at 50 ^{o}C. When treated with CO, the 1,2-$C_6H_4(CO_2Me)_2$ ligand in **3.4** and **3.7** was released to yield the free arene 1,2-$C_6H_4(CO_2Me)_2$, **3.11** with formation of the parent carbonyl cluster complex $Ru_6(\mu_6\text{-}C)(CO)_{17}$.[19]

Two competing products, **3.5** and **3.6**, were also formed in the reaction of **3.2** with DMAD. In these products, the DMAD is coordinated to metal atoms of the cluster as a

bridging ligand. The increase in bonding electrons at the cluster caused by the addition of the DMAD, results in the cleavage of metal – metal bonds with transformation of the cluster into edge-bridged, open-square-pyramidal species. Interestingly, when heated to 50 ^{o}C, compound **3.6** was converted to **3.5** by shifting the π–bonding of the bridging C_4H_4 ligand from the apex-metal atom Ru6 of the open square-pyramid to the edge-bridged metal atom of the square pyramid of **3.5**.

A minor coproduct **3.3** was obtained in the reaction of **3.2** with DMAD. It formed by the addition of two equivalents of CO only to **3.2**. The CO was presumably scavenged from the reaction solution mixture. The increase in the number of CO ligands in the formation of **3.3** caused the Ru_6 cluster to open to yield the first example of a spiked, squared-pyramidal cluster of six ruthenium atoms. Compound **3.2** was found to react with CO (at 1 atm) directly at 25 ^{o}C to yield **3.3** in a good yield. In an effort to obtain **3.5** or **3.6** from **3.3**, a sample of **3.3** was treated directly with DMAD. Instead, the new compound **3.8** was formed by adding one equivalent of DMAD accompanied by the loss of one CO ligand. Compound **3.8** contains a DMAD bridging along a basal edge of the square-pyramid of the spiked, squared-pyramidal cluster of metal atoms. Efforts to obtain **3.5** or **3.6** from **3.8** by heating were unsuccessful.

When heated to 65 ^{o}C, compound **3.5** was converted to yet another isomer, **3.9**, by formation of a carbon – carbon bond between the DMAD ligand and one of the terminal CH groups of the π-coordinated C_4H_4 ligand. In this process the CH bond of that CH group was cleaved and the hydrogen atom was converted to a bridging hydrido ligand on one of the Ru – Ru bonds of the metal cluster.

Finally, an effort was made to condense the metal cluster of **3.3** by decarbonylation by using Me_3NO. While decarbonylation did occur, cluster condensation did not. Instead, a molecule of NMe_3, obtained by the reaction of the Me_3NO with the CO ligand, was added to the metal atom spike, presumably the site of decarbonylation, to yield the compound **3.10**, a NMe_3 derivative of **3.3**.

Conclusions

Reactions of the first octahedral metal cluster complex containing a triply-bridging C_4H_4 ligand formed by the coupling of two molecules of C_2H_2 with a third alkyne (DMAD) have been investigated. Coupling of the DMAD to the C_4H_4 ligand to yield the arene **3.11** ligand was observed. Competing reactions involving additions of the DMAD molecule to the metal atoms produced cluster opening products. Two of the open cluster complexes, **3.5** and **3.6**, exhibit dynamical activities on the ^1H NMR timescale at 25 ^oC that are attributed to flexibility in the open metal clusters at this temperature.

Table 3.1. Crystal Data for the X-Ray Structural Analyses for Compounds **3.3 –3.6**.

Compound	**3.3**	**3.4**	**3.5**	**3.6**
Empirical formula	$C_{21}H_4O_{16}Ru_6$	$C_{25}H_{10}O_{18}Ru_6$	$C_{25}H_{10}O_{18}Ru_6$	$C_{25}H_{10}O_{18}Ru_6$
Formula weight	1118.66	1204.75	1204.75	1204.75
Crystal system	monoclinic	monoclinic	monoclinic	triclinic
Lattice parameters				
a (Å)	9.3269(3)	15.5552(8)	8.9118(3)	9.8368(7)
b (Å)	13.5819(5)	15.4822(8)	18.4294(6)	18.0052(13)
c (Å)	22.3396(8)	26.4000(17)	19.5202(7)	18.4116(13)
α (deg)	90.00	90.00	90.00	90.990(2)
β (deg)	98.315(2)	90.3845(19)	99.6110(10)	93.448(2)
γ (deg)	90.00	90.00	90.00	95.812(2)
V (Å^3)	2800.17(17)	6357.7(6)	3160.98(19)	3237.4(4)
Space group	$P2_1/c$	I2/a	$P2_1/c$	P-1
Z value	4	8	4	4
ρ_{calc} (g/cm^3)	2.654	2.517	2.532	2.472
μ (Mo Kα) (mm^{-1})	3.229	2.859	2.875	2.807
Temperature (K)	100(2)	301(2)	100(2)	300(2)
$2\theta_{max}$ (°)	65.31	55.198	60.078	50.22
No. Obs. (I>2σ(I))	10246	7328	9250	11480
No. of parameters	405	444	461	888
Goodness of fit (GOF)	1.080	1.017	1.119	1.105
Max. shift/error on final cycle	0.005	0.002	0.001	0.001
Residuals 2 σ(I)*: R1; wR2	0.0193;0.0312	0.0323;0.0636	0.0192; 0.0384	0.0590; 0.1218
Absorption Corr, Max/min	Multi-scan 0.3605/ 0.2593	Multi-scan 0.7456/0.6642	Multi-scan 0.7460/0.6478	multi-scan 0.1770/ 0.1224
Largest peak in Final Diff. Map (e$^-$ / Å^3)	0.84	1.09	0.51	0.975

[a] $R1 = \Sigma_{hkl}(||F_{obs}|-|F_{calc}||)/\Sigma_{hkl}|F_{obs}|$; $wR2 = [\Sigma_{hkl}w(|F_{obs}|-|F_{calc}|)^2/\Sigma_{hkl}wF^2_{obs}]^{1/2}$; $w = 1/\sigma^2(F_{obs})$; $GOF = [\Sigma_{hkl}w(|F_{obs}|-|F_{calc}|)^2/(n_{data} - n_{vari})]^{1/2}$

Table 3.2. Crystal Data for the X-Ray Structural Analyses for Compounds **3.7 – 3.10**.

Compound	**3.7**	**3.8**	**3.9**	**3.10**
Empirical formula	$C_{25}H_{10}O_{18}Ru_6$	$C_{26}H_{10}O_{19}Ru_6$	$C_{27}H_{14.5}O_{18}Ru_6$	$C_{32}H_{22}NO_{15}Ru_6$
Formula weight	1204.75	1232.76	1233.31	1266.92
Crystal system	monoclinic	monoclinic	triclinic	triclinic
Lattice parameters				
a (Å)	14.7789(8)	15.3963(4)	12.020(2)	9.3716(3)
b (Å)	11.5156(7)	13.6012(4)	15.548(3)	14.9002(5)
c (Å)	18.4821(11)	16.9225(5)	19.912(4)	15.6455(5)
α (deg)	90.00	90.00	78.488(7)	107.8088(12)
β (deg)	98.3780(10)	111.385(2)	79.644(7)	102.7263(13)
γ (deg)	90.00	90.00	86.467(7)	102.6617(13)
V (Å^3)	3111.9(3)	2509.1(2)	3585.9(12)	1929.92(11)
Space group	$P2_1/c$	$P2_1/c$	P -1	P-1
Z value	4	4	4	2
ρ_{calc} (g/cm^3)	2.571	2.481	2.284	2.180
μ (Mo Kα) (mm^{-1})	2.920	2.759	2.537	2.355
Temperature (K)	100(2)	100(2)	300(2)	100(2)
$2\theta_{max}$ (°)	56.676	56.69	60.386	61.148
No. Obs. (I>2σ(I))	7757	8228	20958	11824
No. of parameters	457	478	921	586
Goodness of fit (GOF)	1.047	1.035	1.137	1.075
Max. shift/error on final cycle	0.001	0.001	0.002	0.002
Residuals 2σ(I)*: R1; wR2	0.0231; 0.0410	0.0230; 0.0431	0.0321; 0.0644	0.0249;0.0400
Absorption Corr, Max/min	multi-scan 0.3343/0.2810	multi-scan 0.6944/0.6059	multi-scan 0.2650/0.1971	multi-scan 0.5645/0.4605
Largest peak in Final Diff. Map (e$^-$ / Å^3)	0.65	0.77	0.854	0.548

[a] $R1 = \Sigma_{hkl}(||F_{obs}| - |F_{calc}||)/\Sigma_{hkl}|F_{obs}|$; $wR2 = [\Sigma_{hkl}w(|F_{obs}| - |F_{calc}|)^2/\Sigma_{hkl}wF^2_{obs}]^{1/2}$; $w = 1/\sigma^2(F_{obs})$; $GOF = [\Sigma_{hkl}w(|F_{obs}| - |F_{calc}|)^2/(n_{data} - n_{vari})]^{1/2}$

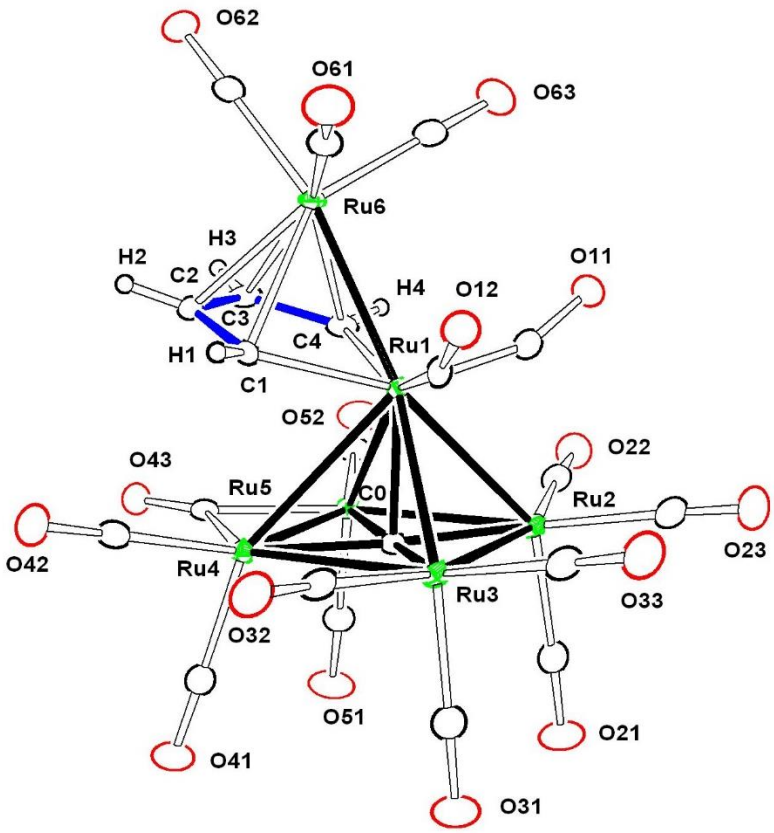

Figure 3.1. An ORTEP diagram of the molecular structure of the compound $Ru_6C(CO)_{16}(\mu-\eta^4-C_4H_4)$, **3.3** showing the 50% thermal ellipsoidal probability. Selected interatomic distances (Å) are as follows: Ru1-Ru2 = 2.80944(19), Ru1-Ru3 = 2.80862(19), Ru1-Ru4 = 2.96963(19), Ru1-Ru5 = 2.96241(19), Ru1-Ru6 = 2.74975(19), Ru2-Ru3 = 2.85374(19), Ru2-Ru5 = 2.9185(2), Ru3-Ru4 = 2.9228(2), Ru4-Ru5 = 2.75116(19), Ru1-C1 = 2.0897(16), Ru1-C4 = 2.0978(16), Ru6-C1 = 2.3026(15), Ru6-C2 = 2.1971(16), Ru6-C3 = 2.2053(16), Ru6-C4 = 2.3006(16), C1-C2 = 1.422(2), C2-C3 = 1.430(2), C3-C4 = 1.422(2), C1-H1 = 0.962(19), C2-H2 = 0.93(2), C3-H3 = 0.93(2), C4-H4 = 0.98(2).

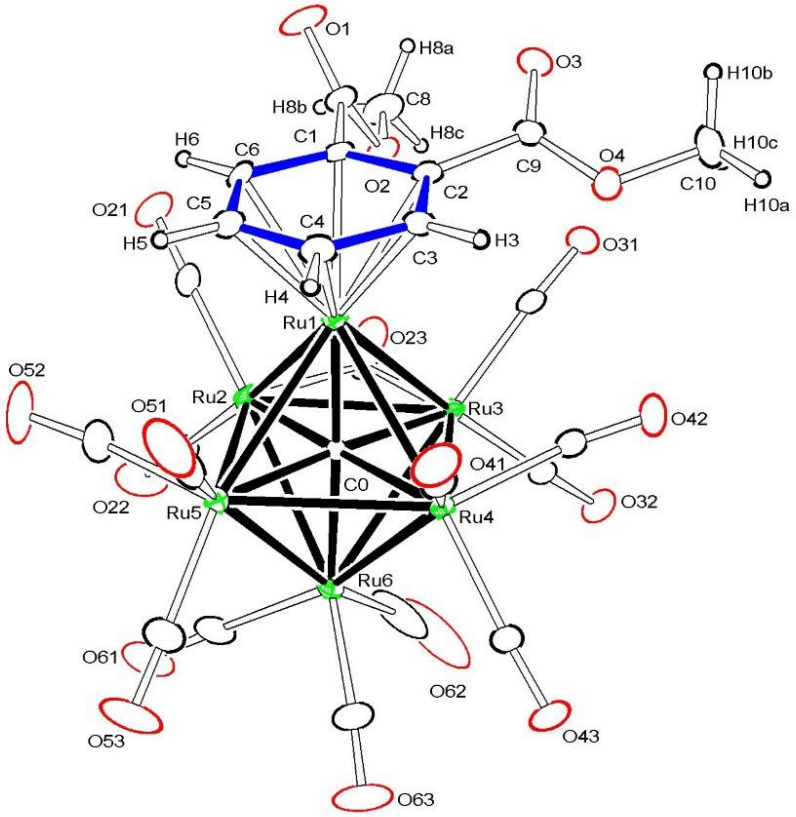

Figure 3.2. An ORTEP diagram of the molecular structure of the compound $Ru_6(\mu_6\text{-}C)(CO)_{14}[\eta^6\text{-}1,2\text{-}C_6H_4(CO_2Me)_2]$, **3.4** showing the 15% thermal ellipsoidal probability. Selected interatomic distances (Å) are as follows: Ru1-C1 = 2.257(4), Ru1-C2 = 2.279(5), Ru1-C3 = 2.242(5), Ru1-C4 = 2.221(5), Ru1-C5 = 2.236(5), Ru1-C6 = 2.253(4), C1-C2 = 1.422(7), C1-C6 = 1.415(7), C1-C7 = 1.510(7), C2-C3 = 1.406(7), C2-C9 = 1.508(7), C3-C4 = 1.402(7), C4-C5 = 1.401(8), C5-C6 = 1.393(7), O1-C7 = 1.194(6), O2-C7 = 1.312(6), O2-C8 = 1.445(6), O3-C9 = 1.199(6), O4-C9 =1.322(6), O4-C10 = 1.452(7).

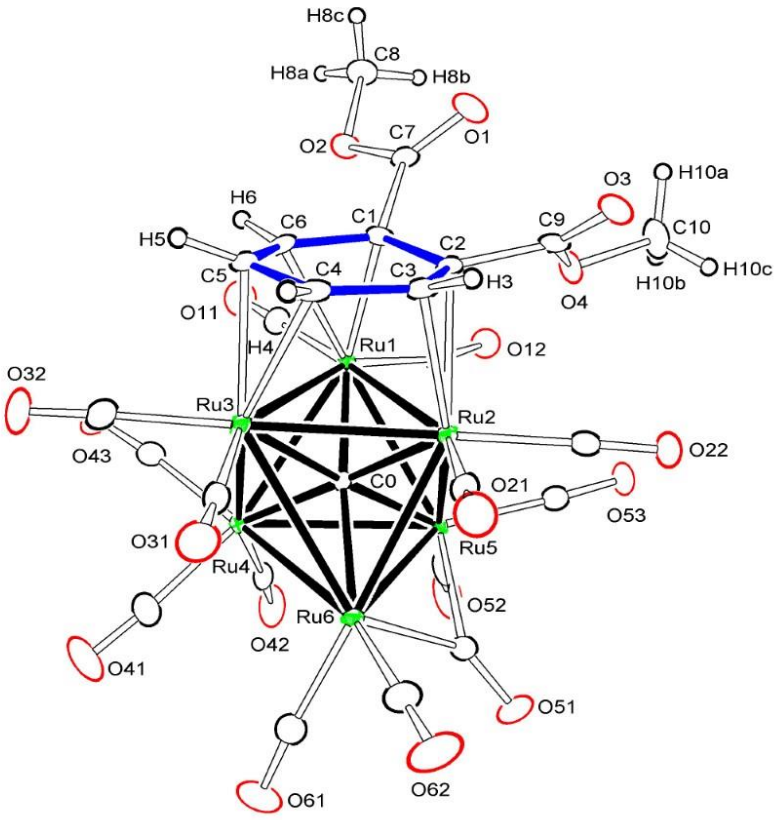

Figure 3.3. An ORTEP diagram of the molecular structure of the compound $Ru_6(\mu_6\text{-}C)(CO)_{14}[\mu_3{-}\eta^6\text{-}1,2\text{-}C_6H_4(CO_2Me)_2]$, **3.7**, showing the 50% thermal ellipsoidal probability. Selected interatomic distances (Å) are as follow: Ru1-C1 = 2.140(3), Ru1-C6 = 2.327(3), Ru2-C2 = 2.365(3), Ru2-C3 = 2.194(3), Ru3-C4 = 2.364(3), Ru3-C5 = 2.217(3), C1-C2 = 1.471(4), C2-C3 = 1.423(4), C3-C4 = 1.451(4), C4-C5 = 1.399(4), C5-C6 = 1.439(4), C1-C6 = 1.438(4), C1-C7 = 1.501(4), C2-C9 = 1.504(4), O1-C7 = 1.202(4), O2-C7 = 1.340(4), O2-C8 = 1.453(3), O3-C9 = 1.205(4), O4-C9 = 1.337(4), O4-C10 = 1.443(4).

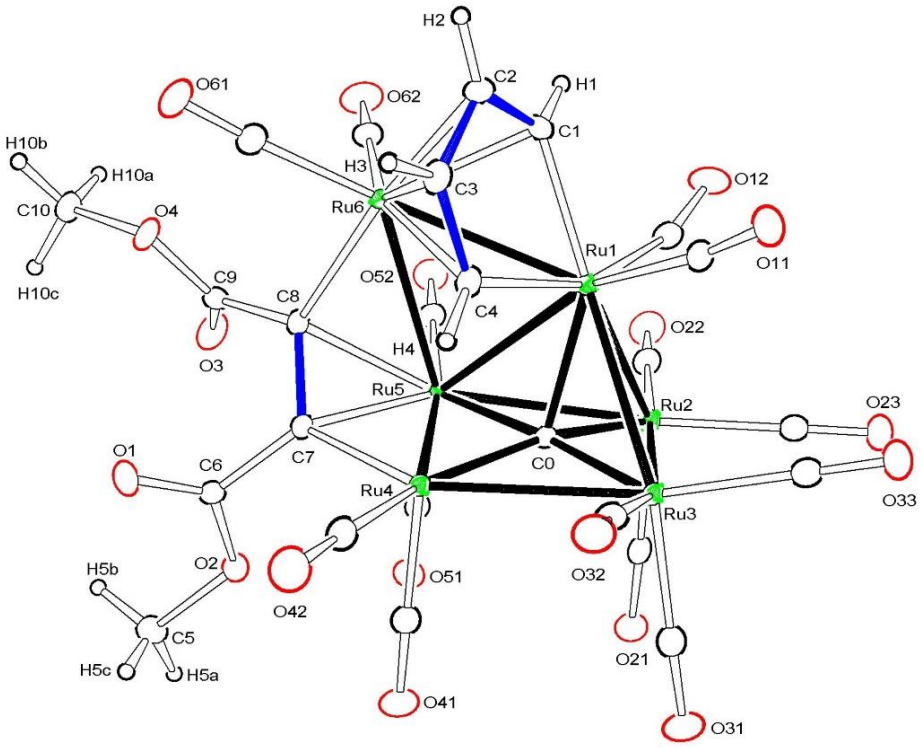

Figure 3.4. An ORTEP diagram of the molecular structure of the compound $Ru_6(\mu_6\text{-}C)(CO)_{14}(\mu\text{–}\eta^4\text{–}C_4H_4)[\mu_3\text{–}C_2(CO_2Me)_2]$, **3.5** showing the 40% thermal ellipsoidal probability. Selected interatomic distances (Å) are as follows: Ru1-Ru2 = 2.8100(2), Ru1-Ru3 = 2.8545(2), Ru1-Ru4 = 3.3627(2), Ru1-Ru5 = 3.0304(2), Ru1-Ru6 = 2.8643(2), Ru2-Ru3 = 2.8622(2), Ru2-Ru5 = 2.8784(2), Ru3-Ru4 = 2.9356(2), Ru4-Ru5 = 2.7074(2), Ru4···Ru6 = 3.750(1), Ru5-Ru6 = 3.0992(2), Ru1-C1 = 2.086(2), Ru1-C4 = 2.106(2), Ru6-C1 = 2.229(2), Ru6-C2 = 2.239(2), Ru6-C3 = 2.251(2), Ru6-C4 = 2.273(2), Ru6-C8 = 2.099(2), Ru5-C7 = 2.191(2), Ru5-C8 = 2.216(2), Ru4-C7 = 2.072(2), C1-H1 = 0.86(3), C1-C2 = 1.395(3), C2-H2 = 0.94(3), C2-C3 = 1.434(3), C3-H3 = 0.92(3), C3-C4 = 1.397(3), C4-H4 = 0.96(3), C6-C7 = 1.497(3), C7-C8 = 1.404(3), C8-C9 = 1.512(3), O1-C6 = 1.206(3), O2-C5 = 1.447(3), O2-C6 = 1.333(3), O3-C9 = 1.202(3), O4-C9 = 1.337(3), O4-C10 = 1.442(3).

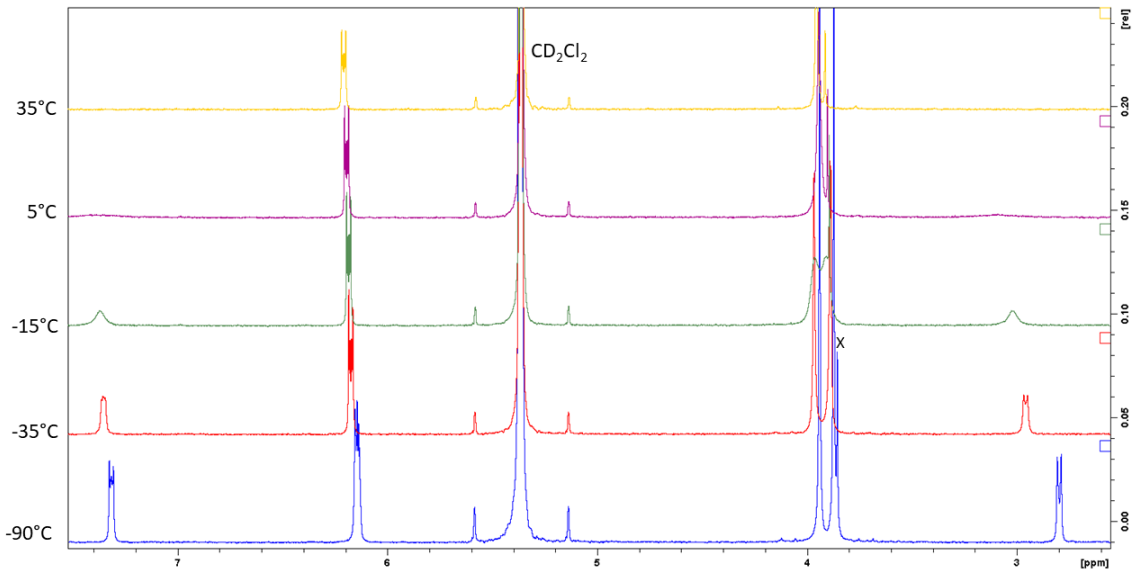

Figure 3.5. A Stacked plot of the ^{1}H NMR spectra of **3.5** at different temperatures in CD_2Cl_2 solvent.

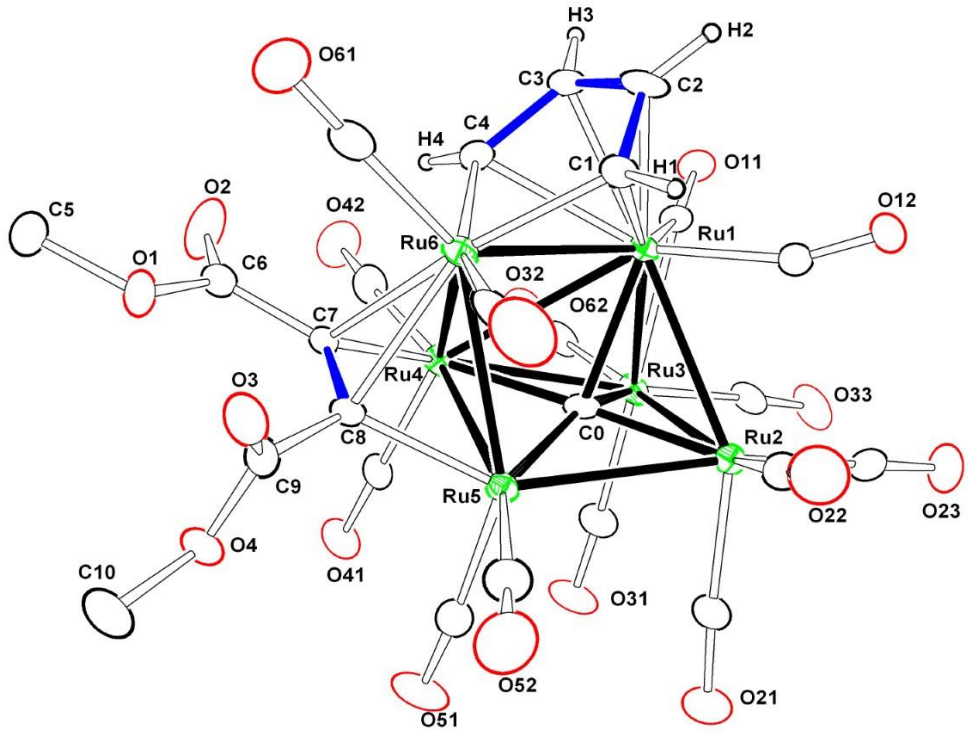

Figure 3.6. An ORTEP diagram of the molecular structure of the compound $Ru_6C(CO)_{14}(\mu-\eta^4-C_4H_4)[\mu_3-C_2(CO_2Me)_2]$, **3.6** showing the 15% thermal ellipsoidal probability. Selected interatomic distances (Å) for molecule **A** are as follows: Ru1A-Ru2A = 2.8259(14), Ru1A-Ru3A = 2.8015(14), Ru1A-Ru4A = 3.0991(13), Ru1A-Ru6A = 2.8523(14), Ru2A-Ru3A = 2.8472(15), Ru2A-Ru5A = 2.9314(14), Ru3A-Ru4A =2.8812(14), Ru4A-Ru5A = 2.8103(13), Ru4A-Ru6A = 3.0388(14), Ru5A-Ru6A = 2.8396(14), Ru1A···Ru5A = 3.604(4), Ru1A-C1A = 2.216(11), Ru1A-C2A = 2.237(12), Ru1A-C3A = 2.261(12), Ru1A- C4A = 2.377(12), Ru4A-C7A = 2.068(12), Ru5A-Ru6A = 2.8396(14), Ru5A-C8A = 2.044(12), Ru6A-C1A = 2.041(12), Ru6A-C4A = 2.095(12), Ru6A-C7A = 2.299(11), Ru6A-C8A = 2.270(11), C1A-C2A = 1.415(17), C2A-H2A = 0.9800, C2A-C3A = 1.411(19), C3A-C4A = 1.431(17), C6A-C7A = 1.483(17), C7A-C8A = 1.392(16), C8A-C9A = 1.496(16).

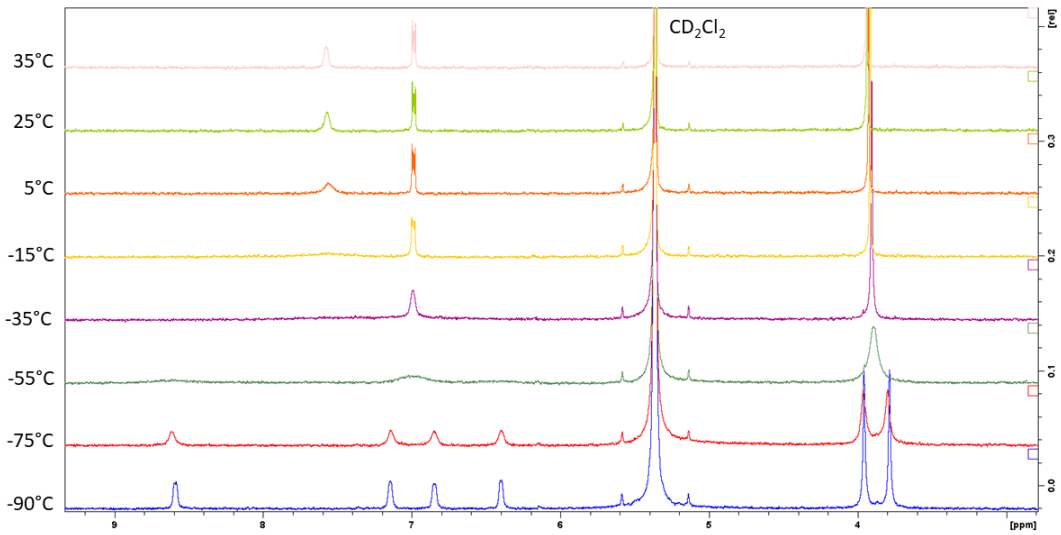

Figure 3.7. A Stacked plot of the ^{1}H NMR spectra of **3.6** at different temperatures.

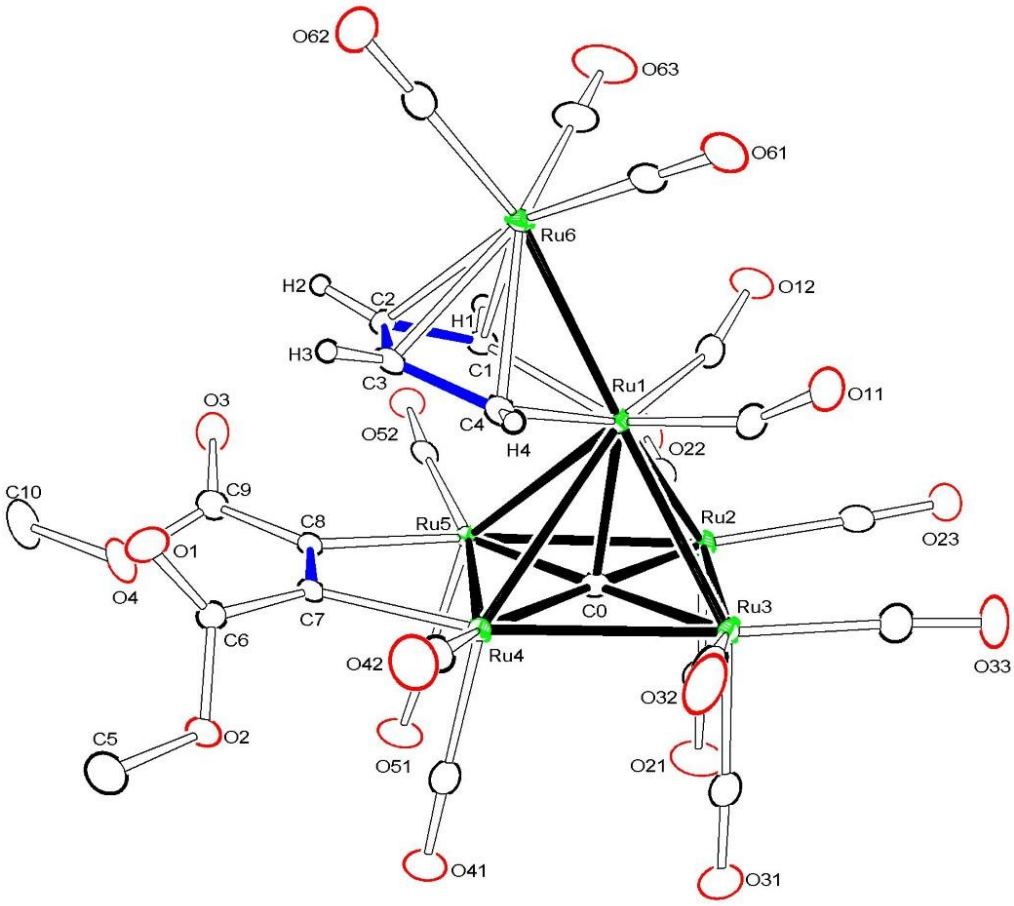

Figure 3.8. An ORTEP diagram of the molecular structure of the compound $Ru_6C(CO)_{15}(\mu-\eta^4-C_4H_4)[\mu-C_2(CO_2Me)_2]$, **3.8** showing the 40% thermal ellipsoidal probability. Selected interatomic distances (Å) are as follows: Ru1-Ru2 = 2.7925(3), Ru1-Ru3 = 2.8079(3), Ru1-Ru4 = 3.0092(3), Ru1-Ru5 = 2.9699(3), Ru1-Ru6 = 2.7436(3), Ru2-Ru3 = 2.8421(3), Ru2-Ru5 = 2.9243(3), Ru3-Ru4 = 2.8818(3), Ru4-Ru5 = 2.8080(3), Ru1-C1 = 2.097(3), Ru1-C4 = 2.102(3), Ru6-C1 = 2.291(3), Ru6-C2 = 2.206(3), Ru6-C3 = 2.216(3), Ru6-C4 = 2.294(3), Ru4-C7 = 2.091(3), Ru5-C8 = 2.095(3), C1-C2 = 1.426(4), C2-C3 = 1.426(4), C3-C4 = 1.410(4), C7-C8 = 1.320(4), C6-C7 = 1.471(4), C8-C9 = 1.479(4), O1-C6 = 1.200(3), O2-C5 = 1.439(4), O2-C6 = 1.342(3), O3-C9 = 1.201(3), O4-C9 = 1.340(4), O4-C10 = 1.449(4).

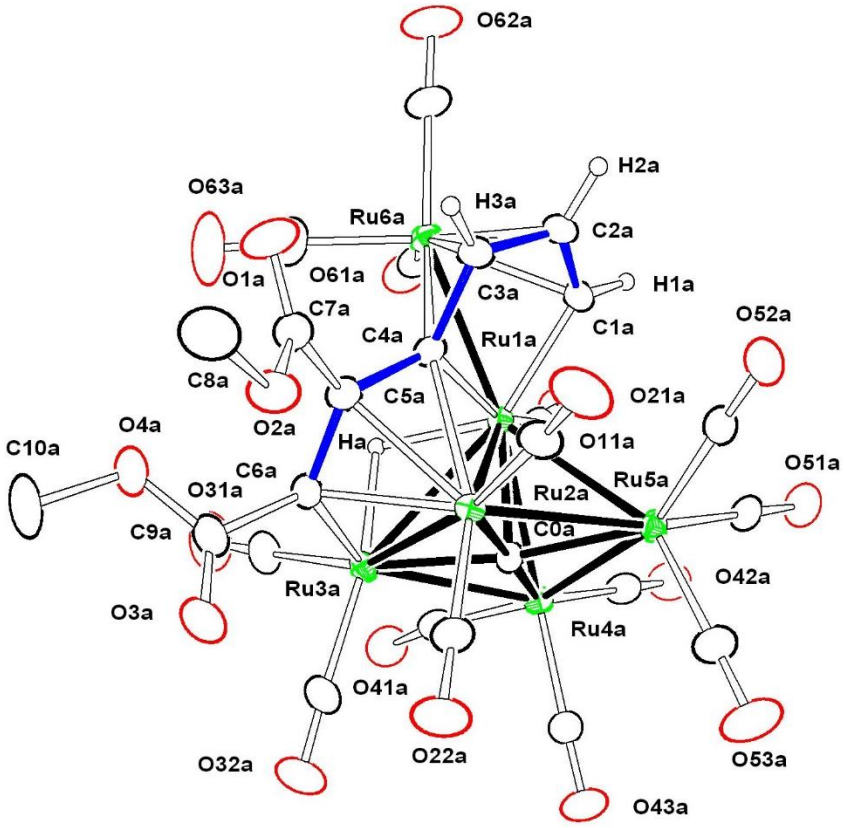

Figure 3.9. An ORTEP diagram of the molecular structure of the compound $Ru_6C(CO)_{14}[\mu_4{-}\eta^6{-}CHCHCHCC(CO_2Me)C(CO_2Me)](\mu\text{-}H)$, **3.9** showing the 20 % thermal ellipsoidal probability. Selected interatomic distances (Å) are as follows: Ru1a-Ru6a = 2.7517(6), Ru1a-C1a = 2.053(4), Ru1a-C4a = 2.142(3), Ru1a-C11a = 1.884(3), Ru2a-C4a = 2.309(3), Ru2a-C5a = 2.204(4), Ru2a-C6a = 2.209(4), Ru3a-C6a = 2.058(4), Ru4a-C0a = 1.971(3), Ru6a-C1a = 2.290(4), Ru6a-C2a = 2.234(4), Ru6a-C3a = 2.188(4), Ru6a-C4a = 2.332(3), C1a-H1a = 0.9800, C1a-C2a = 1.396(5), C2a-H2a = 0.9800, C2a-C3a = 1.413(5), C3a-H3a = 0.9800, C3a-C4a = 1.451(5), C4a-C5a = 1.454(5), C5a-C6a = 1.419(5), Ru1a-Ha = 1.87(3), Ru3a-Ha = 1.89(3).

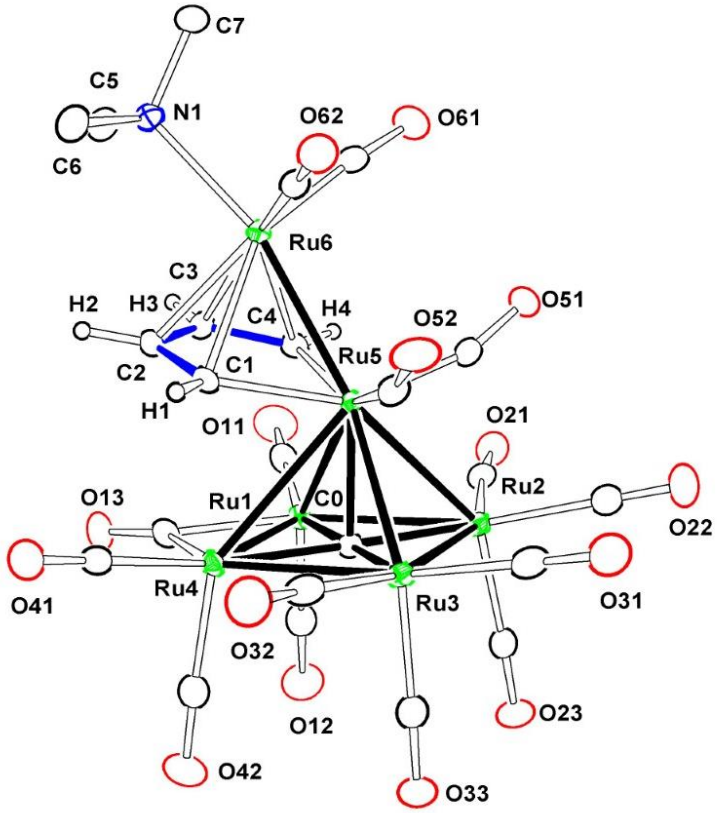

Figure 3.10. An ORTEP diagram of the molecular structure of the compound $Ru_6C(CO)_{15}(\mu-\eta^4-C_4H_4)(NMe_3)$, **3.10** showing the 50% thermal ellipsoidal probability. Selected interatomic distances (Å) are as follows: Ru5-Ru6 = 2.7422(3), Ru5-C1 = 2.119(2), Ru5-C4 = 2.093(2), Ru6-N1 = 2.2241(19), Ru6-C1 = 2.301(2), Ru6-C2 = 2.221(2), Ru6-C3 = 2.217(2), Ru6 -C4 = 2.282(2), N1-C5 = 1.487(3), N1-C6 = 1.489(3), N1-C7 = 1.489(3), C3-C4 = 1.417(3).

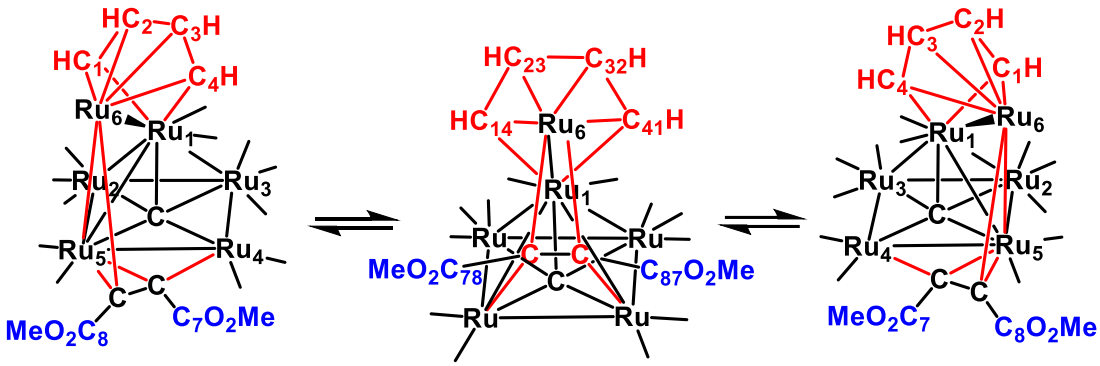

3.5 **3.I** **3.5***

Scheme 3.3

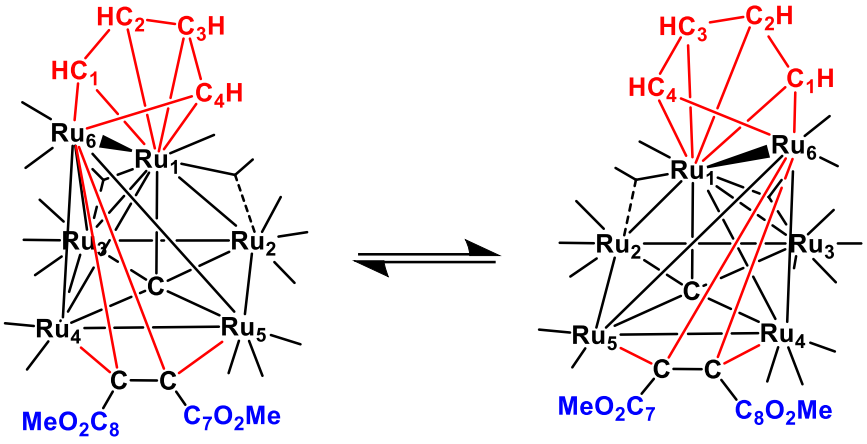

3.6 **3.6***

Scheme 3.4

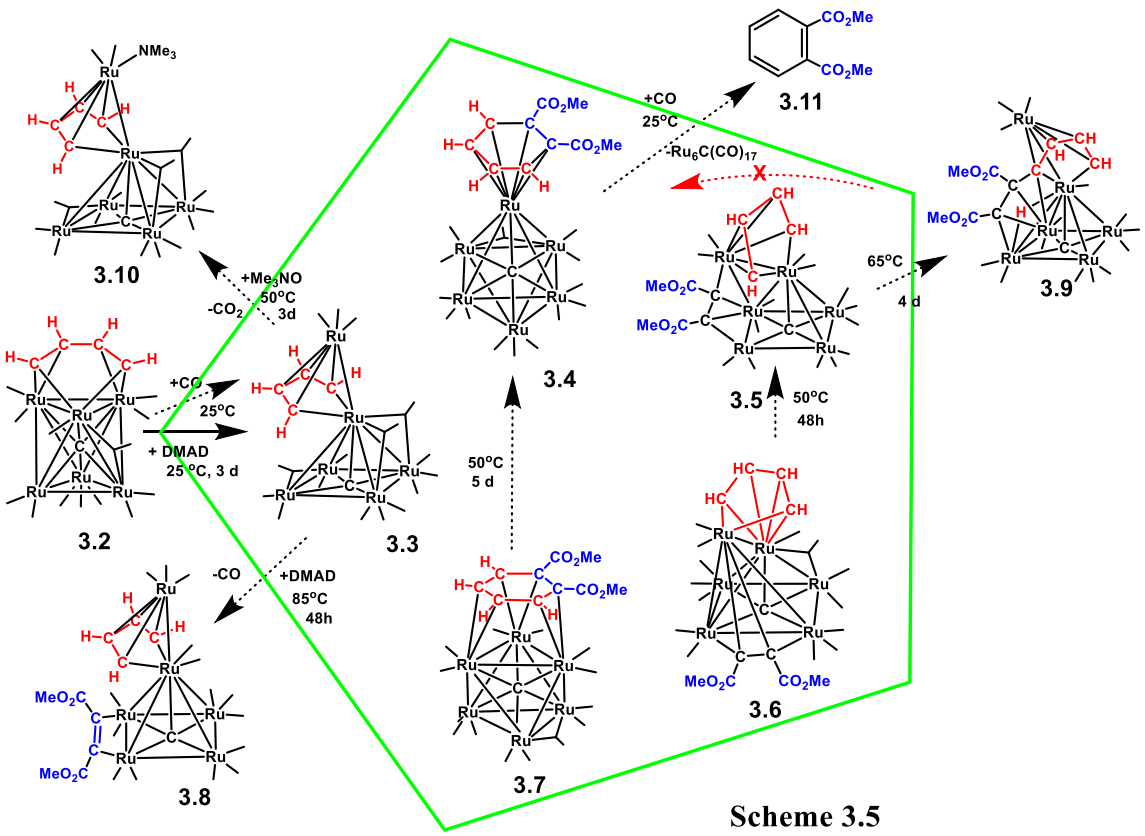
3.10
3.2
3.3
3.4
3.5
3.6
3.7
3.8
3.9
3.11
+Me3NO
50°C
-CO2
3d
+CO
25°C
+ DMAD
25 °C, 3 d
-CO
+DMAD
85°C
48h
50°C
5 d
+CO
25°C
-Ru6C(CO)17
65°C
4 d
50°C
48h

Scheme 3.5

3.4 References

1) Astruc, D. in *Modern Arene Chemistry*, Astruc, D. Ed., Wiley-VCH Pub., Weinheim, **2002**.

2) a) Li, T.; Shoinkhorova, T.; Gascon, J.; Ruiz-Martínez, J., Aromatics Production via Methanol-Mediated Transformation Routes. *ACS Catal*. **2021**, *11*, 7780−7819. (b) Niziolek, A. M.; Onel, O.; Floudas, C. A. Production of benzene, toluene, and xylenes from natural gas via methanol: Process synthesis and global optimization. *AIChE J*. **2016**, *62 (5)*, 1531−1556. (c) Davis, B. H., Alkane dehydrocyclization mechanism. *Catal. Today* **1999**, *53*, 443–516. d) Menon, P. G., Paál, Z., Some Aspects of the Mechanisms of Catalytic Reforming Reactions, *Ind. Eng. Chem. Res.* **1997**, *36*, 3282–3291. e) Heinman, H.; Mills, G. A.; Hattman, J. B.; Kirsch, F. W., Houdriforming Reactions. Studies with Pure Hydrocarbons. *Ind. Eng. Chem*. **1953**, *45*, 130 - 134. f) See *Catalytic Naphtha Reforming*, Anto, G. j.; Aitani, A. M.; Parera, J. M., Eds., Marcel Dekkar Inc., New York, **1995**.

3) a) Link, A.; Sparr, C., Stereoselective arene formation, *Chem. Soc. Rev.*, **2018**, *47*, 3804 – 3815. b) Ito, H.; Segawa, Y.; Murakami, K.; Itami, K., Polycyclic Arene Synthesis by Annulative π-Extension. *J. Am. Chem. Soc*. **2019**, *141*, 3−10.

4) a) Roglans, A.; Pla-Quintana, A.; Solà, M. Mechanistic Studies of Transition-Metal-Catalyzed [2 + 2 + 2] Cycloaddition Reactions, *Chem. Rev*. **2021**, *121*, 1894−1979. b) Xu, L. Li, S.; Jiang, L.; Dong, T.; Zhang, G.; Zhang, W.; Gao, Z. Revisiting reactions of alkynes with $Ru_3(CO)_{12}$: Effects of alkyne substituents and solvents on the structures of ruthenium cluster products. *Inorg. Chim. Acta* **2019**, *485*, 20–25. (c) Varela, J. A.; Saá, C. CpRuCl- and CpCo-Catalyzed or Mediated Cyclotrimerizations of Alkynes and [2 + 2 + 2] Cycloadditions of Alkynes to Alkenes: A Comparative DFT Study. *J. Organomet. Chem*. **2009**, *694*, 143−149. (d) Saito, S.; Yamamoto, Y. Recent Advances in the Transition-Metal-Catalyzed Regioselective Approaches to Polysubstituted Benzene Derivatives. *Chem. Rev*. **2000**, *100*, 2901−2915. (e) Gandon, V.; Aubert, C.; Malacria, M. Recent Progress in Co-Mediated [2 + 2 + 2] Cycloaddition Reactions. *Chem. Commun*. **2006**, 2209−2217. (f) Galan, B. R.; Rovis, T. Beyond Reppe: Building Substituted Arenes by [2 + 2 + 2] Cycloadditions of Alkynes. *Angew. Chem., Int. Ed*. **2009**, *48*, 2830−2834. (g) Domínguez, G.; Pérez-Castells, J. Recent Advances in [2 + 2 + 2] Cycloaddition Reactions. *Chem. Soc. Rev*. **2011**, *40*, 3430−3444. (h) Weding, N.; Hapke, M. Preparation and Synthetic Applications of Alkene Complexes of Group 9 Transition Metals in [2 + 2 + 2] Cycloaddition Reactions. *Chem. Soc. Rev*. **2011**, *40*, 4525−4538. (i) Shibata, Y.; Tanaka, K. Rhodium-Catalyzed [2 + 2 + 2] Cycloaddition of Alkynes for the Synthesis of Substituted Benzenes: Catalysts, Reaction Scope, and Synthetic Applications. *Synthesis* **2012**, *44*, 323−350. (j) Broere, D. L. J., Ruijter, E., Recent Advances in Transition-Metal-Catalyzed [2+2+2]-Cyclo(co)trimerization Reactions, *Synthesis* **2012,** *44*, 2639–2672. (k) Shibata, T.; Tsuchikama, K., Recent advances in enantioselective [2 + 2 + 2] cycloaddition, *Org. Biomol. Chem.*, **2008**, *6*, 1317–1323. (l) Yamamoto, Y.;

Arakawa, T.; Ogawa, R.; Itoh, K., Ruthenium(II)-Catalyzed Selective Intramolecular [2 + 2 + 2] Alkyne Cyclotrimerizations, *J. Am. Chem. Soc*. **2003**, *125*, 12143-12160. (e) Sappa, E. *J. Organomet. Chem.* **1999**, *573*, 139–155

5) (a) Yamazaki, H., Wakatsuki, Y. Cobalt Metallocycles XIII. Preparation and X-ray Crystallography of Cobaltacyclopentadiene and Dinuclear Cobalt Complexes. *J. Organomet. Chem*. **1984**, *272*, 251-263. (b) Wakatsuki, Y.; Nomura, O.; Kitaura, K Morokuma, K.; Yamazaki, H., Cobalt Metallacycles. 11. On the Transformation of Bis(acetylene)cobalt to Cobaltacyclopentadiene. *J Am. Chem. Soc*. **1983**, *105*, 1907 – 1912. (c) Yamazaki, H., Wakatsuki, Y. Cobalt Metallocycles I. One-Step and Stepwise Synthesis of Cobaltacyclopentadiene Complexes from Acetylenes. *J. Organomet. Chem.*, **1977**, *139*, 157 – 167. (d) Gastinger, R. G.; Rausch, M. D.; Sullivan, D. A.; Palenik, G. J., Synthesis and Molecular Structure of 1-(π-Cyclopentadienyl)-1-triphenylphosphine-2,3,4,5-tetrakis(pentafluorophenyl)cobaltole. *J Am. Chem. Soc*. **1976**, *98*, 719 – 723.

6) (a) Dettlaf, G.; Weiss, E., Kristallstruktur, ^{1}H-NMR- und massenspektrum von tricarbonylferracyclopentadienetricarbonyleisen, $C_4H_4Fe_2(CO)_6$, *J. Organomet. Chem*, **1976**, *108*, 213 - 223. (b) Xu, L. Li, S.; Jiang, L.; Dong, T.; Zhang, G.; Zhang, W.; Gao, Z. Revisiting reactions of alkynes with $Ru_3(CO)_{12}$: Effects of alkyne substituents and solvents on the structures of ruthenium cluster products. *Inorg. Chim. Acta* **2019**, *485*, 20–25. (c) Chisholm, M. H.; Folting, K.; Hoffman, D. M.; Huffman, J. C.; Leonelli, J., The remarkable role of steric factors in the reactions of alkynes (HC≡CH and MeC≡CMe)with ditungsten hexa-alkoxides: crystal and molecular structures of $W_2(OPri)_6(py)_2(\mu\text{-}C_2H_2)$, $W_2(OCH_2But)_6(py)_2(\mu\text{-}C_2Me_2)$, and $W_2(OPri)_2(\mu\text{-}C_4R_4)(C_2R_2)$, where R = H and Me (py = pyridine). *J. Chem. Soc., Chem. Commun*.**, 1983**, 589-591. (d) Omori, H.; Suzuki, H.; Morooka, Y., Preparation and structure determination of a dinuclear ruthenacyclopentadiene complex. Coupling of coordinated vinyl ligands. *Organometallics* **1989**, *8*, 1576–1578.

7) (a) Adams, R. D.; Smith, M. D.; Wakdikar, N. D., Zwitterionic Ammoniumalkenyl Ligands in Metal Cluster Complexes. Synthesis, Structures and Transformations of Zwitterionic Trimethylammoniumalkenyl Ligands in Hexaruthenium Carbido Carbonyl Complexes. *Inorg. Chem.* **2020**, *59*, 1513−1521. (b) Blake, A. J.; Haggitt, J. L.; Johnson, B. F. G.; Parsons, S. Alkyne based derivatives of $[Ru_6C(CO)_{17}]$ and the stepwise synthesis of $[Ru_6C(CO)_{13}(\eta^5\text{-}C_5H_5Ph_2)(\mu_3\text{-}CPh)]$. *J. Chem. Soc., Dalton Trans*. **1997**, 991−994. (c) Koridze, A. A.; Astakhova, N. M.; Dolgushin, F. M.; Yanovsky, A. I.; Struchkov, Y. T.; Petrovskii, P. V., A Triosmium Cluster with a Novel Mode of Metallacyclopentadiene Fragment Bonding. X-ray Structure and Reactivity of Os_3 $(\mu_3\text{-}\eta^1\text{:}\eta^1\text{:}\eta^2\text{-}C(SiMe_3)C(Me)C(H)C(Ph)\}(CO)_9$, *Organometallics* **1995**, *14*, 2167 - 2169.

8) (a) Hardesty, J. H.; Koerner, J. B.; Albright, T. A.; Lee, G.Y., Theoretical Study of the Acetylene Trimerization with CpCo, *J. Am. Chem. Soc.* **1999**, *121*, 6055 -

6067. (b) Agenet, N.; Gandon, V.; Vollhardt, K. P. C.; Malacria, M.; Aubert, C., Cobalt-Catalyzed Cyclotrimerization of Alkynes: The Answer to the Puzzle of Parallel Reaction Pathways, *J. Am. Chem. Soc.* **2007**, 129, 8860-8871. (c) Martinez, M.; del Carmen Michelini, M.; Rivalta, I.; Russo, N.; Sicilia, E. Acetylene Cyclotrimerization by Early Second-Row Transition Metals in the Gas Phase. A Theoretical Study, *Inorg. Chem*., **2005**, *44*, 9807 - 9816. (d) Kwon, D.-H.; Proctor, M.; Mendoza, S.; Uyeda, C. Ess, D. H., Catalytic Dinuclear Nickel Spin Crossover Mechanism and Selectivity for Alkyne Cyclotrimerization. *ACS Catal*. **2017**, *7*, 4796−4804. (e) Calderazzo, F.; Pampaloni, G.; Pallavicini, P., Strähle, J.; Wurst, K., Reactions of Zr(η^6-benzene) $(AlCl_4)_2$ with Alkynes: Cyclooligomerization Reactions and Crystal and Molecular Structure of the Seven-Membered Metallacycle $[ZrCPh(CPh)_4CPh][(\mu\text{-}Cl)_2AlCl_2]_2$. *Organometallics* **1991**, *10*, 896 - 901.

9) (a) Yamamoto, K.; Nagae, H.; Tsurugi, H.; Mashima, K., Mechanistic understanding of alkyne cyclotrimerization on mononuclear and dinuclear scaffolds: [4 + 2] cycloaddition of the third alkyne onto metallacyclopentadienes and dimetallacyclopentadienes. *Dalton Trans.* **2016**, *45*, 17072 – 17081. (b) Yamamoto, K.; Tsurug, H.; Mashima, K., Direct Evidence for a [4+2] Cycloaddition Mechanism of Alkynes to Tantallacyclopentadiene on Dinuclear Tantalum Complexes as a Model of Alkyne Cyclotrimerization**.** *Chem. – Eur. J*., **2015**, *21*, 11369 - 11377. (c) Bianchini, C.; Caulton, K. G.; Chardon, C.; Doublet, M.-L.; Eisenstein, O.; Jackson, S. A.; Johnson, T. J., Meli, A.; Peruzzini, M. Streib, W. E.; Vacca, A.; Vizza, F., Mechanism of Acetylene Cyclotrimerization Catalyzed by the *fac*-IrP_3^+ Fragment: Relationship between Fluxionality and Catalysis, *Organometallics* **1994**, *13*, 2010-2023.

10) APEX3 Version 2016.5-0 and SAINT Version 8.37A. Bruker AXS, Inc. Madison, WI, USA.

11) SADABS Version 2016/2. Krause, L., Herbst-Irmer, R., Sheldrick G.M. & Stalke D. *J. Appl. Cryst*. **2015**, *48*, 3-10.

12) (a) SHELXT: Sheldrick, G.M. *Acta Cryst.* **2015**, *A71*, 3-8. (b) SHELXL: Sheldrick, G.M. *Acta Cryst.* **2015**, *C71*, 3-8.

13) **OLEX2**: a complete structure solution, refinement and analysis program. Dolomanov, O. V., Bourhis, L. J., Gildea, R. J., Howard J. A. K. and Puschmann, H. *J. Appl. Cryst.* **2009**, *42*, 339-341.\

14) Kabdas, I.; Keles, A.; Olmez-Hanci, T.; Tunay, O.; Arslan-Alaton, I. *J. Hazard. Mater*. **2009**, *171*, 932 - 940

15) Mingos, D. M. P., Polyhedral Skeletal Electron Pair Approach. *Acc. Chem. Res.* **1984**, *17*, 311–319.

16) Farrar, D. H.; Jackson, P. F.; Johnson, B. F. G.; Lewis, J.; Nichol, J. N.,A High-yield Synthesis of $Ru_5C(CO)_{15}$ by the Carbonylation of $Ru_6C(CO)_{17}$; the X-Ray Structure Analyses of $Ru_5C(CO)_{15}$ and $Ru_5C(CO)_{14}PPh_3$, *J.C.S. Chem. Comm*., **1981**, 415 – 416.

17) (a) Dyson, P. J.; Johnson, B. F. G.; Lewis, J.; Martinelli, M. Braga, D. Grepioni, F., Stepwise Formation of the Bis(benzene)hexaruthenium Carbido Carbonyl Cluster $Ru_6C(CO)_{11}(\eta^6\text{-}C_6H_6)(\mu_3\text{-}\eta^2\text{:}\eta^2\text{:}\eta^2\text{-}C_6H_6)$ from $Ru_6C(CO)_{17}$ *J. Am. Chem. Soc*. **1993**, *115*, 9062 – 9068. (b) Bailey, P. J.; Braga, D. Dyson, P. J.; Grepioni, F.; B. F. G.; Lewis, J.; Sabatino, P., The Synthesis, Molecular Structure and lnterconversion of Two Novel Benzene-coordinated Pentaruthenium-Carbido Cluster Isomers $[Ru_5C(CO)_{12}(\mu_3\text{-}\eta^2\text{:}\eta^2\text{:}\eta^2\text{-}C_6H_6)]$ and $[Ru_5C(CO)_{12}(\eta^6\text{-}C_6H_6)]$, *J . Chem. Soc., Chem. Commun*., **1992**, 177 – 178.

18) (a) Gervasio, G.; Sappa, E.; Marko, L. Synthesis and crystal structure of $[Co_2(CO)_4(PhC{\equiv}CC(O)CH_3)_3]$. Its role in the cyclotrimerization of 1-phenylbut-1-yn-3-one to 1,3,5-triphenyltris(carboxymethyl) benzene. *J. Organomet. Chem*, **1993**, *444*, 203-209. (b) Dickson, R. S.; Fraser, P. J.; Gatehouse, B. M., Crystal and Molecular Structure of a Racemic Complex: η-[1-3,6-η:1,4-6 η-1,3,6-tris(trifluoromethyl)hexa-1,3,5-trien-l,6-diyl]-bis(dicarbonylcobalt)(Co-Co). *J. Chem. Soc., Dalton Trans.*, **1972**, 2278 - 2282. (c) Wilke, G.; Benn, H.; Goddard, R.; Kriiger, C.; Pfeil, B., Intermediates of the cyclotrimerization of 2-butyne with a chromium catalyst. *Inorg. Chim. Acta*, **1992,** *198-200*, 741-748. (d) Green, M.; Kale, P. A.;J. Mercer, R. J., Pathways for Carbon-Chain Growth Reactions at a Dimolybdenum Centre. *J. Chem. Soc, Chem. Commun*., **1987**, 375 – 377. (e) Knox, S. A. R.; Stansfield, R. F. D.; Stone, F. G. A.; Winter, M. J.; Woodward, P., The Sequential Linking of Alkynes at Dichromium and Dimolybdenum Centres; X-Ray Crystal Structure of $[Cr_2(CO)(\mu\text{-}C_4Ph_4)(\mu\text{-}C_5H_5)$. *J. Chem. Soc., Dalton Trans*. **1982**, 173 – 185.

19) Johnson, B. F. G.; Lewis, J.; Sankey, S. W.; Wong, K.; McPartlin, M.; Nelson, W. J. H. An Improved Synthesis of the hexaruthenium carbido Cluster $Ru_6(C)(CO)_{17}$. X-ray structure of the Salt $[Ph_4As]_2[Ru_6(C)(CO)_{16}]$. *J. Organomet. Chem*. **1980**, *191*, C3-C7.

CHAPTER 4

HETEROMETALLIC NITRIDO CLUSTER COMPOUNDS: SYNTHESIS AND CHARACTERIZATIONS OF THE FIRST NITRIDO-CONTAINING RUTHENIUM-GOLD AND RUTHENIUM-COPPER CARBONYL CLUSTER COMPLEXES[3]

[3]Adams, R. D.; Pellechia, P. J.; Smith, M. D.; Tedder, J. D.; Wakdikar, N. D.; *J. Organomet. Chem.* **2019**, 898, 120872

4.1 Introduction

Heterobimetallic catalysts involving the coinage metals, Cu, Ag and Au, have been found to exhibit activity and selectivity that varies significantly from that of their monometallic components.[1,2] Studies have shown that bimetallic complexes can serve as precursors to valuable, bimetallic, homogeneous and heterogeneous catalysts.[3] Over the years there has been much interest in the synthesis, structures and properties of bimetallic complexes containing the coinage metals.[4] Indeed, some of the very first hetero-bimetallic complexes ever prepared involved ligated gold groupings bonded to transition metal carbonyl groups, e.g.[5] Historically, one of the most successful methods for preparing heterometallic cluster complexes has been through reactions of polynuclear metal carbonyl anions with metal halide complexes or complex metal cations.[6] This method has been particularly effective when used with the coinage metals, Cu, Ag and Au.[4]

A range of bimetallic cluster complexes containing interstitial carbido ligands have been prepared over the years.[7] There are also a number of examples of bimetallic cluster complexes containing interstitial borido ligands[8] and there are even a few containing oxo ligands.[9] We have been able to find only one example of heteromultimetallic cluster complexes, namely $[Co_5MoN(CO)_{14}\{AuPPh_3\}]^-$, containing gold atom that also contains an interstitial nitrido ligand in the cluster.[10] In the work reported herein, we have synthesized a number of new bimetallic ruthenium cluster complexes containing an interstitial nitrido ligand by reactions of the anion $[Ru_5(\mu_5\text{-}N)(CO)_{14}]^-$, **4.1**[11] with gold and copper complexes and have investigated their structures and their dynamical activity in solutions.

4.2 Experimental Section.

General Data

All reactions were carried out under an atmosphere of nitrogen by using the standard Schlenk techniques. Reagent grade solvents were dried by standard procedure and were freshly distilled under nitrogen prior to use. Infrared spectra were recorded on a Nicolet IS10 Midinfrared FT-IR spectrophotometer. ^{1}H NMR was recorded on a Bruker AVANCE III-HD 300 spectrometer operating at 300.1 MHz. ^{31}P NMR spectra were recorded on a Bruker AVANCE III-HD 500 spectrometer operating at 202.49 MHz; 85% H_3PO_4 was used as an external reference. The ^{31}P EXSY spectrum was collected on a Bruker AVANCE III-HD 400 MHz spectrometer (161.96 MHz) using the vendor supplied phase sensitive NOESY pulse sequence with a 300 ms mixing time. Exchange rates in exchanged broadened spectra were calculated at the coalescence temperatures by using the standardized equations.[11a] The free energies of activation $\Delta G^{\ddagger}$ at the coalescence temperatures were calculated by using the Eyring equation.[11b] $Ru_3(CO)_{12}$ was purchased from STREM Chemicals. $Au(PPh_3)Cl$ and $[Cu(NCMe)_4][BF_4]$ were purchased from Sigma Aldrich. All reagents were used without further purification. $[PPN][Ru_5(\mu_5\text{-}N)(CO)_{14}]$, **4.1,**[12] $[Cu(PPh_3)Br]_4$[13] and $[Au(PPh_3)]NO_3$[14] were prepared according to previously reported procedures. Unless indicated otherwise, product separations were performed by TLC in air on Analtech 0.50 mm and 0.25 mm silica gel 60 Å F_{254} glass plates. All of the products reported in this paper appear to be air- and light stable when stored in room light under ambient conditions.

Reaction of [PPN][$Ru_5(\mu_5\text{-}N)(CO)_{14}$] (4.1) with $Au(PPh_3)NO_3$ at room temperature.

In a 50 mL three-neck flask, 72.6 mg (0.050 mmol) of **4.1** was added to 20 mL of methylene chloride under a slow purge of nitrogen. To this mixture was added 26.1 mg (0.050 mmol) of $Au(PPh_3)NO_3$. After stirring for 30 min at room temperature, the solvent was removed *in vacuo*. The products were then separated by TLC by using a solvent mixture of hexane/methylene chloride to yield three bands in the order of elution: 1.7 mg of the compound $Ru_4(\mu_4\text{-}N)(CO)_{12}AuPPh_3$, **4.2** (3% yield); 9.1 mg of $Ru_5(\mu_5\text{-}N)(CO)_{14}Au(PPh_3)$, **4.3** (13% yield), and 3.4 mg of $Ru_5(\mu_5\text{-}N)(CO)_{13}[Au(PPh_3)]_3$, **4.4** (3% yield). Compound **4.4** was obtained in a better yield (36%) on the reaction of **4.1** with $[\{(PPh_3)Au\}_3O][BF_4]$, see below. Spectral data for **4.2**: IR spectra, ν_{CO} (cm^{-1} in CH_2Cl_2): 2085.1(w), 2056.7(vs), 2035.1(s), 2005.5(m), 1971.2(vw). ^1H NMR (CD_2Cl_2, δ in ppm): 7.43 – 7.50 (m, 15H, $P(C_6\mathbf{H_5})_3$). ^{31}P NMR (CD_2Cl_2, δ in ppm): 61.245(s, $\mathbf{P}(C_6H_5)_3$). Mass Spectrum (EI^+): M^+ = 1214.6. The isotope distribution pattern is consistent with the presence of four ruthenium and one gold atom. Spectral data for **4.3**: IR spectra, ν_{CO} (cm^{-1} in CH_2Cl_2): 2078.0(w), 2044.1(m), 2036.2(s), 2018.5(vs), 1988.2(vw), 1885.0(vw, br), 1851.9 (vw, br). ^1H NMR (CD_2Cl_2, δ in ppm): 7.53 – 7.73 (m, 15H, $P(C_6H_5)_3$). ^{31}P NMR (CD_2Cl_2, δ in ppm, 25 °C): 68.12 (s, $P(C_6H_5)_3$). Spectral data for **4.4**: IR spectra, ν_{CO} (cm^{-1} in CH_2Cl_2): 2034.9(w), 2002.2(vs), 1957.3(s), 1811.1(m). ^1H NMR (CD_2Cl_2, δ in ppm): 7.35 – 7.68 (m, 45H, $[P(C_6\mathbf{H_5})_3]_3$). VT- ^{31}P NMR (CD_2Cl_2, δ in ppm, -90 °C): 62.52 (s, $\mathbf{P}(C_6H_5)_3$), 61.91 (s, $\mathbf{P}(C_6H_5)_3$), 60.79 (s, $\mathbf{P}(C_6H_5)_3$).

Reaction of [PPN]$Ru_5(\mu_5\text{-}N)(CO)_{14}$ (4.1) with {[$(PPh_3)Au]_3O$}[BF_4] at room temperature

In a 50 mL three-neck flask, 48 mg (0.033 mmol) of **4.1** was added to 20 mL of methylene chloride under a slow purge of nitrogen. To this mixture was added 50 mg (0.034 mmol) of [{$(PPh_3)Au$}$_3$O][BF_4]. After stirring for 30 min, the solvent was removed *in vacuo*. The residue was extracted twice with benzene. The two extracts were combined and reduced to half and filtered. Addition of few drops of hexane to reduced extract induced the formation of red crystals of compound **4.4** (27 mg, 36% yield).

Reaction of [PPN][$Ru_5(\mu_5\text{-}N)(CO)_{14}$], 4.1 with [$Cu(PPh_3)Br]_4$ at room temperature.

In a 100 mL three-neck flask, 97.5 mg (0.067 mmol) of **4.1** was added to 20 mL of methylene chloride under a slow purge of nitrogen. To this mixture was added 129 mg (0.0804 mmol) of [$Cu(PPh_3)Br]_4$ followed by 51.0 mg (0.145 mmol) of Tl[PF_6]. After stirring for 30 min at room temperature, the solvent was removed *in vacuo*, and the products were then separated by TLC by using a solvent mixture of hexane/methylene chloride. The following products were obtained in the order of elution: 6.0 mg of yellow $Ru_4(\mu_4\text{-}N)(CO)_{12}[Cu(PPh_3)]$, **4.5** (8.3% yield); 5.2 mg of red-orange $Ru_5(\mu_5\text{-}N)(CO)_{13}(PPh_3)[\mu_3\text{-}Cu(PPh_3)]$, **4.6**, (5.2% yield), and 6.7 mg of red $Ru_5(\mu_5\text{-}N)(CO)_{13}[\mu\text{-}Cu(PPh_3)][(\mu_3\text{-}Cu(PPh_3)]_2$, **4.7** (5.3% yield). Spectral data for **4.5**: IR spectra, ν_{CO} (cm^{-1} in CH_2Cl_2): 2085.0 (w), 2058.0 (vs), 2031.8 (s), 2006.0 (m). ^{1}H NMR (CD_2Cl_2, δ in ppm): 7.41 – 7.52 (m, 15H, $P(C_6\mathbf{H_5})_3$). ^{31}P NMR (CD_2Cl_2, δ in ppm): 1.44 (s, $\mathbf{P}(C_6H_5)_3$). Spectral data for **4.6**: IR spectra, ν_{CO} (cm^{-1} in CH_2Cl_2): 2055.1(w), 2020.9(s), 2004.7(vs), 1966.1(m), 1860.3(vw, br), 1834.4(vw, br). ^{1}H NMR (CD_2Cl_2, δ in ppm): 7.29 – 7.61 (m, 15H, $P(C_6\mathbf{H_5})_3$), 6.95 – 7.02 (m, 15H, $P(C_6\mathbf{H_5})_3$; ^{31}P NMR (CD_2Cl_2, δ in ppm, 25 ^{o}C):

41.37 (s, Ru**P**), 2.73 (s, Cu**P**). Spectral data for **4.7**: IR spectra, ν_{CO} (cm^{-1} in CH_2Cl_2): 2030.2(w), 1993.9(vs), 1955.7(s), 1943.5(s), 1824.9(m, br). ^1H NMR (CD_2Cl_2, δ in ppm): 7.20 – 7.70 (m, 45H, $[P(C_6\mathbf{H_5})_3]_3$).VT- ^{31}P NMR (d_8-toluene, δ in ppm, -65 °C): 0.37 (s, $\mathbf{P}(C_6H_5)_3$), -4.82 (s, $\mathbf{P}(C_6H_5)_3$), -5.90 (s, $\mathbf{P}(C_6H_5)_3$).

Reaction of [PPN][$Ru_5(\mu_5$-N)$(CO)_{14}$] (4.1) with [$Cu(NCMe)_4$][BF_4] at room temperature.

In a 50 mL three-neck flask, 64 mg (0.044 mmol) of **4.1** was added to 20 mL of methylene chloride under a slow purge of nitrogen. To this mixture was added 14 mg (0.044 mmol) of [$Cu(NCMe)_4$][BF_4]. After stirring for 30 min at room temperature, the solvent was removed *in vacuo*, and the product $Ru_5(\mu_5$-N$)(CO)_{14}[\mu_3$-Cu(NCMe)] (40 mg, 0.039 mmol, 89% yield), **4.8** was then isolated by solvent extraction from the reaction mixture using benzene solvent (10 mL). Spectral data for **4.8**: IR spectra, ν_{CO} (cm^{-1} in CH_2Cl_2): 2076.4(w), 2055.9(m), 2031.9(vs), 2017.3(s), 1981.9(sh). ^1H NMR (CD_2Cl_2, δ in ppm) 2.42 (s, 3H, C$\mathbf{H}_3$).

Crystallographic Analyses.

Crystals of each product suitable for single-crystal X-ray diffraction analyses were grown by slow evaporation of solvent from solutions of the pure compound in the open air at room temperature. Yellow crystals of compound **4.2** were obtained from a benzene/hexane solvent mixture. Dark red crystals of compound **4.3** were obtained from a CH_2Cl_2/benzene/hexane solvent mixture. Dark red crystals of compound **4.4** were obtained from a solution in a CH_2Cl_2/benzene/octane solvent mixture. Yellow crystals of compound **4.5** were obtained from a benzene/hexane solvent mixture. Red crystals of compound **4.6** were obtained from a CH_2Cl_2/benzene/hexane solvent mixture. Red

crystals of compound **4.7** were obtained from a solution in a CH_2Cl_2 /octane solvent mixture. Dark red crystals of **4.8** were obtained from a solution in a CH_2Cl_2/benzene/hexane solvent mixture. X-ray intensity measurements for compounds **4.2**, **4.3** and **4.6** were collected on a Bruker SMART APEX CCD-based diffractometer using Mo Kα radiation (λ = 0.71073 Å). The raw data frames were integrated with the SAINT+ program by using a narrow-frame integration algorithm.[15] Corrections for Lorentz and polarization effects were also applied by using the program SAINT+. Empirical absorption corrections based on the multiple measurements of equivalent reflections was applied by using the program SADABS.[15] All structures were solved by a combination of direct methods and difference Fourier syntheses, and refined by full-matrix least squares on F^2 by using the SHELXTL software package.[16] All non-hydrogen atoms were placed in geometrically idealized positions included as standard riding atoms during the least-squares refinements. X-ray intensity data for compounds **4.4**, **4.5**, **4.7** and **4.8** were collected at 100(2) K by using a Bruker D8 QUEST diffractometer equipped with a PHOTON-100 CMOS area detector and an Incoatec microfocus source (Mo K_α radiation, λ = 0.71073 Å).[17] The data collection strategy consisted of five 180° ω-scans with different φ settings, with a scan width per image of 0.5°. The crystal-to-detector distance was 5.0 cm. The raw area detector data frames were reduced, scaled and corrected for absorption effects using the SAINT[17] and SADABS[18] programs. Crystal data, data collection parameters, and results of these analyses are listed in Table 4.1.

4.3 Results and Discussion

Three gold containing products $Ru_4(\mu_4\text{-}N)(CO)_{12}AuPPh_3$, **4.2** (3% yield), $Ru_5(\mu_5\text{-}N)(CO)_{14}Au(PPh_3)$, **4.3** (13% yield), and $Ru_5(\mu_5\text{-}N)(CO)_{13}[Au(PPh_3)]_3$, **4.4** (3% yield)

were obtained from the reaction of **4.1** with $[Au(PPh_3)]NO_3$ in CH_2Cl_2 solvent at room temperature, see Scheme 4.1. Compound **4.4** was obtained in a much better yield (36%) from the reaction of **4.1** with $[\{(PPh_3)Au\}_3O][BF_4]$ under similar conditions. Each product was characterized by IR and NMR spectroscopy and a single-crystal X-ray diffraction analysis.

An ORTEP diagram of the molecular structure of compound **4.2** is shown in Figure 4.1. This compound contains only four ruthenium atoms arranged in a butterfly tetrahedral structure with a nitrido ligand in the center of the fold. The Ru – N bond distances to the hinge Ru atoms Ru1 and Ru2 are significantly longer, Ru1 – N1 = 2.072(3) Å, Ru2 – N1 = 2.083(3) Å, than those to the wing-tip Ru atoms Ru3 and Ru4, Ru3 – N1 = 1.935(3) Å, Ru4 – N1 = 1.932(3) Å. Similar differences were observed for the hinge Ru – N and wingtip Ru – N bond distances for the complex $Ru_4(\mu_4\text{-}N)(CO)_{11}[P(OMe)_3](\mu\text{-}H)$[19] and the anion $[Ru_4N(CO)_{12}]^-$.[20] An $Au(PPh_3)$ group bridges the hinge bond Ru1 – Ru2 bond, Ru1-Au1 = 2.7729(3) Å and Ru2-Au1 = 2.7503(3) Å. Each Ru atom contains three linear terminally coordinated CO ligands. Compound **4.2** contains a total of 62 cluster valence electrons which is exactly the amount expected for a butterfly tetrahedral cluster of four metal atoms.[21] The most similar RuAu cluster complex that we can find that is related to **4.2** is the carbido cluster complex $Ru_4(\mu_5\text{-}C)(CO)_{12}(\mu\text{-}AuPMe_2Ph)_2$, **4.9** which is a butterfly cluster of four ruthenium atoms with an interstitial carbido ligand in the center and a $Au(PMe_2Ph)$ ligand across the hinge Ru – Ru bond and another $Au(PMe_2Ph)$ group coordinated to the carbido ligand and the two wing-tip ruthenium atoms.[22] Compound **4.9** contains two gold groupings because the carbide ligand contains one less electron than the nitrido ligand in **4.2** and it needs the

second $Au(PMe_2Ph)$ grouping to provide that additional electron to the Ru_4C cluster to complete the bonding requirement of 62 valence electrons.[21]

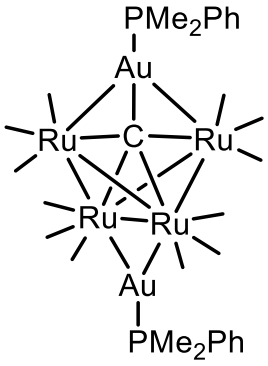

4.9

The molecular structures of the two Ru_5NAu products **4.3** and **4.4** are shown in Figures 4.2 and 4.3, respectively. Both compounds contain a square pyramidal cluster of the five ruthenium atoms with an interstitial nitride ligand in the center of the base of the square pyramid.

Compound **4.3** contains fourteen CO ligands. Two of these, C25-O25 and C34-O34, are semibridging CO ligands on opposite sides of the base of the Ru_5 square pyramid. The $Au(PPh_3)$ group bridges the Ru2 – Ru3 edge of the square pyramid. C45-O45 is a symmetric bridging ligand on the Ru4 – Ru5 bond opposite the bridging $Au(PPh_3)$ bridged Ru – Ru bond, Ru2 - Ru3 bond. The Ru2 - Ru3 bond, 2.9871(7) Å, is the longest Ru – Ru bond in the molecule and is significantly longer (~0.2 Å) than all of the other Ru – Ru bonds. It is also 0.17 Å longer than the corresponding distance in the cluster of the anion **4.1**, itself which has no bridging atom on this bond.[23] It is well known that the edge-bridging hydrido ligand which is one electron donor like the $Au(PPh_3)$ group also produces a significant lengthening of the metal – metal bonds that it bridges.[24] It appears that the structural bond lengthening of metal – metal bonds maybe be extended

to bridging coinage metal groupings as well. The Ru – Au bond distances, Ru2-Au1 = 2.7751(6) Å and Ru3-Au1 = 2.7561(5) Å, are very similar to those in **4.2**. The nitrido ligand occupies the base of the Ru_5 square pyramid. The Ru – N distances to Ru2 and Ru3 which are opposite from the bridging CO ligand, Ru2 – N1 = 1.994(5) Å, Ru3 – N1 = 1.999(5) Å are significantly shorter than those to the other Ru atoms, Ru 1 – N1 = 2.091(5) Å, Ru4 - N1 = 2.038(5) Å, Ru5 – N1 = 2.062(5) Å. A similar distortion was found for the Ru – N bond distances in the square pyramid anion $[Ru_5(\mu_5\text{-}N)(CO)_{14}]^-$, **4.1** from which **4.3** was made.[23] Indeed, the structure of the $Ru_5(\mu_5\text{-}N)(CO)_{14}$ cluster of **4.3** is extremely similar to that of the parent anion except for the presence of the bridging $Au(PPh_3)$ group. Compound **4.3** contains a total of 74 cluster valence electrons which is in accord with the observed square pyramidal structure for the five ruthenium atoms.[21]

Housecroft et al. reported a related square pyramidal Ru_5Au cluster complex $Ru_5(\mu_5\text{-}B)(CO)_{15}(AuPPh_3)$, **4.10**[25] which contains an interstitial borido ligand instead of the nitrido ligand in **4.3**, but **4.10** has fifteen CO ligands. The increase in the number of CO ligands in **4.10** is required in order to make up for the fact that B atom in **4.10** donates only 3-electrons to the cluster as compared to the nitrogen atom in **4.3** which donates 5-electrons to the cluster. Interestingly, the $Au(PPh_3)$ group in **4.10** bridges two of the ruthenium atoms in the base of the Ru_5 square pyramid, but it is also bonded to the boron atom. The change in location of the $Au(PPh_3)$ group from **4.3** to **4.10** may be due to an increase in the steric crowding on the upper portion of the Ru_5 cluster caused by the addition of the fifteenth CO ligand.

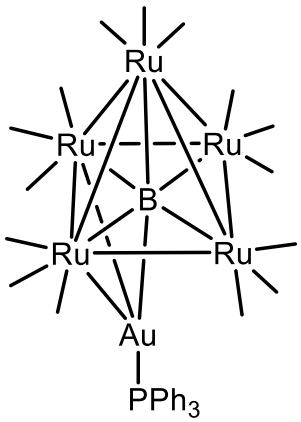

4.10

Compound **4.4** contains a square pyramidal cluster of five ruthenium atoms similar to that of **4.3**, but there are three $Au(PPh_3)$ groups on the surface of this Ru_5 cluster. One of these bridges the Ru2 – Ru3 edge of the base of the square pyramid similar to that in **4.3**. The other two $Au(PPh_3)$ groups are mutually bonded through the gold atoms. As in **4.3**, the longest Ru – Ru bond is Ru2 - Ru3 bond, 2.9381(6) Å, that contains the lone edge bridging $Au(PPh_3)$ group. The Au – Au bond distance, Au2 – Au3 = 2.8159(3) Å is similar to that found in other related complexes, such as $Ru_6C(CO)_{16}Au_2(Ph_2PCH_2PPh_2)$, Au – Au = 2.863(1) Å,[26] $Ru_5(\mu_5\text{-}C)(CO)_{14}[Au_2(PPh_2CH_2CH_2PPh_2)]$, Au – Au = 2.811(1) Å,[27] $Ru_5(\mu_5\text{-}C)(CO)_{11}(\mu\text{-}CO)_2[\mu\text{-}Au(PPh_3)]_2$, Au - Au = 2.8817(5)[28] and $Ru_5(\mu_5\text{-}C)(CO)_{11}(\mu\text{-}CO)_2[\mu\text{-}Au(PPh_3)]_4$, Au - Au = 2.8277(6)[28,] but it is significantly shorter than the Au – Au bond distance in the trigold compound $Ru_5(\mu_5\text{-}B)(CO)_{14}(\mu\text{-}AuPPh_3)\{\mu_4\text{-}(AuPPh_3)_2\}$, **4.11**, Au – Au = 2.918(3) Å which contains an interstitial boride atom. Interestingly, the $(AuPPh_3)_2$ group in **4.11** bridges the entire base of the Ru_5 square pyramid and includes bonding to the boron atom.[29] Like **4.10**, compound **4.11** contains one more CO ligand than **4.4** which may induce the relocation of the Au_2 grouping to the Ru_4 base due to steric crowding. Each

$Au(PPh_3)$ group in **4.4** contributes one valence electron to the cluster, which then achieves a total of 74 valence electrons which is in accord with the observed square-pyramidal structure of the Ru_5 cluster.[21]

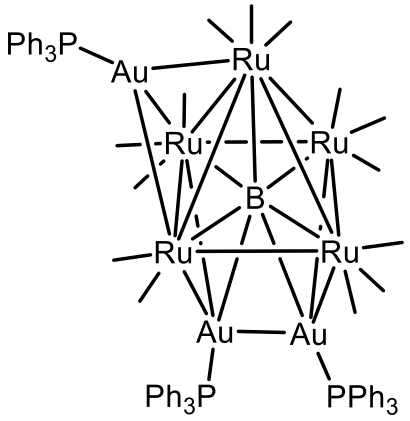

4.11

The ^{31}P NMR spectra of compound **4.4** exhibits single broad resonance at 63.92 ppm at 25 ^oC for the three PPh_3 ligands. The ^{31}P NMR spectra of **4.4** at a variety of temperatures are in shown in Figure 4.4. At -90 ^oC, three slightly broadened phosphorus resonances of equal intensity are observed at 62.52, 61.91 and 60.79 ppm. The resonances at 62.52 and 61.91 ppm broaden and coalesce into a single sharp resonance of intensity 2 at -50 ^oC. The third resonance has sharpened to a singlet of intensity 1. At higher temperatures, the two resonances observed at -50 ^oC broaden and then merge into the single broad resonance observed at 63.92 ppm at 25 ^oC. These changes can be explained by the coexistence of two dynamical exchange processes. The most likely processes involve intramolecular permutations of the $Au(PPh_3)$ groups about the central Ru_5 cluster. Other examples of dynamical stereochemistry of $Au(PR_3)$[30] groups in bimetallic cluster complexes have been reported including that of compound **4.11.**[29]

There are only three different ways to permute the $Au(PPh_3)$ groups in **4.4** intramolecularly by one on one exchanges. These are shown in Scheme 4.2. Mechanisms and possible intermediates are not shown in Scheme 4.2. Pathway **4.1** would exchange the two mutually bonded $Au(PPh_3)$ labeled Au2 and Au3. Mechanistically, this could be as simple as a two-fold rotation about an axis perpendicular to the Au2 – Au3 bond. Pathway **4.2** would exchange the two $Au(PPh_3)$ labeled Au1 and Au2, and Pathway **4.3** would exchange the two $Au(PPh_3)$ groups labeled Au1 and Au3. Pathways 2 and 3 would require a cleavage of the Au2 – Au3 bond followed by a shift of one to those $Au(PPh_3)$ groups to the other side of the Ru_5 cluster. Unfortunately, there is no way to distinguish between these three exchange processes from the site to site exchanges shown in NMR data alone. From the coalescence temperatures of the NMR resonances it is possible to estimate, $\Delta G^{\ddagger}$, the free energy of activation, for the two observed exchange processes.[31] The resonances at 62.52 ppm and 61.91 ppm coalesce at -75 ^{o}C, $\Delta G^{\ddagger}_{198}$ = 9.3(3) kcal/mol. The coalescence for the higher energy exchange process is found at 63.92 ppm at 25 ^{o}C, $\Delta G^{\ddagger}_{298}$ = 13.9(3) kcal/mol.[11] We prefer the exchange Pathway 1 for the lower energy exchange process simply because it would involve the making and breaking of fewer metal – metal bonds than Pathways 2 or 3.

In addition to these two intramolecular exchange processes, there is also a higher energy intermolecular exchange process that involves the phosphine ligands of **4.4** with free PPh_3, but this is only observed in the presence of added quantities of PPh_3. This process is slow on the NMR timescale at room temperature, and it does not influence the dynamics of the intramolecular exchanges of the phosphine ligands shown in Figure 4.4. The slow intermolecular exchange process was revealed in an EXSY magnetization

transfer experiment by the observation of the cross peaks for the resonances of free PPh_3 added to a solution of **4.4** and the averaged resonance for the phosphine ligands of complex, see Figure 4.5.

Three RuCu carbonyl cluster complexes with each containing a nitrido ligand: $Ru_4(\mu_4\text{-}N)(CO)_{12}[\mu\text{-}Cu(PPh_3)]$, **4.5** (8.3% yield); $Ru_5(\mu_5\text{-}N)(CO)_{13}(PPh_3)[\mu_3\text{-}Cu(PPh_3)]$, **4.6**, (5.2% yield), and $Ru_5(\mu_5\text{-}N)(CO)_{13}[\mu\text{-}Cu(PPh_3)][\mu_3\text{-}\{Cu(PPh_3)_2\}]$, **4.7** (5.3% yield) were obtained in low yields from the reaction of **4.1** with $[Cu(PPh_3)Br]_4$ at room temperature for 30 min. $Tl[PF_6]$ was used to activate the copper reagent by assisting in removal of its bromide ligand. Each of the products was characterized by IR and ^{31}P NMR spectroscopy and by single-crystal X-ray diffraction analysis. A schematic of the synthesis and structures of the products is shown in Scheme 4.3.

An ORTEP diagram of the molecular structure of **4.5** is shown in Figure 4.6. Compound **4.5** is the copper homologue of compound **4.2**. The $Cu(PPh_3)$ group bridges the hinge edge of the butterfly tetrahedron of the four ruthenium atoms of the cluster as found for the Au atom in **4.2**. The Ru – Cu distances, Ru1-Cu1 = 2.5862(3) Å, Ru2-Cu1 = 2.5966(3) Å, are similar to those in the related Ru_3Cu bimetallic cluster complexes: $Ru_3(CO)_9(C_2Bu^t)(CuPPh_3)$, Ru – Cu = 2.603(1) Å[32] and $Ru_3(\mu_3\text{-}PPhCH_2PPh_2)(CO)_9(CuPPh_3)$, Ru – Cu = 2.607(1) Å.[33] The Ru – N distances to the interstitial nitrido ligand in **4.5** are very similar to the corresponding distances in **4.2**, Ru1 – N1 = 2.0852(15) Å, Ru2 – N1 = 2.0790(15) Å Ru3 – N1 = 1.9352(15) Å, Ru4 – N1 = 1.9359(15) Å.

An ORTEP diagram of the molecular structure of compound **4.6** is shown in Figure 4.7. Like **4.3**, compound **4.6** contains a square pyramidal cluster of five ruthenium atoms. There is a $Cu(PPh_3)$ group in **4.6**, but unlike the $Au(PPh_3)$ in **4.3**, it bridges one of the triangular faces of the square pyramid, Cu1-Ru1 = 2.6722(6) Å, Cu1-Ru2 = 2.6855(7) Å, Cu1-Ru3 = 2.7075(7) Å. The Ru – Ru bond distances are similar to those in **4.3**, and the Cu-bridged Ru2-Ru3 bond in the base of the square pyramid is the longest in the cluster, 2.8844(5) Å. Unlike **4.3**, the Ru_5 cluster of **4.6** contains thirteen CO ligands and one PPh_3 ligand. The latter is coordinated to one of the basal ruthenium atoms, Ru4 – P2 = 2.3076(12) Å. As in **4.3**, there is a bridging CO ligand across the Ru4 – Ru5 bond and a semibridging CO ligand on both the Ru3 – Ru4 and Ru2 – Ru5 metal – metal bonds. The Ru – N distances in **4.6** are similar to those in **4.3**.

The crystal of compound **4.7** contains two independent molecular units in the asymmetric crystal unit. Both molecules are structurally similar. An ORTEP diagram of the molecular structure of one of the two independent molecules in the crystal of **4.7** is shown in Figure 4.8. Compound **4.7** is very similar to **4.4** except that it contains three copper atoms in the locations of the three gold atoms in **4.4**. Two of the $Cu(PPh)_3$ groups are mutually bonded. The Cu – Cu bond distance, Cu2-Cu3 = 2.6211(9) Å, is significantly shorter than that found in the complex $Ru_6C(CO)_{16}\{\mu_3\text{-}Cu(NCMe)\}_2$, Cu(l)-Cu(2) 2.691(1) Å, despite the presence of the less bulky NCMe ligands in the latter compound.[34] As in **4.4**, the two copper-bridged Ru - Ru bonds in the base of the Ru_5 square pyramid, Ru2-Ru3 = 2.8767(6) Å, Ru4-Ru5 = 2.9603(6) Å, are much longer than all of the other Ru – Ru bonds. The Ru – Cu bond distances to the edge bridging copper atom Cu(1), Ru2-Cu1 = 2.6129(7) Å, Ru3-Cu1 = 2.6101(7) Å are significantly shorter

than those to the other copper atoms which are triply bridging atoms. Each $Cu(PPh_3)$ group contributes one valence electron to the Ru_5 cluster, which then achieves a total of 74 valence electrons which is in accord with the observed square-pyramidal structure.[21]

Compound **4.7** also exhibits dynamical activity on the NMR time scale similar to that of compound **4.4**, see Figure 4.7. The ^{31}P NMR spectrum of compound **4.7** also shows three broad resonances at 0.37 ppm, -4.83 ppm and -5.91 ppm for the three different PPh_3 ligands at -65 ^oC. The two resonances at -4.83 and -5.91 ppm broaden and coalesce when the temperature is raised to -40 ^oC, δ = -5.38, $\Delta G^{\ddagger}_{233}$ = 10.9(3) kcal/mol, and become a sharp singlet of intensity 2 at -5 ^oC. This exchange averaged resonance and the one at 0.12 ppm (-25 ^oC) then broaden and coalesce at δ = -4.00 at 35 ^oC as the temperature is raised still further, $\Delta G^{\ddagger}_{308}$ = 14.0(3) kcal/mol.[11] Both exchange processes are believed to be similar to those described above for compound **4.4** although they both occur at slightly higher temperatures with accordingly higher activation energies, $\Delta G^{\ddagger}$.

The reaction of **4.1** with $[Cu(NCMe)_4][BF_4]$ yielded the new compound $Ru_5(\mu_5\text{-}N)(CO)_{14}[\mu_3\text{-}Cu(NCMe)]$, **4.8** in 89% yield, see Scheme 4.4. Compound **4.8** was also characterized crystallographically, and an ORTEP diagram of the molecular structure of compound **4.8** is shown in Figure 4.10. Compound **4.8** contains a square pyramidal cluster of five ruthenium atoms with an interstitial nitrido ligand N1 and a triply bridging Cu(NCMe) group on one of the triangular Ru_3 groups of the Ru_5 square pyramid. It is structurally similar to that of compound **4.6**, but it has an NCMe ligand on the copper atom Cu1 instead of a PPh_3 ligand and it has a CO ligand on the basal Ru atom in the place of the PPh_3 ligand in **4.6**. The Ru – Cu bonds in **4.8** are similar to those in **4.6**, Ru1-

Cu1 = 2.7404(6) Å, Ru3-Cu1 = 2.5902(6) Å, Ru4-Cu1 = 2.6487(6) Å. Interestingly, as in **4.3** and **4.4**, the Cu bridged Ru – Ru bond, Ru3-Ru4 = 2.9684(5) Å, is nearly 0.2 Å longer than all of the other Ru – Ru bonds in the complex. The Ru – N bond distances in **4.8** are similar to those in **4.6**. The resonance of the methyl group of the NCMe ligand was observed at $\delta = 2.42$ in the ^{1}H NMR spectrum.

4.4 Conclusions

It has been shown that the anion **4.1** can serve as a reagent for the synthesis of bimetallic ruthenium nitrido carbonyl cluster complexes with gold and copper. Three new ruthenium-gold cluster complexes **4.2**, **4.3** and **4.4** containing an interstitial nitrido ligand were obtained in low yields from the reaction of the anion **4.1** with $Au(PPh_3)NO_3$. One of them, compound **4.4**, was obtained in a much better yield (36%) from the reaction of **4.1** with the more reactive gold reagent $[\{(PPh_3)Au\}_3O][BF_4]$. Similarly, three new nitrido-ruthenium-copper cluster complexes **4.5**, **4.6** and **4.7** containing an interstitial nitrido ligand were obtained in low yields from the reaction of the **4.1** with $[Cu(PPh_3)Br]_4$. The ruthenium-copper complex **4.8** was obtained in a good yield by using the more reactive copper reagent $[Cu(NCMe)_4][BF_4]$. Compounds **4.2** and **4.5** contain only four ruthenium atoms due to a loss of one ruthenium atom from the reagent **4.1** in the course of the reaction. All of the pentaruthenium complexes contain square pyramidal Ru_5 clusters that are capped with gold phosphine, copper phosphine or copper acetonitrile groups. Compounds **4.4** and **4.7** exhibit dynamical activity on the NMR time scale via exchange processes involving intramolecular shifts of the $M(PPh_3)$ groups, M = Au and Cu, about the surface of the square pyramidal Ru_5 cluster framework.

Table 4.1. Crystal Data for the X-Ray Structural Analyses of Compounds **4.2** – **4.4**.

Compound	**4.2**	**4.3**	**4.4**
Empirical formula	$Ru_4AuPNO_{12}C_{30}H_{15}$	$Ru_5AuPNO_{14}C_{32}H_{15}$	$Ru_{10}Au_6P_6N_2O_{26}C_{159}H_{116}Cl_2$
Formula weight	1213.65	1370.74	4919.76
Crystal system	Monoclinic	Triclinic	Monoclinic
Lattice parameters			
a (Å)	9.2077(3)	9.4985(3)	36.8398(17)
b (Å)	24.7662(7)	14.8369(5)	14.3624(6)
c (Å)	16.3896(5)	15.2066(5)	16.4081(8)
α (deg)	90.00	68.048(1)	90.00
β (deg)	99.418(1)	76.868(1)	114.787(1)
γ (deg)	90.00	81.233(1)	90.00
V ($Å^3$)	3687.10(19)	1930.28(11)	7881.8(6)
Space group	$P2_1/n$	*P*-1	*C*2
Z value	4	2	2
ρ_{calc} (g/cm^3)	2.186	2.358	2.073
μ (Mo Kα) (mm^{-1})	5.667	5.798	6.648
Temperature (K)	294(2)	294(2)	100(2)
$2\theta_{max}$ (°)	56.60	50.06	50.06
No. Obs. ($I>2\sigma(I)$)	9159	6829	13895
No. of parameters	442	481	885
Goodness of fit (GOF)	1.091	1.018	1.029
Max. shift/error on final cycle	0.002	0.007	0.006
Residuals $2\sigma(I)$*: R1; wR2	0.0292; 0.0586	0.0373;0.0960	0.0230;0.055
Absorption Corr, Max/min	Semi-empirical from equivalents 1.000/ 0.698	Semi-empirical from equivalents 1.000/0.639	Semi-empirical from equivalents 0.381/0.217
Largest peak in Final Diff. Map (e^- / $Å^3$)	0.440	2.397	1.514

[a] $R1 = \Sigma_{hkl}(\,|\,|F_{obs}|-|F_{calc}|\,|\,)/\Sigma_{hkl}|F_{obs}|$; $wR2 = [\Sigma_{hkl}w(|F_{obs}|-|F_{calc}|)^2/\Sigma_{hkl}wF^2_{obs}]^{1/2}$; $w = 1/\sigma^2(F_{obs})$; $GOF = [\Sigma_{hkl}w(|F_{obs}|-|F_{calc}|)^2/(n_{data} - n_{vari})]^{1/2}$

Table 4.2. Crystal Data for the X-Ray Structural Analyses of Compounds **4.5** – **4.6**

Compound	**4.5**	**4.6**
Empirical formula	$Ru_4CuPNO_{12}C_{30}H_{15}$	$Ru_5CuP_2NO_{13}C_{49}H_{30}$
Formula weight	1080.22	1471.57
Crystal system	Monoclinic	Triclinic
Lattice parameters		
a (Å)	8.8225(4)	10.1176(4)
b (Å)	24.0608(10)	13.7516(5)
c (Å)	16.5979(7)	19.4975(7)
α (deg)	90.00	104.826(1)
β (deg)	99.827(2)	100.763(1)
γ (deg)	90.00	99.811(1)
V ($Å^3$)	3471.6(3)	2507.39(16)
Space group	$P2_1/n$	*P*-1
Z value	4	2
ρ_{calc} (g/cm^3)	2.067	1.949
μ (Mo Kα) (mm^{-1})	2.410	2.012
Temperature (K)	100(2)	294(2)
$2\theta_{max}$ (°)	62.64	50.06
No. Obs. ($I>2\sigma(I)$)	11343	8849
No. of parameters	442	640
Goodness of fit (GOF)	1.055	1.122
Max. shift/error on final cycle	0.002	0.001
Residuals*:R1; wR2	0.0253; 0.0405	0.0333; 0.0909
Absorption Corr., Max/min	Semi-empirical from equivalents 0.494/0.372	Semi-empirical from equivalents 1.000/0.819
Largest peak in Final Diff. Map ($e^-/Å^3$)	0.765	0.978

[a] $R1 = \Sigma_{hkl}(||F_{obs}|-|F_{calc}||)/\Sigma_{hkl}|F_{obs}|$; $wR2 = [\Sigma_{hkl}w(|F_{obs}|-|F_{calc}|)^2/\Sigma_{hkl}wF^2_{obs}]^{1/2}$; $w = 1/\sigma^2(F_{obs})$; $GOF = [\Sigma_{hkl}w(|F_{obs}|-|F_{calc}|)^2/(n_{data} - n_{vari})]^{1/2}$

Table 4.3. Crystal Data for the X-Ray Structural Analyses of Compounds **4.7** – **4.8**

Compound	**4.7**	**4.8**
Empirical formula	$Ru_5Cu_3P_3NO_{13}C_{71}H_{45}$	$Ru_5CuN_2O_{14}C_{16}H_3$
Formula weight	1908.96	1016.09
Crystal system	Triclinic	Triclinic
Lattice parameters		
a (Å)	14.1380(6)	9.3373(5)
b (Å)	19.9764(9)	9.4936(5)
c (Å)	26.6054(12)	15.2090(8)
α (deg)	75.9745(18)	73.695(2)
β (deg)	86.7730(18)	78.047(2)
γ (deg)	71.7564(16)	75.971(2)
V ($Å^3$)	6922.1(5)	1241.30(11)
Space group	*P*-1	*P*-1
Z value	4	2
ρ_{calc} (g/cm^3)	1.832	2.719
μ (Mo Kα) (mm^{-1})	2.095	3.877
Temperature (K)	100(2)	100(2)
$2\theta_{max}$ (°)	54.26	55.20
No. Obs. ($I>2\sigma(I)$)	30578	5737
No. of parameters	1730	355
Goodness of fit (GOF)	1.035	1.084
Max. shift/error on final cycle	0.010	0.001
Residuals*:R1; wR2	0.0451; 0.0892	0.0286; 0.0478
Absorption Corr., Max/min	Semi-empirical from equivalents 0.959/0.850	Semi-empirical from equivalents 0.793/0.746
Largest peak in Final Diff. Map ($e^-/Å^3$)	2.210	0.940

[a] $R1 = \Sigma_{hkl}(||F_{obs}|-|F_{calc}||)/\Sigma_{hkl}|F_{obs}|$; $wR2 = [\Sigma_{hkl}w(|F_{obs}|-|F_{calc}|)^2/\Sigma_{hkl}wF^2_{obs}]^{1/2}$; $w = 1/\sigma^2(F_{obs})$; $GOF = [\Sigma_{hkl}w(|F_{obs}|-|F_{calc}|)^2/(n_{data} - n_{vari})]^{1/2}$

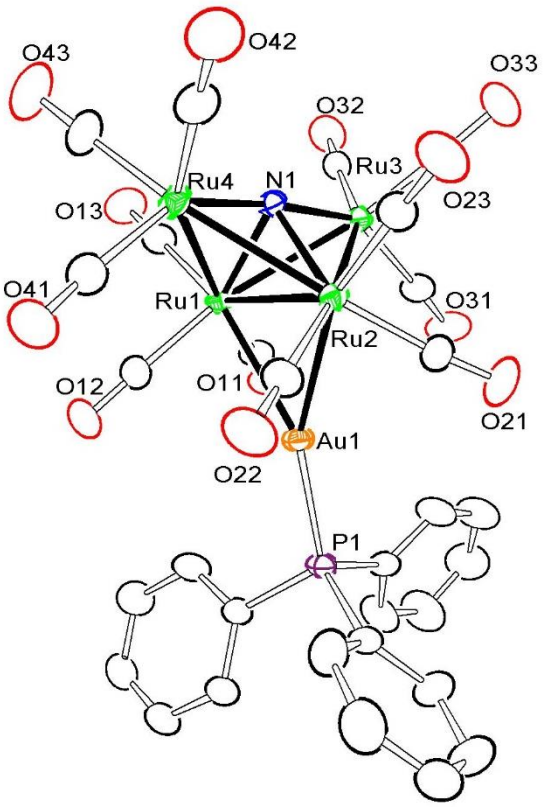

Figure 4.1. An ORTEP diagram of the molecular structure of the compound $Ru_4(\mu_4\text{-}N)(CO)_{12}(\mu\text{-}AuPPh_3)$, **4.2**, showing the 20% thermal ellipsoidal probability. Selected interatomic bond distances (Å) are as follow: Ru1-Au1 = 2.7729(3), Ru2-Au1 = 2.7503(3), Ru1-Ru2 = 2.8311(4), Ru1-Ru4 = 2.7847(4), Ru2-Ru4 = 2.7663(4), Ru1-Ru3 = 2.7825(4), Ru2-Ru3 = 2.7726(4), Ru1 – N1 = 2.072(3), Ru2 – N1 = 2.083(3), Ru3 – N1 = 1.935(3), Ru4 – N1 = 1.932(3), Au1-P1 = 2.2860(10).

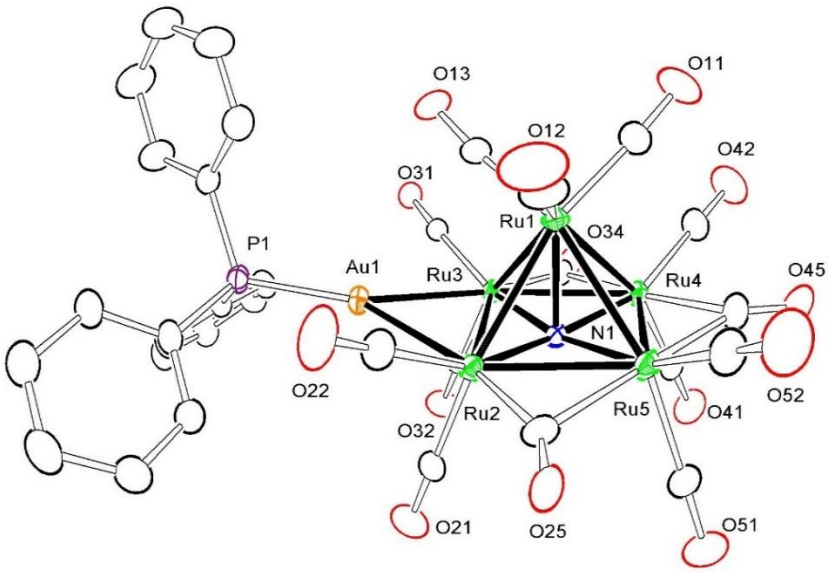

Figure 4.2. An ORTEP diagram of the molecular structure of the compound $[Ru_5(\mu_5\text{-}N)(CO)_{14}(\mu\text{-}AuPPh_3)]$, **4.3**, showing the 20% thermal ellipsoidal probability. Selected interatomic distances (Å) are as follow: Ru2-Au1 = 2.7751(6), Ru3-Au1 = 2.7561(5), Ru1-Ru2 = 2.7680(7), Ru1-Ru3 = 2.8004(7), Ru1-Ru4 = 2.7991(7), Ru1-Ru5 = 2.7497(7), Ru2-Ru3 = 2.9871(7), Ru2-Ru5 = 2.8151(7), Ru3-Ru4 = 2.8020(7), Ru4-Ru5 = 2.7873(7), Ru 1 – N1 = 2.091(5), Ru2 – N1 = 1.994(5), Ru3 – N1 = 1.999(5), Ru4 - N1 = 2.038(5) , Ru5 – N1 = 2.062(5), Au1 – P1 = 2.3012(17).

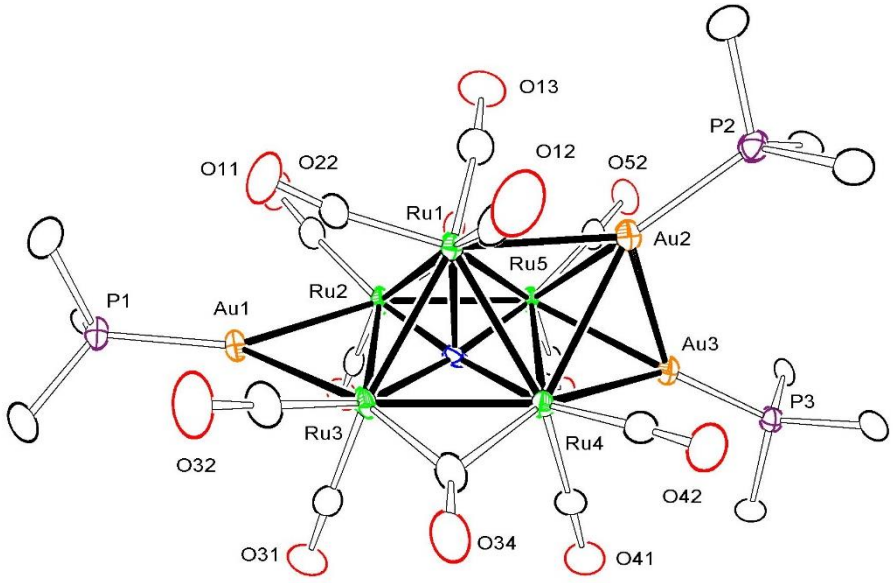

Figure 4.3. An ORTEP diagram of the molecular structure of the compound $Ru_5(\mu_5\text{-}N)(CO)_{13}(\mu\text{-}AuPPh_3)[\mu_3\text{-}(AuPPh_3)_2]$, **4.4**, showing the 25% thermal ellipsoidal probability. For clarity only the *ipso*-carbon atoms of the phenyl rings on the phosphorus atoms are shown. Selected interatomic bond distances (Å) are as follow: Au2-Au3 = 2.8159(3), Ru1-Ru3 = 2.8005(7), Ru1-Ru2 = 2.8034(6), Ru1-Ru5 = 2.8476(6), Ru1-Ru4 = 2.8523(6), Ru2-Ru5 = 2.7773(6), Ru2-Ru3 = 2.9381(6), Ru3-Ru4 = 2.7860(6), Ru4-Ru5 = 2.9722(6), Ru2-Au1 = 2.7391(5), Ru3-Au1 = 2.7616(5), Ru1-Au2 = 2.7804(5), Ru4-Au3 = 2.8024(5), Ru4-Au2 = 2.9573(5), Ru5-Au3 = 2.7876(5), Ru5-Au2 = 2.9147(5), Ru1-N1 = 2.136(5), Ru2-N1 = 2.029(5), Ru3-N1 = 2.030(5), Ru4-N1 = 2.040(5), Ru5-N1 = 2.045(5), Au1-P1 = 2.2721(15), Au2-P2 = 2.2928(16), Au3-P3 = 2.2770(15).

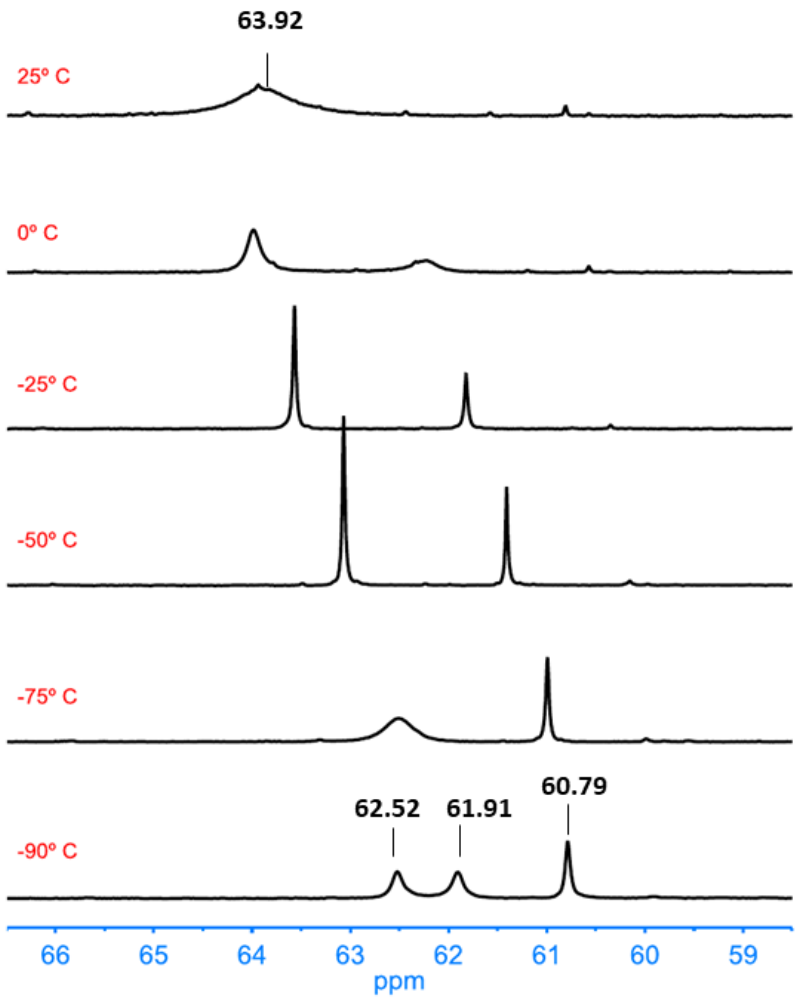

Figure 4.4. A stacked plot of ^{31}P NMR spectra of compound **4.4** in CD_2Cl_2 solvent recorded at different temperatures showing the resonances for the PPh_3 ligands.

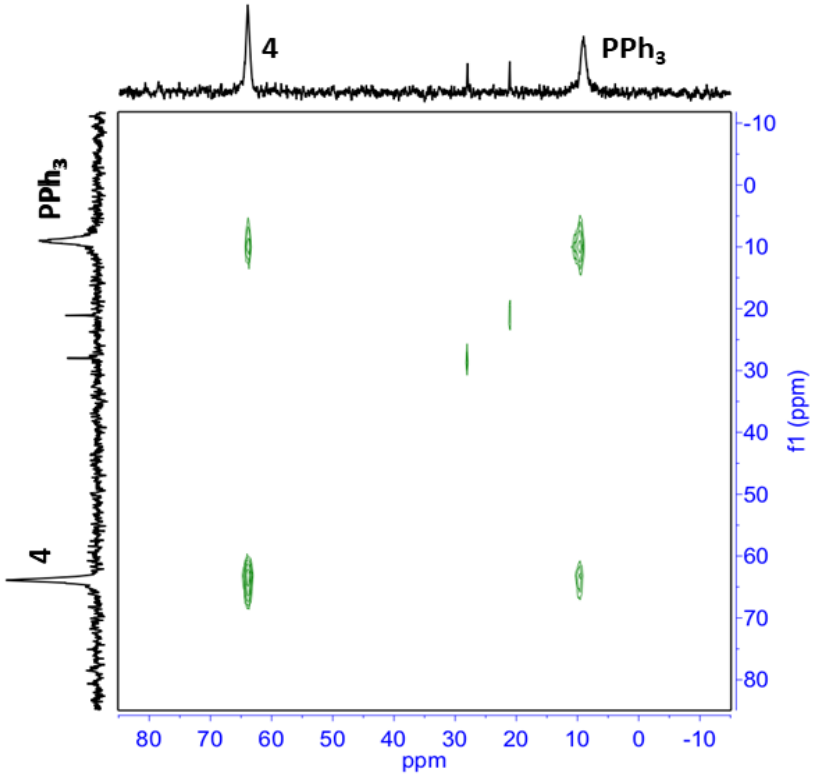

Figure 4.5. A ^{31}P 2D EXSY NMR spectrum of a mixture of compound **4.4** and free PPh_3 in a CD_2Cl_2 solution at room temperature.

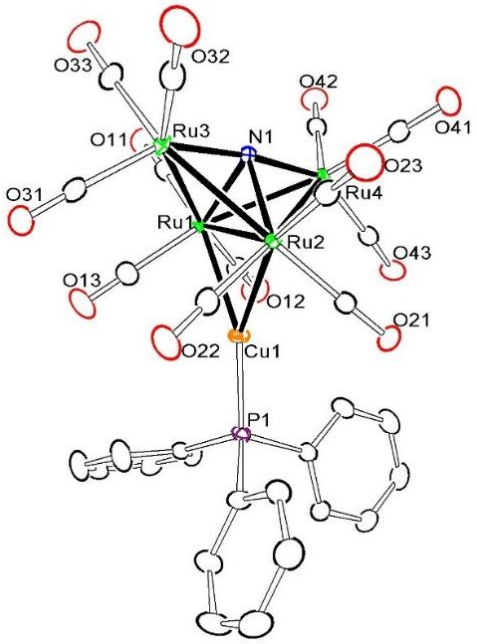

Figure 4.6. An ORTEP diagram of the molecular structure of the compound $Ru_4(\mu_4\text{-}N)(CO)_{12}[\mu\text{-}Cu(PPh_3)]$, **4.5**, showing the 50% thermal ellipsoidal probability. Selected interatomic bond distances (Å) are as follow: Ru1-Cu1 = 2.5865(3), Ru2-Cu1 = 2.5966(3), Ru1-Ru2 = 2.7546(2), Ru1-Ru4 = 2.7807(2), Ru2-Ru4 = 2.7790(2), Ru1-Ru3 = 2.7717(2), Ru2-Ru3 = 2.7826(2), Ru1 – N1 = 2.0852(15), Ru2 – N1 = 2.0790(15), Ru3 – N1 = 1.9352(15), Ru4 – N1 = 1.9359(15), Cu1-P1 = 2.2048(5).

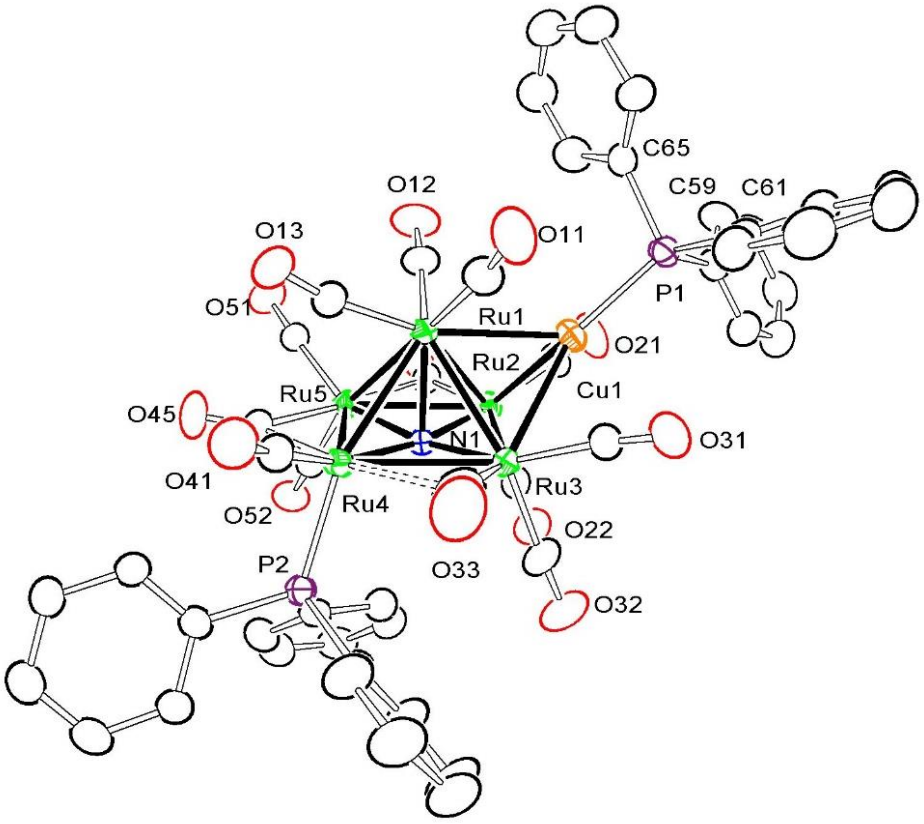

Figure 4.7. An ORTEP diagram of the molecular structure of the compound $Ru_5(\mu_5\text{-}N)(CO)_{13}(PPh_3)[\mu_3\text{-}Cu(PPh_3)]$, **4.6**, showing the 30% thermal ellipsoidal probability. Selected interatomic bond distances (Å) are as follow: Cu1-P1 = 2.2508(13), Cu1-Ru1 = 2.6722(6), Cu1-Ru2 = 2.6855(7), Cu1-Ru3 = 2.7075(7), Ru1-Ru2 = 2.7985(5), Ru1-Ru3 = 2.7820(5), Ru1-Ru4 = 2.848(7), Ru1-Ru5 = 2.7907(5), Ru2-Ru3 = 2.8844(5), Ru2-Ru5 = 2.8265(5), Ru3-Ru4 = 2.8980(5), Ru4-Ru5 = 2.8201(5), Ru1-N1 = 2.128(3), Ru2-N1 = 2.023(3), Ru3-N1 = 2.013(3), Ru4-N1 = 2.048(3), Ru5-N1 = 2.032(3), Ru4-P2 = 2.3076(12).

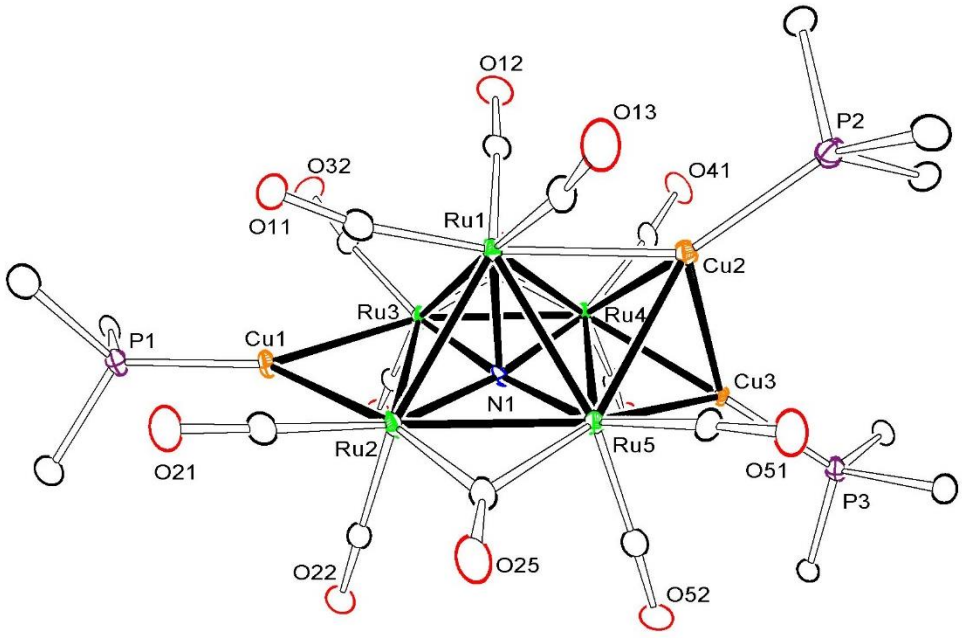

Figure 4.8. An ORTEP diagram of the molecular structure of the compound $Ru_5(\mu_5\text{-}N)(CO)_{13}[\mu\text{-}Cu(PPh_3)][\mu_3\text{-}\{Cu(PPh_3)_2\}]$, **4.7**, showing the 25% thermal ellipsoidal probability. For clarity only the *ipso*-carbon atoms of the phenyl rings are shown. Selected interatomic bond distances (Å) are as follow: Cu2-Cu3 = 2.6211(9), Ru1-Ru3 = 2.7755(6), Ru1-Ru2 = 2.8178(6), Ru1-Ru5 = 2.8006(6), Ru1-Ru4 = 2.7917(6), Ru2-Ru5 = 2.7994(6), Ru2-Ru3 = 2.8767(6), Ru3-Ru4 = 2.8089(6), Ru4-Ru5 = 2.9603(6), Ru1-Cu2 = 2.7252(7), Ru2-Cu1 = 2.6129(7), Ru3-Cu1 = 2.6101(7), Ru4-Cu2 = 2.6794(7), Ru4-Cu3 = 2.6199(7), Ru5-Cu2 = 2.7029(7), Ru5-Cu3 = 2.6968(7), Ru1-N1 = 2.132(4), Ru2-N1 = 2.034(4), Ru3-N1 = 2.028(4), Ru4-N1 = 2.034(4), Ru5-N1 = 2.039(4), Cu1-P1 = 2.2182(15), Cu2-P2 = 2.2633(15), Cu3-P3 = 2.2259(15).

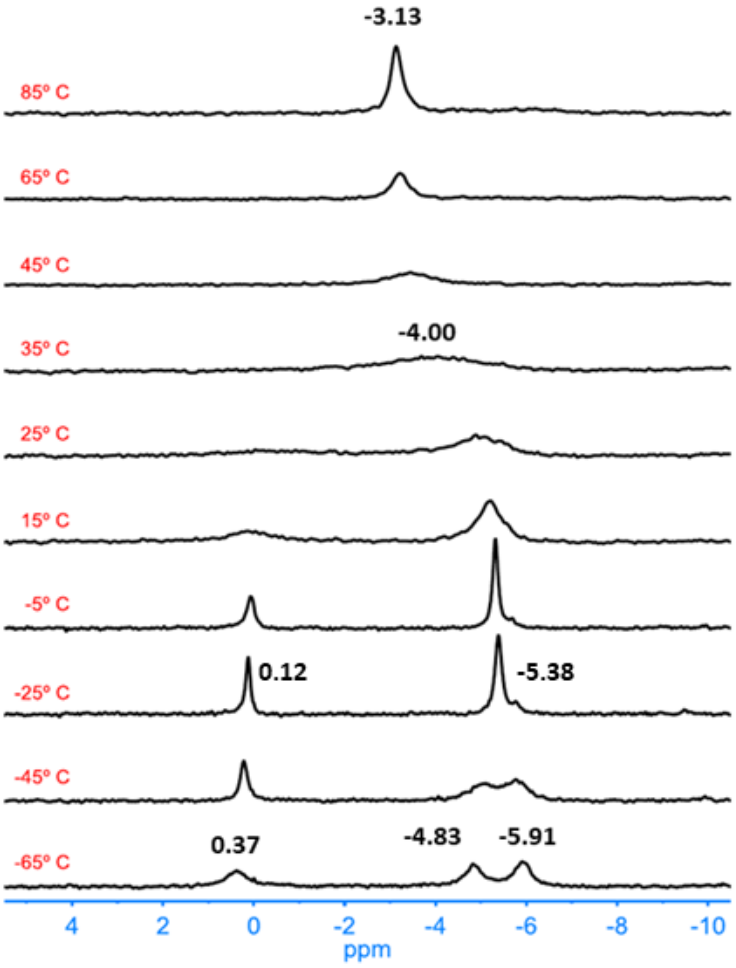

Figure 4.9. A stacked plot of ^{31}P NMR spectra of compound **4.7** in toluene-d_8 solvent showing the resonances for the PPh_3 ligands recorded at different temperatures.

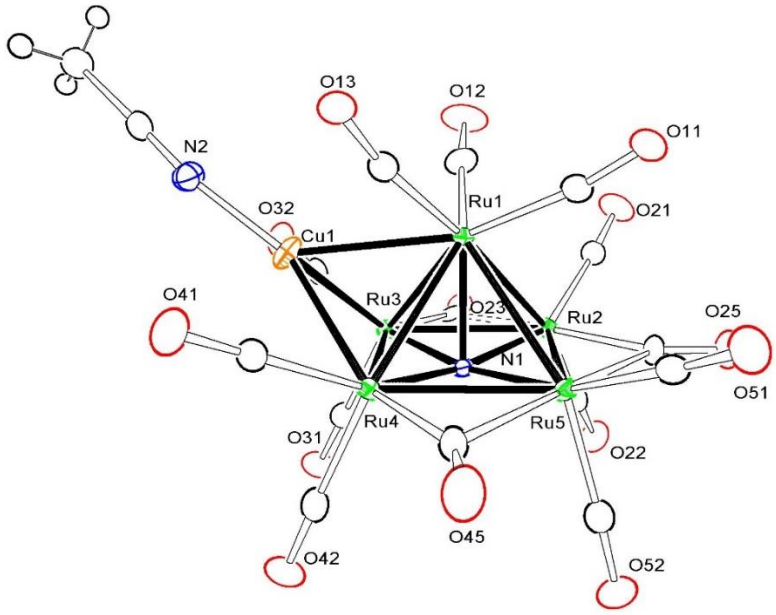

Figure 4.10. An ORTEP diagram of the molecular structure of the compound $Ru_5(\mu_5\text{-}N)(CO)_{14}[\mu_3\text{-}Cu(NCMe)]$, **4.8**, showing the 50% thermal ellipsoidal probability. Selected interatomic bond distances (Å) are as follow: Ru1-Cu1 = 2.7404(6), Ru3-Cu1 = 2.5902(6), Ru4-Cu1 = 2.6487(6), Ru1-Ru2 = 2.7771(4), Ru1-Ru3 = 2.7991(4), Ru1-Ru4 = 2.7661(4), Ru1-Ru5 = 2.8100(5), Ru2-Ru3 = 2.8302(5), Ru2-Ru5 = 2.7993(5), Ru3-Ru4 = 2.9684(5), Ru4-Ru5 = 2.7984(5), Ru1-N1 = 2.126(3), Ru2-N1 = 2.037(3), Ru3-N1 = 2.009(3), Ru4-N1 = 2.019(3), Ru5-N1 = 2.037(3), Cu1-N2 = 1.909(4).

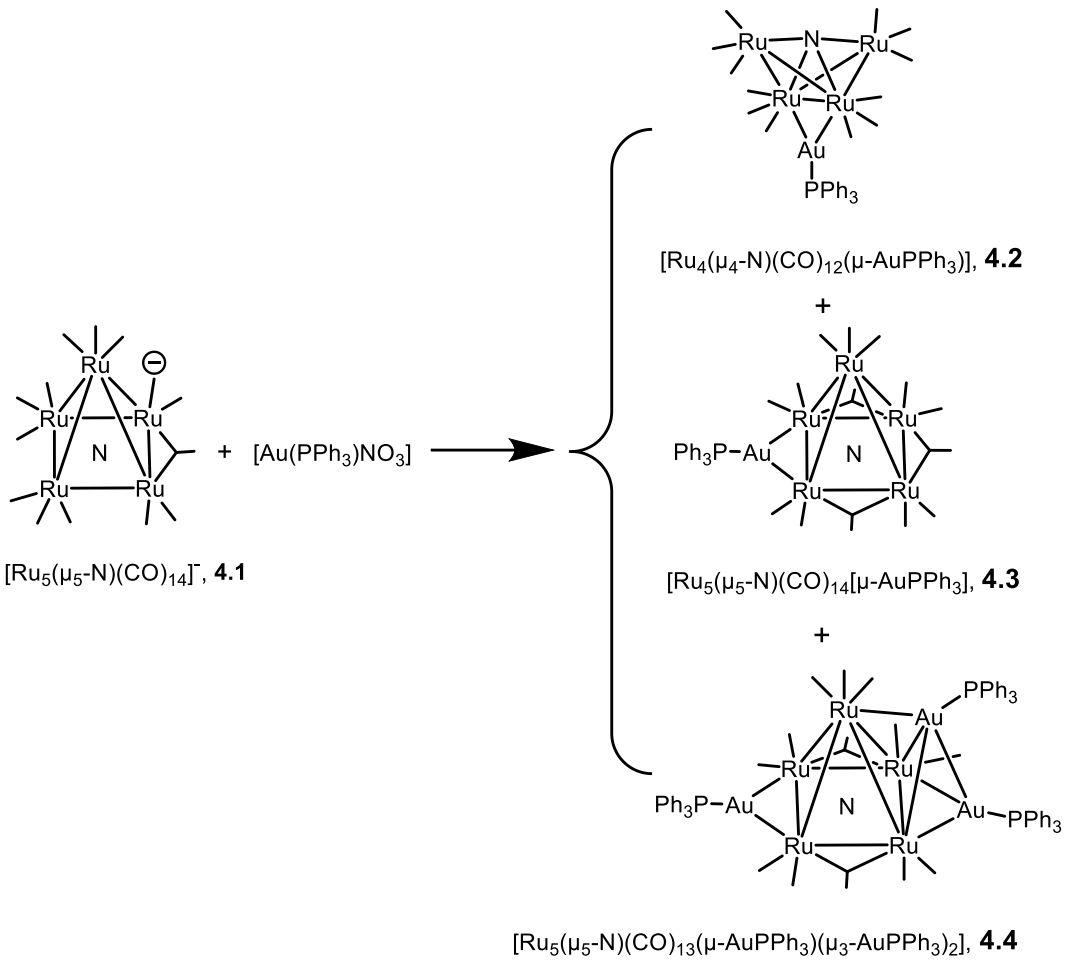

Scheme 4.1. A schematic of the products obtained from the reaction of anion **4.1** with $Au(PPh_3)NO_3$.

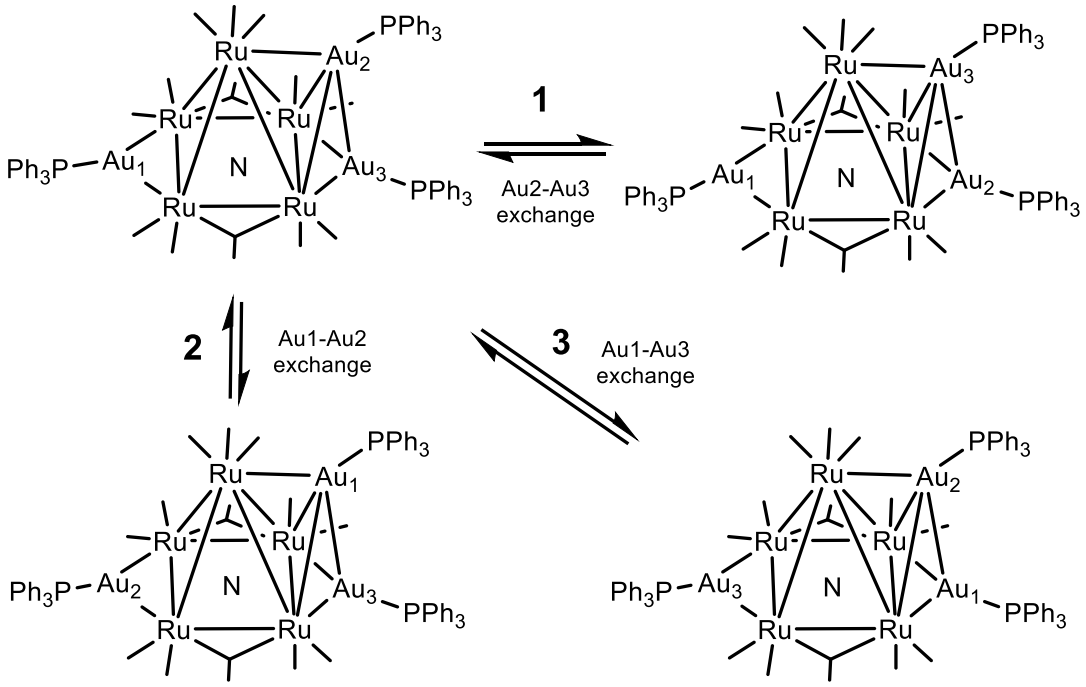
Ru
Au2
PPh3
Ru
Ru
Ph3P
Au1
N
Au3
PPh3
Ru
Ru
1
Au2-Au3
exchange
Ru
Au3
PPh3
Ru
Ru
Ph3P
Au1
N
Au2
PPh3
Ru
Ru
2
Au1-Au2
exchange
3
Au1-Au3
exchange
Ru
Au1
PPh3
Ru
Ru
Ph3P
Au2
N
Au3
PPh3
Ru
Ru
Ru
Au2
PPh3
Ru
Ru
Ph3P
Au3
N
Au1
PPh3
Ru
Ru

Scheme 4.2

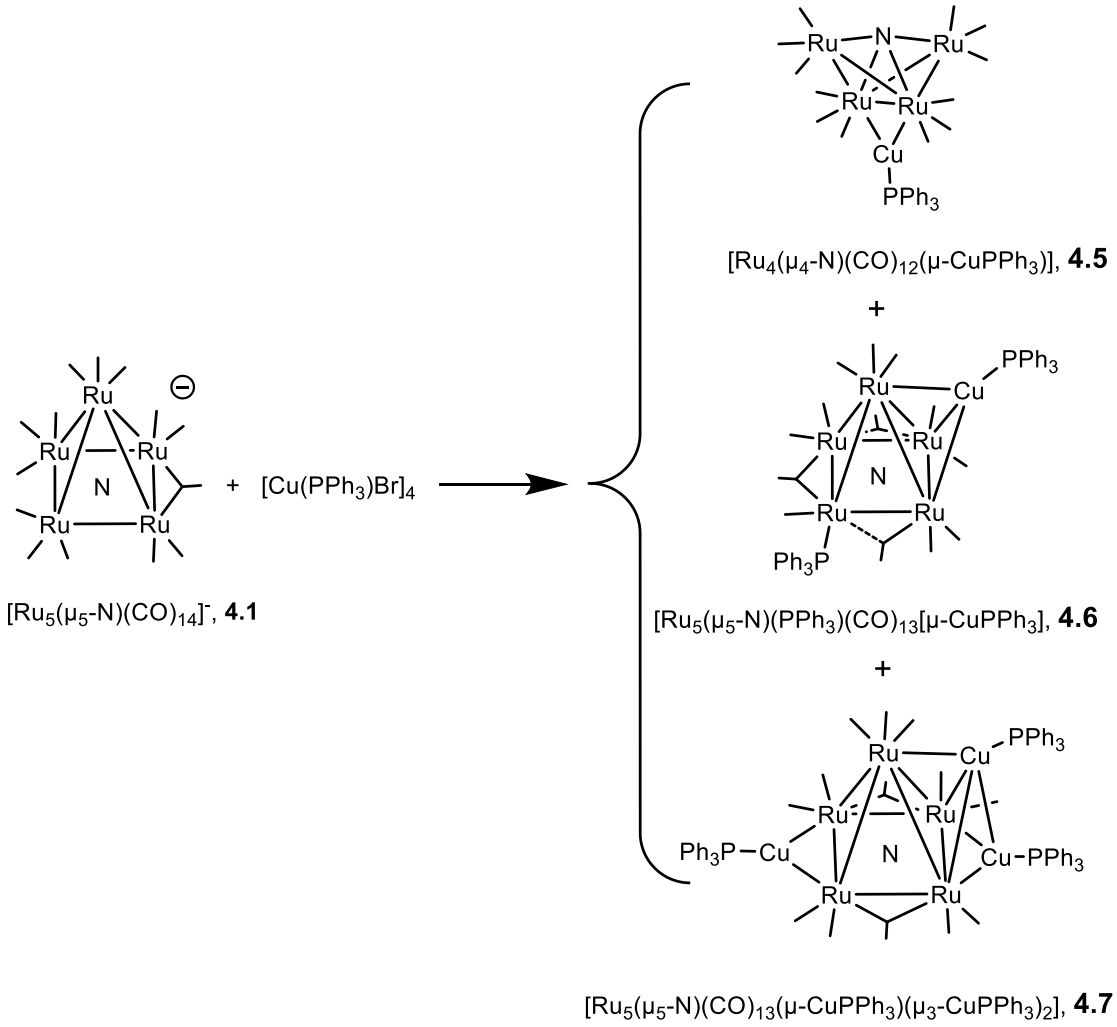

Scheme 4.3. A schematic of the products obtained from the reaction of anion **4.1** with $[Cu(PPh_3)Br]_4$.

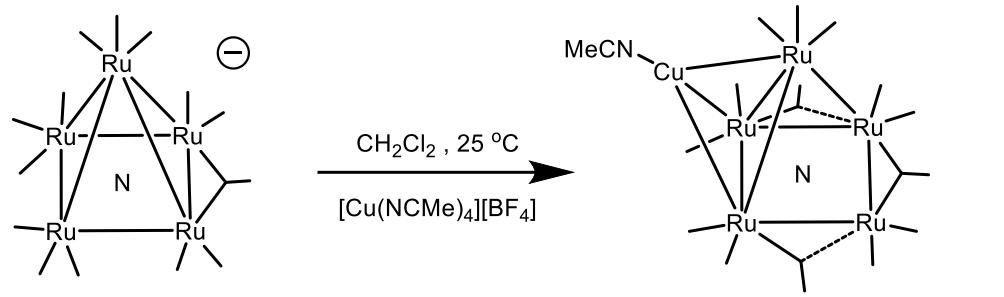

[PPN][$Ru_5(\mu_5\text{-}N)(CO)_{14}$] [$Ru_5(\mu_5\text{-}N)(CO)_{14}\{\mu_3\text{-}Cu(NCMe)\}$], **4.8**

Scheme 4.4. A schematic for the reaction of **4.1** with $[Cu(NCMe)_4][BF_4]$.

4.5 References

1. (a) H.-L. Jiang, Q. Xu, Recent progress in synergistic catalysis over heterometallic nanoparticles, *J. Mater. Chem.* **2011**, *21*, 13705 - 13725. (b) G. Kyriakou, A. M. Marquez, J. P. Holgado, M. J. Taylor, A. E. H. Wheatley, J. P. Mehta, J. F. Sanz, S. K. Beaumont, Comprehensive Experimental and Theoretical Study of the CO + NO Reaction Catalyzed by Au/Ni Nanoparticles, *ACS Catal*. **2019**, *9*, 4919−4929. (c) F. Gao, D. W. Goodman, Pd–Au bimetallic catalysts: understanding alloy effects from planar models and (supported) nanoparticles, *Chem. Soc. Rev.* **2012**, *41*, 8009–8020. (d) M. Chen, D. Kumar, C.-W. Yi, D.W. Goodman, The Promotional Effect of Gold in Catalysis by Palladium-Gold, *Science* **2005**, *310*, 291 – 293. (e) G. J. Hutchings, Selective oxidation using supported gold bimetallic and trimetallic nanoparticles, *Catalysis Today*, **2014**, *238*, 69–73. (f) Y. Zhang, X. Cui, F. Shi, Y. Deng, Nano-Gold Catalysis in Fine Chemical Synthesis, *Chem. Rev.* **2012**, *112*, 2467–2505. (g) G. J. Hutchings, Nanocrystalline gold and gold palladium alloy catalysts for chemical Synthesis, *Chem. Commun.* **2008**, 1148 – 1164. (h) J. A. Lopez-Sanchez, N. Dimitratos, N. Glanvilla, L. Kesavan, C. Hammond, J. K. Edwards, A. F. Carley, C. J. Kiely, G. J. Hutchings, Reactivity studies of Au–Pd supported nanoparticles for catalytic applications, *Applied Catalysis A: General* **2011**, *391*, 400 – 406. (i) M. Sharma, B. Das, M. J. Baruah, S. Biswas, S. Roy, A. Hazarika, S. K. Bhargavad, K. K. Baniaa, Pd-Au-Y as Efficient Catalyst for C-C Coupling Reactions, Benzylic C-H Bond Activation and Oxidation of Ethanol for Synthesis of Cinnamaldehydes, *ACS Catal.* **2019**, *9*, 5860−5875. (j) M. Hasbi Ab Rahim, R. D. Armstrong, C. Hammond, N. Dimitratos, S. J. Freakley, M. M. Forde, D. J. Morgan, G. Lalev, R. L. Jenkins, J. A. Lopez-Sanchez, S. H. Taylor, G. J. Hutchings, Low temperature selective oxidation of methane to methanol using titania supported gold palladium copper catalysts, *Catal. Sci. Technol.*, **2016**, *9*, 3410-3418. (k) P. Buchwalter, J. Rosé, P. Braunstein, Multimetallic Catalysis Based on Heterometallic Complexes and Clusters, *Chem. Rev.* **2015**, *115*, 28–126. (l) M. Böhmer, F. Kampert, T. T. Y. Tan, G. Guisado-Barrios, E. Peris, F. E. Hahn, IrIII/AuI and RhIII/AuI Heterobimetallic Complexes as Catalysts for the Coupling of Nitrobenzene and Benzylic Alcohol, *Organometallics* **2018**, *37*, 4092 - 4099. (m) J. Wisniewska, C.-M. Yang, M, Ziolek, Changes in bimetallic silver–platinum catalysts during activation and oxidation of methanol and propene, *Catalysis Today* **2019**, *333*, 89–96. (n) M. Zhu, X.-L. Du, Y. Zhao, B. Mei, Q. Zhang, F. Sun, Z. Jiang, Y.-M. Liu, H.-Y. He, and Y. Cao, Ring-Opening Transformation of 5-Hydroxymethylfurfural Using a Golden Single-Atomic-Site Palladium Catalyst, *ACS Catal.* **2019**, *9*, 6212−6222.

2. (a) D. S. Shephard, T. Maschmeyer, G. Sankar, J. M. Thomas, D. Ozkaya, B. F. G. Johnson, R. Raja, R. D. Oldroyd, R. G. Bell, Preparation, Characterisation and Performance of Encapsulated Copper - Ruthenium Bimetallic Catalysts Derived from Molecular Cluster Carbonyl Precursors, *Chem. Eur. J.* **1998**, *4*, 1214 – 1224. (b) J. F. Sinfelt, Catalysis by Alloys and Bimetallic Clusters, *Accts. Chem. Res.* **1977**, *10*, 15 - 20. (c) J. F. Sinfelt, Supported "Bimetallic Cluster" Catalysts, *J. Catal.* **1973**, *29*, 308-315. (d) J. F. Sinfelt, Catalysis by Alloys and Bimetallic Clusters, Acc. Chem. Res., *1977, 10*, 15–20. (e) J. F. Sinfelt, Y. L. Lam, J. A. Cusumano, A. E. Barnett, Nature of Ruthenium-Copper Catalysts, *J. Catal.* **1976**, *42*, 227- 237.

3. (a) P. Buchwalter, J. Rosé, P. Braunstein, Multimetallic Catalysis Based on Heterometallic Complexes and Clusters, *Chem. Rev.* **2015**, *115*, 28−126. (b) M. H. Perez-Temprano, J. A. Casares, P. Espinet, Bimetallic Catalysis using Transition and Group 11 Metals: An Emerging Tool for C-C Coupling and Other Reactions, *Chem. Eur. J.* **2012**, *18*, 1864 – 1884. (c) W. Yu, M. D. Porosoff, J. G. Chen, Review of Pt-Based Bimetallic Catalysis: From Model Surfaces to Supported Catalysts, *Chem. Rev.* **2012**, *112*, 5780−5817. (d) P. Braunstein, J. Rosé, Heterometallic Clusters in Catalysis, in "Metal Clusters in Chemistry", Edited by P. Braunstein, L. A. Oro, P. R. Raithby, Wiley-VCH, Weinheim, **1999**, Ch. 2.2, pp 616 - 677.

4. (a) C. Ciabatti, M. Femoni, S. Carmela Iapalucci, S. Ruggieri, S. Zacchini**,** The role of gold in transition metal carbonyl clusters, *Coord. Chem. Rev.* **2018**, *355*, 27–38. (b) I. D. Salter, Cluster Complexes with Bonds Between Transition Element and Copper, Silver and Gold, in "Comprehensive Organometallic Chemistry II" E. W. Abel, F. G. A. Stone, G. Wilkinson, Eds., Pergamon, Oxford, **1995**, Vol. 10, Ch. 5, 255 – 322. (c) D.M.P. Mingos, M.J. Watson, Heteronuclear Gold Cluster Compounds, *Adv. Inorg. Chem.* **1992**, *39*, 327–399. (d) I.D. Salter, Heteronuclear Cluster Chemistry of Copper, Silver and Gold, *Adv. Organomet. Chem.* **1989**, *29*, 249–343. (e) T. Nakajimaa, H. Konomotob, H. Ogawab, Y. Wakatsuki, Synthesis of three-component high nuclearity cluster complexes with ruthenium carbido carbonyl clusters as a building block, *J. Organomet. Chem.* **2007**, *692*, 5071–5080 (f) P. Braunstein, J. Rose, Gold in Bimetallic Molecular Clusters, *Gold Bull.* **1985**, *18*, 17–30. (g) M. A. Beswick, J. Lewis, P. R. Raithby, M. C. Ramirez de Arellano, The High Nuclearity Mixed-Metal Cluster Dianions $[Ru_8H_2Cu_7Cl_3(CO)_{24}]^{2-}$ and $[Ru_{12}H_2Cu_6Cl_2(CO)_{34}]^{2-}$ *Angew. Chem. Int. Ed. Engl.* **1997**, *36*, 291 – 293.

5. C. E. Coffey, J. Lewis, R. S. Nyholm, *J. Chem. Soc*. **1964**, 1741 – 1749.

6. (a) R. D. Adams, Synthesis of Compounds Containing Heteronuclear Metal-Metal Bonds, in "Comprehensive Organometallic Chemistry II" G. Wilkinson, F. G. A. Stone, E. W. Abel, Eds. Pergamon, Oxford, **1995**, Vol. 10, Ch. 1, 1-22. (b) D. A. Roberts, G. L. Geoffroy, Synthesis of Compounds Containing Heteronuclear Metal-Metal Bonds, in "Comprehensive Organometallic Chemistry I" E. W. Abel, F. G. A. Stone, G. Wilkinson, Pergamon, Eds., Oxford, **1982**, Vol. 6, Ch. 40, 763 - 877.

7. (a) M. Tachikawa, A. C. Sievert, E. L. Muetterties, M. R. Thompson, C. S. Day, V. W. Day, Metal Clusters. 24.1 Synthesis and Structure of Heteronuclear Metal Carbide Clusters, *J. Am. Chem. Soc.* **1980**, *102*, 1725 – 1727. (b) M. Bortoluzzi, I. Ciabatti, C. Femoni, T. Funaioli, M. Hayatifar, M. C. Iapalucci, G. Longoni, S. Zacchini, Homoleptic and heteroleptic Au(I) complexes containing the new $[Co_5C(CO)_{12}]^-$ cluster as Ligand, *Dalton Trans.* **2014**, *43*, 9633 - 9646. (c) I. Ciabatti, C. Femoni, M. Hayatifar, M. C. Iapalucci, S. Zacchini, Co_5C and Co_4C carbido carbonyl clusters stabilized by $[AuPPh_3]^+$ fragments, *Inorg. Chim. Acta*, **2015**, *428*, 203 – 211. (d) B. F. G. Johnson, J. Lewis, W. J. H. Nelson, J. N. Nicholls, M. D. Vargas, *J. Organomet. Chem.* **1983**, *249*, 255 – 272.

8. (a) *C. E. Housecroft*, Transition metal boride clusters at the molecular level, *Coord. Chem. Rev.* **1995**, *143*, 297 – 330. (b) *C. E. Housecroft*, Boron atoms in transition metal clusters, *Adv. Organomet. Chem.* **1991**, *33*, 1 – 50.

9. (a) C. K. Schauer, E. J. Voss, M. Sabat, D. F. Shriver, Synthesis and structure of a capped square-pyramidal five-metal oxo cluster, $[Fe_2Ru_3(CO)_{14}(\mu_4\text{-}O)]^{2-}$, *J. Am. Chem. Soc.* **1989**, *111*, 7662-7664. (b) C. K. Schauer, D. F. Shriver, Synthesis and Structure of $[(PPh_3)_2N][Fe_3Mn(CO)_{12}(\mu_4\text{-}O)]$: A Butterfly Oxo Cluster, *Angew. Chem., Int. Ed.* **1987**, *26*, 255 - 256.

10. R. Della Pergola, A. Fumagalli, F. Fabrizi de Biani, L. Garlaschelli, F. Laschi, M. Carlotta Malatesta, M. Manassero, E. Roda, M. Sansoni, and P. Zanello, Carbonyl-Nitrido Mixed-Metal Clusters: Synthesis, Reactivity, Electrochemical Behavior and Solid-State Structure of $[Co_5MoN(CO)_{14}]^{2-}$ and $[Co_5MoN(CO)_{14}AuPPh_3]^{-}$, *Eur. J. Inorg. Chem.* **2004** 3901-3906.

11. Binsch, G. in *Dynamic Nuclear Magnetic Resonance Spectroscopy*, Jackman, L. M.; Cotton, F. A., Academic Press, New York, **1975**, Ch. 3, (a) Sec. II.B, p 50; (b) Sec. V.B p 76.

12. M. L. Blohm, W. L. Gladfelter, *Inorg. Synth.* **1989**, *26*, 286 **–** 289.

13. G.B. Kauffman, L. A. Teter, *Inorg. Synth.* **1963**, *7*, 9.

14. L. Malatesta, L. Naldini, G. Simonetta, F. Cariati, *Coord. Chem. Rev.* **1966**, *1*, 255−262.

15. SAINT+, version 6.2a, Bruker Analytical X-ray Systems, Inc., Madison, WI, **2001**.

16. G. M. Sheldrick, SHELXTL, version 6.1, Bruker Analytical X-ray Systems, Inc., Madison, WI, **1997**.

17. APEX3 Version 2016.5-0 and SAINT Version 8.37A. Bruker AXS, Inc. Madison, WI, USA.

18. SADABS Version 2016/2. L. Krause, R. Herbst-Irmer, G. M. Sheldrick, D. Stalke, J. *Appl. Cryst.* **2015**, *48*, 3-10.

19. D. Braga, B. F. G. Johnson, J. Lewis, J. M. Mace, M. McPartlin, J. Puga, W. J. H. Nelson, P. R. Raithby, K. H. Whitmire, The reaction of NO^+ with some anions of osmium and ruthenium: synthesis and X-ray characterization of $[H_3Os_4(CO)_{12}(\mu_2\text{-}NO)]$ and $[HRu_4N(CO)_{11}P(OMe)_3]$, *J. Chem. Soc., Chem. Commun.* 1982, **1081-1083.**

20. S. Harris, M. L. Blohm, W. L. Gladfelter, Comparison of the Electronic Structures of Homo- and Heteronuclear Butterfly Clusters Containing Carbide, Nitride, and Oxide

Ligands. Crystal and Molecular Structure of [PPN][$Ru_4N(CO)_{12}$], *Inorg. Chem.* **1989**, *28*, 2290-2297.

21. D. M. P. Mingos, D. M. P.; May, A. S., in The Chemistry of Metal Cluster Complexes. D. F. Shriver, H. D. Kaesz, R. D. Adams, VCH Publishers, New York, **1990**, Ch. 2.

22. A. G. Cowie, B. F. G. Johnson, J. Lewis, P. R. Raithby, Synthesis of the Tetraruthenium Carbido Cluster [$Ru_4(H)_2C(CO)_{12}$)] via Mixed Ruthenium-Gold Carbido Intermediates: X-Ray Crystal Structures of [$Ru_4C(CO)_{12}$)($AuPMe_2Ph)_2$], [$Ru_4C(CO)_{12}$)(I)($AuPEt_3)_2$], and [$Ru_4(H)C(CO)_{12}$)($AuPPh_3$)], *J. Chem. Soc., Chem. Commun.* 1984**, 1710-1712.**

23. M. L. Blohm, D. E. Fjare, W. L. Gladfelter, Formation of a new nitrido cluster from a cluster coordinated isocyanate, *Inorg. Chem.* **1983**, *22*, 1004- 1006.

24. (a) R. Bau, M.H. Drabnis, Structures of transition metal hydrides determined by neutron diffraction, *Inorg. Chim. Acta* **1997**, *259*, 27. (b) R.G. Teller, R. Bau, Crystallographic studies of transition metal hydride complexes, *Struct. Bonding, Berlin, Ger.* **1981**, *41*, 1.

25. C. E. Housecroft, D. M. Matthews, A. L. Rheingold, $Ru_5(CO)_{15}B(AuPPh_3)$: A Novel Boride Cluster Formed by the Degradation of $Ru_6(CO)_{17}B(AuPPh_3)$, *Organometallics* **1992**, *11*, 2959-2961.

26. P. J. Bailey, M. A. Beswick, J. Lewis, P. R. Raithby, M. C. Ramirez de Arellano, Reactions of the hexaruthenium cluster anions $[Ru_6C(CO)_{16}]^{2-}$ and $[Ru_6(CO)_{18}]^{2-}$ with $Au_2(Ph_2PCH_2PPh_2]Cl$,: crystal and molecular structures of $Ru_6C(CO)_{16}Au_2(Ph_2PCH_2PPh_2)$ and $Ru_5(CO)_{15}Au_2(Ph_2PCH_2PPh_2)$, *J. Organomet. Chem.* **1993**, *459*, 293-301.

27. A. J. Amoroso, A. J. Edwards, B. F.G. Johnson, J. Lewis, M. R. Al-Mandhary, P. R. Raithby, V. P. Saharan and W.-T. Wong, Synthesis of bridged and linked ruthenium and osmium carbonyl clusters containing a [$Au_2(PPh_2CH_2CH_2PPh_2)$] unit. The crystal and molecular structures of $Ru_5C(CO)_{14}[Au_2(PPh_2CH_2CH_2PPh_2)]$ and $Os_4H_3(CO)_{12}\}_2[Au_2(PPh_2CH_2CH_2PPh_2)]$ *J. Organomet. Chem.*, **1993**, *443*, C11 - C13.

28. R. D. Adams, J. Tedder, Organometallic chemistry of pentaruthenium-gold carbonyl cluster complexes, *J. Organomet. Chem.* **2017**, *443*, 58 - 65.

29. C. E. Housecroft, D. M. Nixon, A. L. Rheingold, Pentaruthenium-Based Borides Stabilized by Gold(I) Phosphine Units, *J. Cluster Sci.* **2001**, *12*, 89 – 99.

30. (a) L. J. Farrugia, M. J. Freeman, M. Green, A. G. Orpen, F. G. A. Stone, I. D. Salter, Metal Framework Arrangements in Pentanuclear Gold-Ruthenium Clusters Crystal Structures of [$Au_2Ru_3(\mu_3\text{-}S)(CO)_8(PPh_3)_3$] and [$Au_2Ru_3(\mu\text{-}H)(\mu_3\text{-}COMe)(CO)_9(PPh_3)_2$],

J. Organomet. Chem. **1983**, *249*, 273-288. (b) C. J. Brown, P. J. McCarthy, I. D. Salter, The Heteronuclear Cluster Chemistry of the Group 1B Metals. Part 15. Effect of the Nature of the Group 1B Metals and the Cone Angles of the Attached Phosphine Ligands on the Metal Framework Structures of Heteronuclear Cluster Compounds. Synthesis, Structures, and Dynamic Behaviour of the Bimetallic Hexanuclear Cluster Compounds $[M_2Ru_4H_2(CO)_{12}(PR_3)_2]$ (M = Cu, R = $CHMe_2$ or C_6H_{11}; M = Ag or Au, R = $CHMe_2$, C_6H_{11}, or CMe_3), *J. Chem. Soc., Dalton Trans.* **1990**, 3583 – 3590. (c) I. D. Salter, V. Sik, S. A. Williams, T. Adatia, Variable-temperature nuclear magnetic resonance spectroscopic studies of the dynamic behaviour of the mixed-metal cluster compounds $[MM'Ru_4H_2(\mu\text{-dppf})(CO)_{12}]$ [M = M' = Cu, Ag or Au; M = Cu, M' = Au; dppf = $Fe(\eta^5\text{-}C_5H_4PPh_2)_2$] and the crystal structures of $[MM'Ru_4H_2(\mu\text{-dppf})(CO)_{12}]$ (M = Cu or Au, M' = Au), *J. Chem. Soc., Dalton Trans.*, **1996**, 643 – 652.

31. R. K. Harris, in Nuclear Magnetic Resonance Spectroscopy, Longman Scientific & Technical, Essex, England, **1986**, Ch. 5, p. 116.

32. R. A. Brice, S. C. Pearse, I. D. Salter, The Heteronuclear Cluster Chemistry of the Group 1B Metals. Part 1. Structural Similarities and Differences Among Mixed-metal Cluster Compounds containing Copper, Silver, or Gold Atoms ligated by Phosphines. X-Ray Crystal Structures of $[CuRu_4(\mu_3\text{-}H)_3(CO)_{12}(PMePh_2)]$ and $[CuRu_3(CO)_9(C_2Bu^t)(PPh_3)]$, *J. Chem. Soc. Dalton Trans.* **1986**, 2181 – 2192.

33. M. I. Bruce, M. L. Williams, J. M. Patrick, B. W. Skelton, A. H. White, Cluster chemistry. Part 45. Synthesis and some reactions of $[Ru_3(\mu_3\text{-}PPhCH_2PPh_2)(CO)_9]^-$: X-ray crystal structures of $[MRu_3(\mu_3\text{-}PPhCH_2PPh_2)(CO)_9(PPh_3)]$ (M = Cu, Ag, or Au), *J. Chem. Soc., Dalton Trans.* **1986**, 2557 – 2567.

34. J. S. Bradley, R. L. Pruett, E. Hill, G. B. Ansell, M. E. Leonowicz, M. A. Modrick, Synthesis and Molecular Structure of Bis(acetonitrilecuprio)carbidohexadecacarbonylhexaurthenium, $[(CH_3CN)_2Cu_2Ru_6C(CO)_{16}]$, a Bimetallic Carbidocarbonyl Cluster Containing a Copper-Copper Bond, *Organometallics* **1982,** *1*, 748 – 752.

CHAPTER 5

COPPER CARBENE COMPLEXES. SYNTHESIS AND STRUCTURAL ANALYSIS OF A CHLORO-BRIDGED DICOPPER CATION AND THE TRIOSMIUM-COPPER CARBENE CLUSTER COMPLEX $HOs(CO)_{11}[\mu\text{-}Cu(IPr)]^{+}$ [4]

[4]Adams, R. D.; Smith, M. D.; Tedder, J. D.; Wakdikar, N. D.; *J. Organomet. Chem.* **2021**, 941, 121799

Reprinted here with permission from publisher

5.1 Introduction

The Group 11 elements, Cu, Ag and Au, widely referred to as the "coinage metals", are well-known for their stability in their elemental forms and because of their monetary value, they have been used as forms of currency throughout the world.[1] In recent years, a variety of ligated forms of ions of these metals have been synthesized and shown to exhibit useful chemistry including catalytic transformations of organic compounds.[2-6] Copper has been one of the more chemically investigated members of this family of metals,[3-4] and N-heterocyclic carbenes have been shown to be particularly effective ligands for ions of copper.[7] In the present study, we have prepared the new chloro-bridged dicopper complex $[\{(IPr)Cu\}_2(\mu\text{-}Cl)][PF_6]$, **5.1**, IPr = N,N′-bis(2,6-diisopropylphenyl)imidazolin-2- ylidene from the reaction of (IPr)CuCl with $Tl[PF_6]$ and investigated its structure and reactivity.

Recently, there has been great interest in the potential of heterometallic materials to perform heterogeneous catalysis.[8] These materials frequently exhibit improved activity, selectivity and longevity compared to their homometallic components. Copper has been shown to be an effective modifier and cocatalyst for bimetallic catalysts.[9] It has been shown that bi- and polymetallic cluster complexes can serve as excellent precursors to heterometallic catalysts and this has stimulated interest in the synthesis of heterometallic cluster complexes for this purpose.[10]

Efforts have been made successfully to introduce carbene ligated-copper groupings into metal carbonyl cluster complexes.[11] but to date there are no examples of copper carbene complexes containing osmium. In the present work, we have investigated the reaction of the new dicopper cation of **5.1** with the triosmium carbonyl anion

$[HOs_3(CO)_{11}]^-$ obtained via the salt $[PPN][HOs_3(CO)_{11}]$, **5.2**. This reaction has yielded the new bimetallic complex $Os_3(CO)_{11}(H)[\mu\text{-}Cu(IPr)]$, **5.3**, the first example of Cu – Os carbonyl cluster complex containing a N-heterocyclic carbene ligand. Compounds **5.1** and **5.3** were both characterized by IR and ^1H NMR spectroscopy and structurally by single-crystal X-ray diffraction analyses.

5.2 Experimental data

General data

All reactions were performed under an atmosphere of nitrogen by using standard Schlenk techniques. Reagent grade solvents were dried by the standard procedure and were freshly distilled under nitrogen prior to use. Infrared spectra were recorded on a Nicolet IS10 Midinfrared FT-IR spectrophotometer. ^1H NMR spectra were obtained by using a Varian Mercury 300 spectrometer operating at 300 MHz. Mass spectrometric (MS) measurements performed by a direct-exposure probe by using electron impact ionization (EI) or electrospray ionization (ESI) on a VG 70S instrument. $Os_3(CO)_{12}$ and $TlPF_6$ were obtained from STREM and used without further purification. (IPr)CuCl, IPr = [N,N′-bis(2,6-diisopropylphenyl)imidazolin-2-ylidene] was purchased from Sigma Aldrich and was used without further purification. $[PPN][Os_3(CO)_{11}(\mu\text{-}H)]$, **5.2**, PPN = $[Ph_3PNPPh_3]^+$ was prepared according to a previously reported procedure.[12]

Preparation of the dicopper carbene complex, $[\{(IPr)Cu\}_2(\mu\text{-}Cl)][PF_6]$, 5.1.

100.0 mg (0.205 mmol) of (IPr)CuCl was added to 5 mL of methylene chloride in a 100 mL three-neck flask under nitrogen. In an another 100 ml three-neck flask, 143 mg (0.41 mmol) of $TlPF_6$ was added to 5mL of methanol and stirred until it was completely dissolved. The methanol solution of $Tl[PF_6]$ was then added dropwise into the methylene

chloride solution of the (IPr)CuCl. After stirring for 30 min at room temperature, this mixture was passed through a frit containing a celite bed into a 100 ml three-neck flask. Then the solvent was removed *in vacuo* and compound [{(IPr)Cu}$_2$(μ-Cl)][PF_6], **5.1** was isolated by solvent extraction and filtration by using methylene chloride solvent. After reducing the extract and adding few drops of hexane, small white crystals of **5.1** (71% yield) were obtained. Spectral data for **5.1**: ^{1}H NMR (CD_2Cl_2, δ): 7.53 (t, 4H, J = 7.8Hz, para C**H**-$(CH)_2$), 7.30 (d, 8H, J = 7.8Hz, meta CH-(C**H**)$_2$), 7.20 (s, 4H, N(C**H**)$_2$), 2.46 (sept, 8H, J = 6.9Hz, C**H**-$(CH_3)_2$), 1.21 (d, 24H, J = 6.9Hz, CH-(C**H**$_3$)$_2$), 1.12 (d, 24H, J = 6.9Hz, CH-(C**H**$_3$)$_2$). Mass Spec. ESI+/MS *m*/*z*: 939, M^+

Preparation of Cu-Os_3 heterometallic cluster complex, $HOs_3(CO)_{11}$[μ-Cu(IPr)], **5.3.**

In a 100 mL flask, 54.7 mg (0.039mmol) of [PPN][$HOs_3(CO)_{11}$], **5.2** was added to 10 mL of methylene chloride under a slow purge of nitrogen. To this mixture was added 72.4 mg (0.067 mmol) of **5.1**. After stirring for 15 min at room temperature, the solvent was removed *in vacuo.* The product, $HOs_3(CO)_{11}$[μ-Cu(IPr)], **5.3 (**10% yield) was then obtained in a pure form by a combination of extraction using hexane, filtration and crystallization from pure hexane at -78˚C. Spectral data for **5.3**: IR spectra, ν_{CO} (cm^{-1} in hexane): 2106.1(w), 2069.1(w), 2052.6(m), 2037.6(s), 2020.0(vs), 2002.6(w), 1979.3(w), 1960.4(vw), 1955.3(vw). ^{1}H NMR (CD_2Cl_2, δ in ppm): 7.45 (t, 2H, J = 7.5Hz, para C**H**-$(CH)_2$), 7.33 (d, 4H, J = 7.5Hz, meta CH-(C**H**)$_2$), 7.18 (s, 2H, N(C**H**)$_2$), 2.82 (sept, 4H, J = 6.3Hz, C**H**-$(CH_3)_2$), 1.38 (d, 12H, J = 6.3Hz, CH(C**H**$_3$)$_2$), 1.16 (d, 12H, J = 6.3Hz, CH(C**H**$_3$)$_2$), -10.04 (s, 1H). Mass Spec. ESI/MS *m*/*z*: 1333, M^+.

Crystallographic Analyses.

Single crystals of compounds **5.1** and **5.3** suitable for X-ray diffraction analyses were obtained by slow evaporation of solvent from solutions at room temperature. Each data crystal was glued onto a glass fiber. X-ray diffraction intensity data for compound **5.1** was obtained by using a Bruker SMART APEX CCD-based diffractometer by using Mo Kα radiation (λ = 0.71073 Å). The raw data frames were integrated with the SAINT + program by using a narrow frame integration algorithm.[13] Correction for Lorentz and polarization effects were also applied with SAINT+. An empirical absorption correction based on the multiple measurements of equivalent reflections was applied by using the program SADABS were applied in each analysis.[13] X-ray intensity data for compound **5.3** was obtained by using a Bruker D8 QUEST diffractometer equipped with a PHOTON-100 CMOS area detector and an Incoatec microfocus source (Mo Kα radiation, λ = 0.71073 Å). The data collection strategy consisted of three 180° ω-scans at different φ settings and one 360° φ-scan, with a scan width per image of 0.5°. The crystal-to-detector distance was 4.0 cm and each image was measured for 5 s in shutterless mode. The average reflection redundancy was 9.6. The raw area detector data frames were reduced, scaled and corrected for absorption effects using the SAINT[14] and SADABS[15] programs. All structures were solved by a combination of direct methods and difference Fourier syntheses, and refined by full-matrix least squares refinement on F^2 by using the SHELXTL software package.[16] All non-hydrogen atoms were refined with anisotropic thermal parameters. All hydrogen atoms were placed in geometrically idealized positions and were included as standard riding atoms during the final least-squares refinements with C-H distances fixed at 0.96

Å. Compound **5.1** crystallized in the monoclinic crystal system whereas compound **5.3** crystallized in the orthorhombic crystal system. The space group $P2_1/c$ was uniquely identified for compound **5.1** based on systematic absences observed in the intensity data. The space group *C*mcm was identified for compound **5.3** on the basis of the systematic absences observed in the intensity data. Crystal data, data collection parameters, and results for the analyses for both compounds are listed in Table 5.1.

5.3 Results and Discussion

The dicopper cation $[\{(IPR)Cu\}_2(\mu\text{-}Cl)]^+$ of the salt $[\{(IPr)Cu\}_2(\mu\text{-}Cl)][PF_6]$, **5.1**, was obtained in 71% yield from the reaction of (IPr)CuCl with $Tl[PF_6]$ in CH_2Cl_2 solvent at room temperature in 30 min, see Scheme 5.1. A number of ligand-bridged bis(copper carbene) complexes have been reported in recent years,[17] but very few of them contain bridging chloro ligands. Compound **5.1** was characterized by ^1H NMR spectroscopy and electrospray ionization (ESI+) mass spectrometry and single-crystal X-ray diffraction analysis.

An ORTEP diagram of the molecular structure of compound **5.1** is shown in Figure 5.1. This cation of **5.1** contains two Cu(IPr) groupings linked to each other via a nonlinear, bridging chloro ligand. The Cu – Cl bond distances are equal in length within experimental error, Cu1 – Cl1 = 2.120(15) Å, Cu2 – Cl1 = 2.124(15) Å, but are slightly longer than the Cu – Cl bond distance, 2.089 Å, in the precursor complex (IPr)CuCl in which the Cl ligand is bonded to only one Cu atom.[18] Each copper atom in **5.1** exhibits an almost linear coordination geometry, C1-Cu1-Cl1 = 172.53(16) and C28-Cu2-Cl1 = 171.52(15)^o. The Cu1-Cl1-Cu2 angle is nonlinear, 115.2(7)^o. The nonlinearity could be interpreted as bonding to a sp^3-hybridized octet of electrons in Cl which is expanded due

to steric repulsions between the bulky carbene ligands on the copper atoms. Floriani also found a nonlinear, bridging chloro ligand in the cationic dicopper complex $[\{Cu(Me_2NCH_2CH_2NMe_2)(CO)\}_2(\mu\text{-}Cl)]^+$, Cu – Cl – Cu = 103.0(1)°.[19] On the other hand, Kunz found a linear bridging chloro ligand in the cationic dicopper(carbene) complex, $[\{Cu(bimcaMe)\}_2(\mu\text{-}Cl)]^+$, bimca = bis(imidazolin-2-ylidene)carbazolide, which contains a very bulky chelating bis(NHC) carbazolide pincer ligand on each copper atom.[20] Interestingly, for comparison, the Cu – S – Cu angle in the neutral molecule $\{(IPr^*)Cu\}_2(\mu\text{-}S)$ is 120.15(9)°.[21]

The reaction of the dinuclear copper cation **5.1** with the triosmium cluster anion $[Os_3(CO)_{11}(\mu\text{-}H)]^-$, **5.2** at room temperature yielded the heterometallic Cu – Os cluster complex $HOs_3(CO)_{11}[\mu\text{-}Cu(IPr)]$, **5.3** containing the IPr ligand in 10% yield, see Scheme 5.2. Compound **5.3** was characterized structurally by using single-crystal X-ray diffraction analysis.

An ORTEP diagram of the molecular structure of compound **5.3** is shown in Figure 5.2.

Compound **5.3** consists of a triangular cluster of three osmium atoms with a bridging copper carbene ligand lying in the plane of the Os_3 triangle on one edge of the cluster. The compound crystallizes in the space group *C*mcm with only ¼ of the molecule in the asymmetric crystal unit. Thus, the molecule is disordered about a crystallographic C_2 axis. Atoms Os(2), Cu(1) and C(1) lie on this axis. In addition, the three osmium atoms and the copper atom also lie on a crystallographic symmetry plane. In addition, there is a second crystallographic symmetry plane that lies perpendicular to the first symmetry plane. The CN_2C_2 plane of the carbene ligand lies in the second symmetry plane. The two symmetry planes intersect on the C_2 axis. Overall, the molecule contains

C_{2v} crystallographic symmetry. One of the CO ligands, C(13) – O(13), that lies in the first symmetry plane is equally disordered between the two sites, C(13), O(13) and $C(13)^i$, $O(13)^i$, by virtue of the C_2 axis and the second symmetry plane, see Figure 5.2. This ligand has 50% occupancy in each of these two sites. This hydrido ligand was not observed directly in the crystallographic analysis. It is believed to located proximate to the two carbon atoms sites, C(13) and $C(13)^i$, of the disordered carbonyl ligand in the remaining 50% occupancy of these two positions. The bridging copper atom Cu(1) in **5.3** is bonded equally to the two osmium atoms Os(1) and $Os(1)^i$, Os1-Cu1 = $Os1^i$-Cu1 = 2.6654(19) Å. The Os – Cu bond distances to the bridging Cu atom in the related triosmium – copper phosphine complex, $H_3Os_3(CO)_{10}[\mu\text{-}Cu(PPh_3)]$, were 2.695(5) Å and 2.726(5) Å.[22] The Cu-bridged Os1-Os1' bond in this structure is elongated, Os1-$Os1^i$ = 2.9319(17) Å, as compared to the unbridged Os - Os bonds Os1 - Os2 = Os2 - Os1' = 2.8858(10) Å. For comparison, the Os – Os bond lengths in the parent compound $Os_3(CO)_{12}$ are 2.8771(27) Å.[23] The Cu - C distance to the carbene ligand in **5.3**, Cu1-C1= 1.915(17) Å, is slightly longer than Cu - C bonds to the carbene ligands in the cation of **5.1**, 1.874(4) Å and 1.876(5) Å. This may be due to steric interactions between the carbene ligand and the carbonyl ligands on the osmium cluster.

The hydrido ligand in **5.3** exhibits a resonance in the ^1H NMR spectrum at δ = -10.03. The resonance shift is consistent with its assignment as a terminally-coordinated ligand. For reference, the resonances of the terminally-coordinated and bridging hydrido ligands in $Os_3(CO)_{11}H(\mu\text{-}H)$, **5.4** occur at δ = -10.25 and δ = -19.96, respectively, see Scheme 5.3.[23] It is interesting to compare the structure of **5.3** with the structure of **5.4** which contains a bridging hydrido ligand in the location corresponding to the bridging

Cu(IPr) grouping in **5.3**.[24] In **5.4** the terminally-coordinated hydrido ligand is positioned perpendicular to the plane of the Os_3 triangle. By comparison, our structural studies, see above, have indicated that the terminally-coordinated hydrido ligand in **5.3** lies in the plane of the Os_3 triangle proximate to the bridging Cu atom, Scheme 5.3.

The hydrido ligand and the bridging Cu(IPr) grouping in **5.3** each serve only as a 1-electron donor to the Os_3 cluster. Thus, the three osmium atoms in **5.3** contain a total of 48 valence electrons which is consistent with the observed triangular cluster having three Os – Os single bonds, as also found in **5.4.**[24]

5.4 Conclusions

In this work, we have reported the synthesis of the salt $[\{(IPr)Cu\}_2(\mu\text{-}Cl][PF_6]$, **5.1** containing the dicopper cation $[\{(IPr)Cu\}_2(\mu\text{-}Cl]^+$, obtained by using $Tl[PF_6]$ to assist in the removal of one of the chloro ligands from one of two copper complexes, (IPr)CuCl, involved in the synthesis. The second equivalent of (IPr)CuCl then combines with the chloro-deficient one to form the dicopper cation having a bridging chloro ligand. The dicopper cation of **5.1** was found to react with the anion $[Os_3H(CO)_{11}]^-$ of **5.2** at room temperature to yield the heterometallic Cu – Os cluster complex, $HOs_3(CO)_{11}[\mu\text{-}Cu(IPr)]$, **5.3** which contains a IPr ligand on the copper atom that bridges a pair of osmium atoms in the triangular Os_3 cluster. The hydride ligand was not directly observed in the study, but it is believed to lie in the plane of the Os_3 triangular cluster in a terminal coordination site proximate to the Cu atom.

Table 5.1 Crystal data, and results of the X-ray Analyses for compounds **5.1** and **5.3**.

Compound	**5.1**	**5.3**
Empirical formula	$Cu_2PF_6ClN_4C_{54}H_{72}$	$Os_3CuN_2O_{11}C_{38}H_{36}{\cdot}C_6H_6$
Formula weight	1084.66	1408.94
Crystal system	Monoclinic	Orthorhombic
Lattice parameters		
a (Å)	10.8448(7)	14.6728(8)
b (Å)	27.6185(17)	19.4402(11)
c (Å)	19.4284(12)	18.5256(11)
α (deg)	90.00	90.00
β (deg)	92.615(2)	90.00
γ (deg)	90°	90.00
V ($Å^3$)	5813.1(6)	5284.3(5)
Space group	$P2_1/n$	*C*mcm
Z value	4	4
ρ_{calc} (g/cm^3)	1.239	1.771
μ (Mo Kα) (mm^{-1})	0.860	7.638
Temperature (K)	294(2)	302(2)
θ_{max} (°)	27.94	23.50
No. Obs. ($I>2\sigma(I)$)	6657	1571
No. of parameters	629	163
Goodness of fit (GOF)	1.054	1.065
Max. shift/error on final cycle	0.092	0.001
Residuals*: R1; wR2	0.0714; 0.2038	0.0467;0.1323
Absorption Correction, Max/min	Semi-empirical from equivalents 1.000/ 0.856	Semi-empirical from equivalents 0.862/0.461
Largest peak in Final Diff. Map (e^- / $Å^3$)	1.262	1.054

[a] $R1 = \Sigma_{hkl}(||F_{obs}|-|F_{calc}||)/\Sigma_{hkl}|F_{obs}|$; $wR2 = [\Sigma_{hkl}w(|F_{obs}|-|F_{calc}|)^2/\Sigma_{hkl}wF^2_{obs}]^{1/2}$; $w = 1/\sigma^2(F_{obs})$; $GOF = [\Sigma_{hkl}w(|F_{obs}|-|F_{calc}|)^2/(n_{data} - n_{vari})]^{1/2}$

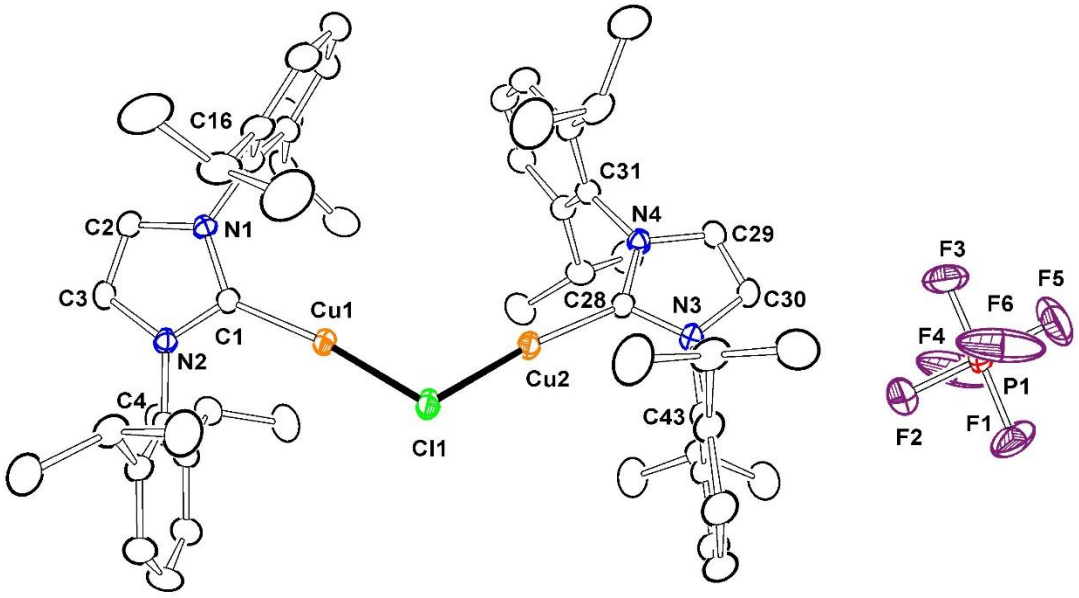

Figure 5.1. ORTEP diagram of the molecular structure of $[\{(IPr)Cu\}_2(\mu\text{-}Cl][PF_6]$, **5.1** showing 15% thermal ellipsoidal probabilities. Selected interatomic distances (Å) and angles (°) are as follows: Cu1-Cl1 = 2.1207 (15), Cu2-Cl1 = 2.1247 (15), Cu1-C1 = 1.874(4), Cu2-C28 = 1.876(5). C1-Cu1-Cl1 = 172.53(16), C28-Cu2-Cl1 = 171.52(15), Cu1-Cl1-Cu2 = 115.24(7).

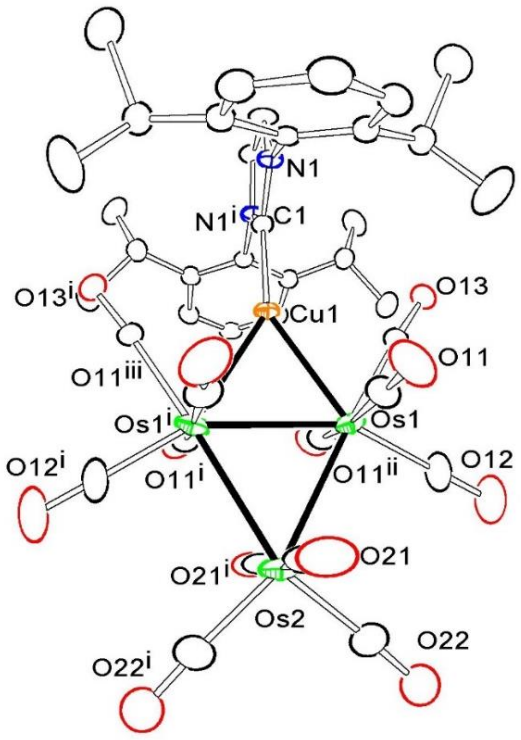

Figure 5.2. ORTEP diagram of the molecular structure of the disordered molecule in the crystal of $HOs_3(CO)_{11}[\mu\text{-}Cu(IPr)]$, **5.3** at 10% ellipsoidal probability. C(13) - O(13) and $C(13^i)$ - $O(13^i)$ have only 50% occupancy at each site and are equally disordered with the one hydrido ligand in the complex. Selected interatomic distances (Å) and angles (^{o}) are as follows: Os1-Cu1 = Cu1-$Os1^i$ = 2.6654(19), Os1-$Os1^i$ = 2.9319(17), Os1-Os2 = 2.8858(10), Cu1-C1 = 1.915(17), C1-N1 = 1.361(14).

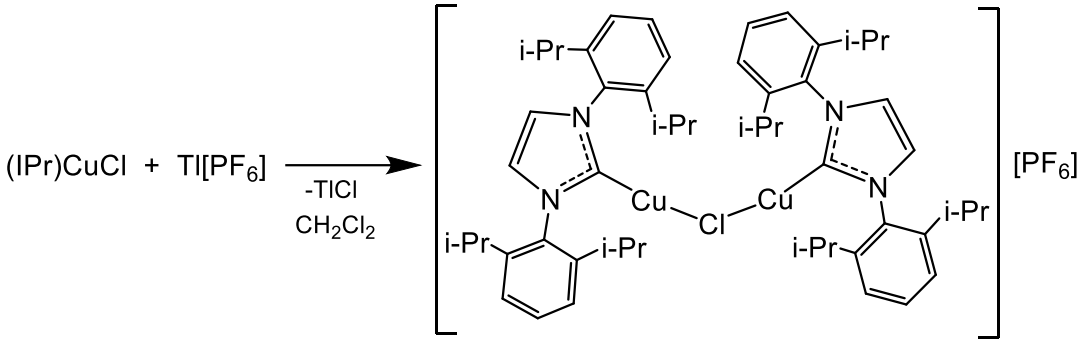

Scheme 5.1. A schematic for the synthesis of cation **5.1**.

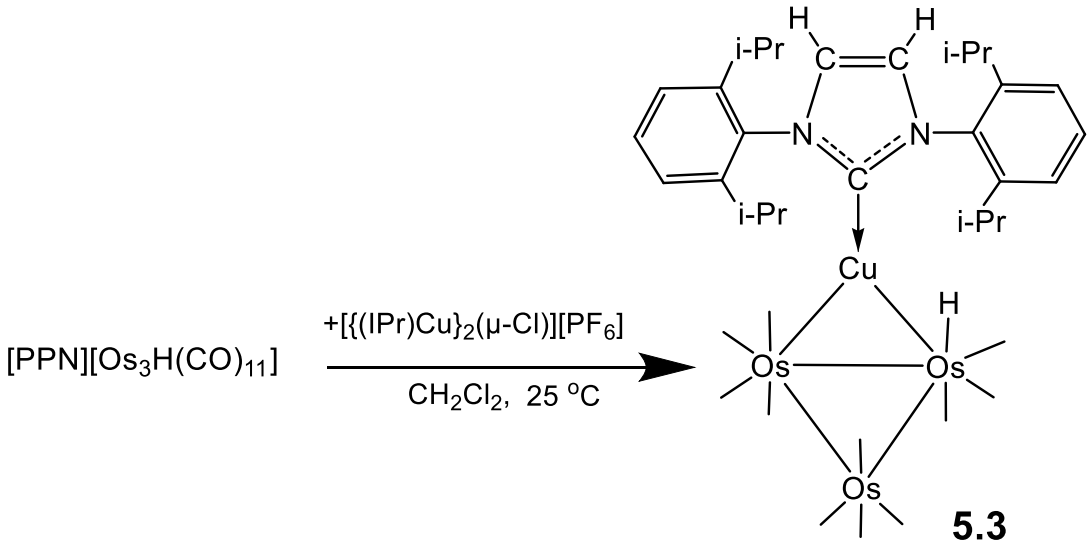

Scheme 5.2. A schematic of the synthesis and structure of the Cu – Os_3 cluster complex **5.3**. The CO ligands in **5.3** are represented only as lines from the Os atoms.

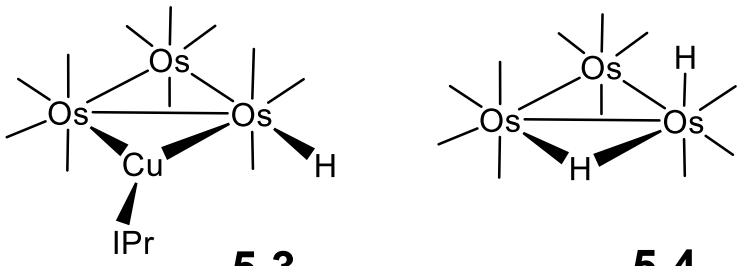

5.3 **5.4**

Scheme 5.3. Line structures of **5.3** and **5.4** comparing the relative positions of the hydrido ligands.

5.5 References

1. Group 11 element, in *Wikipedia*, https://en.wikipedia.org/wiki/Group_11_element**.**

2. A. M. Echavarren, N. Jiao, V. Gevorgyan, Coinage metals in organic synthesis, *Chem. Soc. Rev.* **2016**, *45,* 4445 – 4447.

3. (a) J. Hassan, M. Sevignon, C. Gozzi, E. Schulz, M. Lemaire, Aryl-Aryl Bond Formation One Century after the Discovery of the Ullmann Reaction, *Chem. Rev.* 2002*, 102,* 1359–1470. (b) I. P. Beletskaya, A. V. Cheprakov, Copper in cross-coupling reactions. The post-Ullmann chemistry, *Coord. Chem. Rev.* **2004**, *248,* 2337–2364. (c) F. Monnier, M. Taillefer, Catalytic C-C, C-N, and C-O Ullmann-Type Coupling Reactions, *Angew. Chem. Int. Ed*. **2009**, *48,* 6954 – 6971. (d) M. V. Kirillova, Y N. Kozlov, L. S. Shul'pina, O. Y. Lyakin, A. M. Kirillov, E. P. Talsi, A. J. L. Pombeiro, G. B. Shul'pin, Remarkably fast oxidation of alkanes by hydrogen peroxide catalyzed by a tetracopper(II) triethanolaminate complex: Promoting effects of acid co-catalysts and water, kinetic and mechanistic features, *J. Catal*. **2009**, *268,* 26-38. (e) M. Yamada, K. D. Karlin, S. Fukuzumi, One-step selective hydroxylation of benzene to phenol with hydrogen peroxide catalysed by copper complexes incorporated into mesoporous silica–alumina, *Chem. Sci*., **2016**, *7,* 2856–2863. (f) C.-J. Li, Cross-Dehydrogenative Coupling (CDC): Exploring C-C Bond Formations beyond Functional Group Transformations, *Acc. Chem. Res*. **2009**, *42,* 335 – 344. (g) L. S. Shul'pina, M. M. Vinogradov, Y. N. Kozlov, Y. V. Nelyubina, N. S. Ikonnikov, G. B. Shul'pin, Copper complexes with 1,10-phenanthrolines as efficient catalysts for oxidation of alkanes by hydrogen peroxide, *Inorg. Chim. Acta* **2020**, *512,* 119889. (h) M. Meldal, C. W. Tornøe, Cu-Catalyzed Azide−Alkyne Cycloaddition, *Chem. Rev.* 2008*, 108,* 2952–3015. (i) X. Zhu, S. Chiba, Copper-catalyzed oxidative carbon–heteroatom bond formation: a recent update, *Chem. Soc. Rev.,* **2016**, *45,* 4504 – 4523. (j) S. D. McCann, S. S. Stahl, Copper-Catalyzed Aerobic Oxidations of Organic Molecules: Pathways for Two-Electron Oxidation with a Four-Electron Oxidant and a One-Electron Redox-Active Catalyst, *Acc. Chem. Res*. **2015**, *48,* 1756−1766.

4. (a) S. C. Allen, R. R. Walvoord, R. Padilla-Salinas, M. C. Kozlowski, Aerobic Copper-Catalyzed Organic Reactions. *Chem. Rev.* **2013**, *113,* 6234−6458. (b) X. X. Guo, D.-W. Gu, Z. X. Wu, W. B. Zhang, Copper-Catalyzed C−H Functionalization Reactions: Efficient Synthesis of Heterocycles, *Chem. Rev*. **2015**, *115,* 1622−1651. (c) X. Tang, W. Wu, W. Zeng, H. Jiang, Copper-Catalyzed Oxidative Carbon−Carbon and/or Carbon−Heteroatom Bond Formation with O_2 or Internal Oxidants, *Acc. Chem. Res*. **2018**, *51,* 1092−1105. (d) R. Trammell, K. Rajabimoghadam, I. Garcia-Bosch, Copper-Promoted Functionalization of Organic Molecules: from Biologically Relevant Cu/O_2 Model Systems to Organometallic Transformations, *Chem. Rev.* **2019**, *119,* 2954−3031.

5. For recent reviews, see: a) H. Pellissier, Enantioselective Silver-Catalyzed Transformations, *Chem. Rev.* 2016*, 116,* 14868–14917. b) Q.-Z. Zheng, N. Jiao, Ag-catalyzed C–H/C–C bond functionalization, *Chem. Soc. Rev***. 2016**, *46,* 4590-4627. c) K. Sekine, T. Yamada, Silver-catalyzed carboxylation, *Chem. Soc. Rev*. **2016**, *45,* 4524-

4532. d) J.-M. Weibel, A. Blanc,P. Pale Ag-Mediated Reactions: Coupling and Heterocyclization Reactions, *Chem. Rev*. **2008**, *108*, 3149–3173. d) Z.G. Li, C. He, Recent Advances in Silver-Catalyzed Nitrene, Carbene, and Silylene-Transfer Reactions, *Eur. J. Org. Chem*. **2006**, 4313–4322. e) R. Karmakar, D. Lee, Reactions of arynes promoted by silver ions, *Chem. Soc. Rev.* **2016**, *45*, 4459-4470.

6. For recent reviews, see: a) A. S. K. Hashmi, Homogeneous Catalysis by Gold. *Gold Bull*. **2004**, *37*, 51−65. b) A. S. K. Hashmi, G. J. Hutchings, Gold Catalysis. *Angew. Chem., Int. Ed*. **2006**, *45*, 7896−7936. c) A. Fürstner, P. W. Davies, Catalytic Carbophilic Activation: Catalysis by Platinum and Gold π-Acids. *Angew. Chem., Int. Ed*. **2007**, *46*, 3410−3449. d) S. Witzel, A. S. K. Hashmi, and J. Xie, Light in Gold Catalysis, *Chem. Rev*. **2021**, *121*, ASAP. e) E. Jiménez-Núñez, A. M. Echavarren, Gold-Catalyzed Cycloisomerizations of Enynes: A Mechanistic Perspective. *Chem. Rev*. **2008**, *108*, 3326−3350. f) C. Obradors, A. M. Echavarren, Gold-Catalyzed Rearrangements and Beyond, *Acc. Chem. Res.* 2014, *47*, 902–912. g) R. J. Harris and R. A. Widenhoefer, Gold carbenes, gold-stabilized carbocations, and cationic intermediates relevant to gold-catalysed enyne cycloaddition, *Chem. Soc. Rev*. **2016**, *45*, 4533 – 4551. h) D. Pflästerer and A. S. K. Hashmi, Gold catalysis in total synthesis – recent achievements, *Chem. Soc. Rev*. **2016**, *45*, 1331 – 1367. i) A. M. Asiri, A. S. K. Hashmi, Gold-catalysed reactions of diynes, *Chem. Soc. Rev*. **2016**, *45*, 4471 – 4503.

7. a) C. Fliedel, A. Labande, E. Manoury, R. Poli, Chiral N-heterocyclic carbene ligands with additional chelating group(s) applied to homogeneous metal-mediated asymmetric catalysis, *Coord. Chem. Rev*. **2019**, *394*, 65 – 103. b) F. Lazreg, F. Nahra, C. S. J. Cazin, Copper–NHC complexes in catalysis, *Coord. Chem. Rev*. **2015**, *293–294*, 48 - 79. c) J. D. Egbert, C. S. J. Cazin, S. P. Nolan, Copper N-heterocyclic carbene complexes in catalysis, *Catal. Sci. Technol*. **2013**, *3*, 912 – 926. d) R. Jazzar, M. Soleilhavoup, G. Bertrand, Cyclic (Alkyl)- and (Aryl)-(amino)carbene Coinage Metal Complexes and Their Applications, I. **2020**, *120*, 4141−4168. e) J. C. Y. Lin, R. T. W. Huang, C. S. Lee, A. Bhattacharyya, W. S. Hwang, I. J. B. Lin, Coinage Metal-N-Heterocyclic Carbene Complexes, *Chem. Rev*. **2009**, *109*, 3561–3598. f) A. A. Danopoulos, T. Simler, P. Braunstein, N-Heterocyclic Carbene Complexes of Copper, Nickel, and Cobalt, *Chem. Rev*. **2019**, *119*, 3730−3961. g) S. Díez-González, E. D. Stevens, N. M. Scott, J. L. Petersen, S. P. Nolan, Synthesis and Characterization of $[Cu(NHC)_2]X$ Complexes: Catalytic and Mechanistic Studies of Hydrosilylation Reactions, *Chem. Eur. J*. **2008**, *14*, 158 – 168.

8. a) J. H. Sinfelt, *Acc. Chem. Res.* 1977, *10*, 15–20. b) J. H. Sinfelt, *Acc. Chem. Res.* 1987, *20*, 134–139. c) J. H. Sinfelt, Supported Bimetallic Cluster" Catalysts, *J. Catal*. **1973**, *29*, 308-315. d) J. A. Lopez-Sanchez, N. Dimitratos, N. Glanvilla, L. Kesavan, C. Hammond, J. K. Edwards, A. F. Carley, C. J. Kiely, G. J. Hutchings, Reactivity studies of Au–Pd supported nanoparticles for catalytic applications, *Appl. Catal. A: Gen.* **2011**, *391*, 400 – 406. e) G. J. Hutchings, Nanocrystalline gold and gold palladium alloy catalysts for chemical Synthesis, *Chem. Commun*. **2008**, 1148 – 1164. f) J. Wisniewska, C.-M. Yang, M. Ziolek, Changes in bimetallic silver–platinum catalysts during activation and oxidation of methanol and propene, *Catal. Today* **2019**, *333*, 89–96. g) Rice, R.W.; Lu,

K., Comparison of Platinum and Platinum-Iridium Catalysts for Heptane Reforming at Different Pressures, *J. Catal*. **1982**, *77*, 104-117. h) R. D. Adams, M. Chen, G. Elpitiya, M. E. Potter, R. Raja, Iridium-Bismuth Cluster Complexes yield Bimetallic Nano-Catalysts for the Direct Oxidation of 3-Picoline to Niacin, *ACS Catal.* **2013**, *3*, 3106−3110.

9. a) D. S. Shephard, T. Maschmeyer, G. Sankar, J. M. Thomas, D. Ozkaya, B. F. G. Johnson, R. Raja, R. D. Oldroyd, R. G. Bell, Preparation, Characterisation and Performance of Encapsulated Copper - Ruthenium Bimetallic Catalysts Derived from Molecular Cluster Carbonyl Precursors, *Chem. Eur. J*. **1998**, *4*, 1214 – 1224.(b) C. L. Bracey, P. R. Ellis, G. J. Hutchings, Application of copper–gold alloys in catalysis: current status and future perspectives, *Chem. Soc. Rev*. **2009**, *28*, 2231–2243. c) C. Rhodes, G. J. Hutchings, A. M. Ward, Water-gas shift reaction: finding the mechanistic boundary, *Catal. Today* **1995**, *23*, 43-58. d) H. Iwai, T. Umeki, M. Yokomatsu and C. Egawa, Methanol partial oxidation on Cu–Zn thin films grown on Ni(1 0 0) surface**,** *Surf. Sci*. **2008**, *602*, 2541 - 2546. e) J.-D. Grunwaldt, A. M. Molenbroek, N.-Y. Topsøe, H. Topsøe, and B. S. Clausen, Investigations of Structural Changes in Cu/ZnO Catalysts, *J. Catal*. **2000**, *194*, 452–460, doi:10.1006/jcat.2000.2930 f) B H. Lipshutz, D. M. Nihan, E. Vinogradova, B. R. Taft, Z. V. Boskovic, Copper + Nickel-in-Charcoal (Cu-Ni/C): A Bimetallic, Heterogeneous Catalyst for Cross-Couplings, *Org. Lett*. **2008**, *10*, 4279 – 4282. g) J. H. Sinfelt, Catalysis by Alloys and Bimetallic Clusters, *Acc. Chem. Res*. **1977**, *10*, 15 – 20. h) A. B. Boricha, H. C. Bajaj, T. H. Kim, S. H. R. Abdi, R. V. Jasra, Preparation of Highly Dispersed Pd–Cu on Silica for the Aerobic Hydroxylation of Benzene to Phenol Under Ambient Conditions, *Catal. Lett*. **2010**, *137*, 202–209.

10. a) P. Buchwalter, J. Rosé, P Braunstein, Multimetallic Catalysis Based on Heterometallic Complexes and Clusters, *Chem. Rev*. **2015**, *115*, 28−126. b) J. M. Thomas, B. F. G. Johnson, R. Raja, G. Sankar, P. A. Midgley, High-Performance Nanocatalysts for Single-Step Hydrogenations, *Acc. Chem. Res*. **2003**, *35*, 20 - 30. c) P. Braunstein, J. Rosé, Heterometallic Clusters in Catalysis, in *Metal Clusters in Chemistry*, P Braunstein, L. A. Oro, P. R. Raithby, Eds. Wiley-VCH, Weinheim, **1999**, Vol. 2, Sec. 2.2, 616 – 677. d) P. Braunstein, J. Rosé, Heterometallic Clusters for Heterogeneous Catalysis, in *Catalysis by Di- and Polynuclear Metal Complexes*, R. D. Adams and F. A. Cotton,, Eds. Wiley-VCH, New York, **1998**, Ch. 13, 443 – 508. e) R. D. Adams and E. Trufan, Ruthenium-Tin Cluster Complexes and their Applications as Bimetallic Nanoscale Heterogeneous Hydrogenation Catalysts, *Phil. Trans Royal. Soc*. **2010**, *368*, 1473-1493. f) A. B. Hungria, R. Raja, R. D. Adams, B. Captain, J. M. Thomas, P. A. Midgley, V. Golvenko and B. F. G. Johnson, Single-Step Conversion of Dimethyl Terephthalate to Cyclohexanedimethanol with A Trimetallic Nanoparticle Catalyst: Ru_5PtSn, *Angew. Chem. int. Ed.* **2006**, *45*, 4782-4785. g) R. D. Adams, D. A. Blom, B. Captain, R. Raja, J. M. Thomas, and E. Trufan, Toward Less Dependence on Platinum Group Metal Catalysts: The Merits of Utilizing Tin, *Langmuir*, **2008**, *24*, 9223-9226.

11. a) B. Berti, M. Bortoluzzi, C. Cesari,.C. Femoni, M. C. Iapalucci, R. Mazzoni, S. Zacchini, A Comparative Experimental and Computational Study of Heterometallic Fe-M (M = Cu, Ag, Au) Carbonyl Clusters Containing N-Heterocyclic Carbene Ligands, *Eur.*

J. Inorg. Chem. **2020**, 2191–2202. b) R.D. Pergola, A. Sironi, A. Rosehr, V. Colombo, A. Sironi, N-heterocyclic carbene copper complexes tethered to iron carbidocarbonyl clusters, *Inorg. Chem. Commun*. **2014**, *49,* 27- 29. c) M. Shieh, Y.-H. Liu, Y.-H. Li, C.-N. Lin, C.-C. Wang, Functionalized NHC-incorporated Te–Fe–Cu clusters: Facile synthesis, electrochemistry, and catalytic reaction, *J. Organomet. Chem*. **2018**, *867,* 161 – 169. d) M. Shieh, Y.-H. Liu, C.-C. Wang, S.-H. Jian, C.-N. Lin, Y.-M. Chen, C.-Y. Huang, A comparative study on NHC-functionalized ternary Se/Te–Fe–Cu compounds: synthesis, catalysis, and the effect of chalcogens, *New J. Chem*. **2019**, *43,* 11832 -11843. e) C.-N. Lin, C.-Y. Huang, C.-C. Yu, Y.-M. Chen, W.-M. Ke, G.-J. Wang, G.-A. Lee, M. Shieh, Iron carbonyl cluster-incorporated Cu(I) NHC complexes in homocoupling of arylboronic acids: an effective $[TeFe_3(CO)_9]^{2-}$ ligand, *Dalton Trans*. **2015**, *44,* 16675 – 16679.

12. C. R. Eady, B. F. G. Johnson, J. Lewis, *J. Chem. Soc., Dalton Trans*, **1978**, 1358 – 1363.

13. SAINT+, version 6.2a, Bruker Analytical X-ray Systems, Inc., Madison, WI, **2001**.

14. APEX3 Version 2016.5-0 and SAINT Version 8.34A. Bruker AXS, Inc. Madison, WI, USA.

15. SADABS Version 2016/2. L. Krause, R. Herbst-Irmer, G. M. Sheldrick, D. Stalke, *J. Appl. Cryst*. **2015**, *48,* 3-10.

16. G.M. Sheldrick, SHELXTL, Version 6.1, Bruker Analytical X-ray Systems, Inc, Madison, WI, **1997**.

17. M. Trose, F, Nahra, C. S.J. Cazin, Dinuclear N-heterocyclic carbene copper(I) complexes, *Coord. Chem. Rev*. **2018**, *355,* 380–403.

18. H. Kaur, F. K. Zinn, E. D. Stevens, S. P. Nolan, (NHC)CuI(NHC)N-Heterocyclic Carbene) Complexes as Efficient Catalysts for the Reduction of Carbonyl Compounds, *Organometallics* **2004**, *23,* 1157-1160.

19. M. Pasquali, C. Floriani, A. Gaetani-Manfredotti, Carbon Monoxide Absorption by Copper(I) Halides in Organic Solvents: Isolation and Structure of μ-Halogeno-dicopper(I) Carbonyl Complexes, *Inorg. Chem*. **1981**, *20,* 3382-3388.

20. E. Jürgens, O. Back, J. J. Mayer, K. Heinze, D. Kunz, Synthesis of copper(II) and gold(III) bis(NHC)-pincer complexes, *Z. Naturforsch*. **2016**, *71,* 1011–1018.

21. J. Zhai, A. S. Filatov, G. L. Hillhouse, M. D. Hopkins, Synthesis, structure, and reactions of a copper-sulfido cluster comprised of the parent Cu_2S unit: $\{(NHC)Cu\}_2(\mu\text{-}S)$, *Chem. Sci*. **2016**, *7,* 589 – 595.

22. B. F. G. Johnson, J. Lewis, P. R. Raithby, S. N. Azman, B. Syed-Mustaffa, M. J. Taylor, K. H. Whitmire, Synthesis of Mixed-metal Clusters by the Reaction of the Unsaturated Cluster $[Os_3(\mu\text{-}H)_2(CO)_{10}]$ transition-metal Hydrides; the X-Ray Crystal Structures $[Os_3H_3(CO)_{10}\{Cu(PPh_3)\}]$ and $[Os_3H_3(CO)_{11}\{Ir(PPh_3)\}]$, *J. Chem. Soc., Dalton Trans.* **1984**, 2111 – 2118.

23. J. R. Shapley, J. B. Keister, M. R. Churchill, B, G, DeBoer, Synthesis and Characterization of the Fluxional Species $H_2Os_3(CO)_{10}L$. The Crystal Structure of $H_2Os_3(CO)_{11}$, *J. Am. Chem. Soc.* **1975**, *97*, 4145 – 4146.

24. M. R. Churchill, B. G. DeBoer, Structural Studies on Polynuclear Osmium Carbonyl Hydrides. 1. Crystal Structures of the Isomorphous Species $H_2Os_3(CO)_{11}$ and $Os_3(CO)_{12}$. Direct Information on the Role of an Equatorial 2-Bridging Hydride Ligand in Perturbing the Arrangement of Carbonyl Ligands in a Triangular Cluster, *Inorg. Chem.* **1977**, *16*, 878 – 884.

APPENDIX A

COPYRIGHT RELEASES

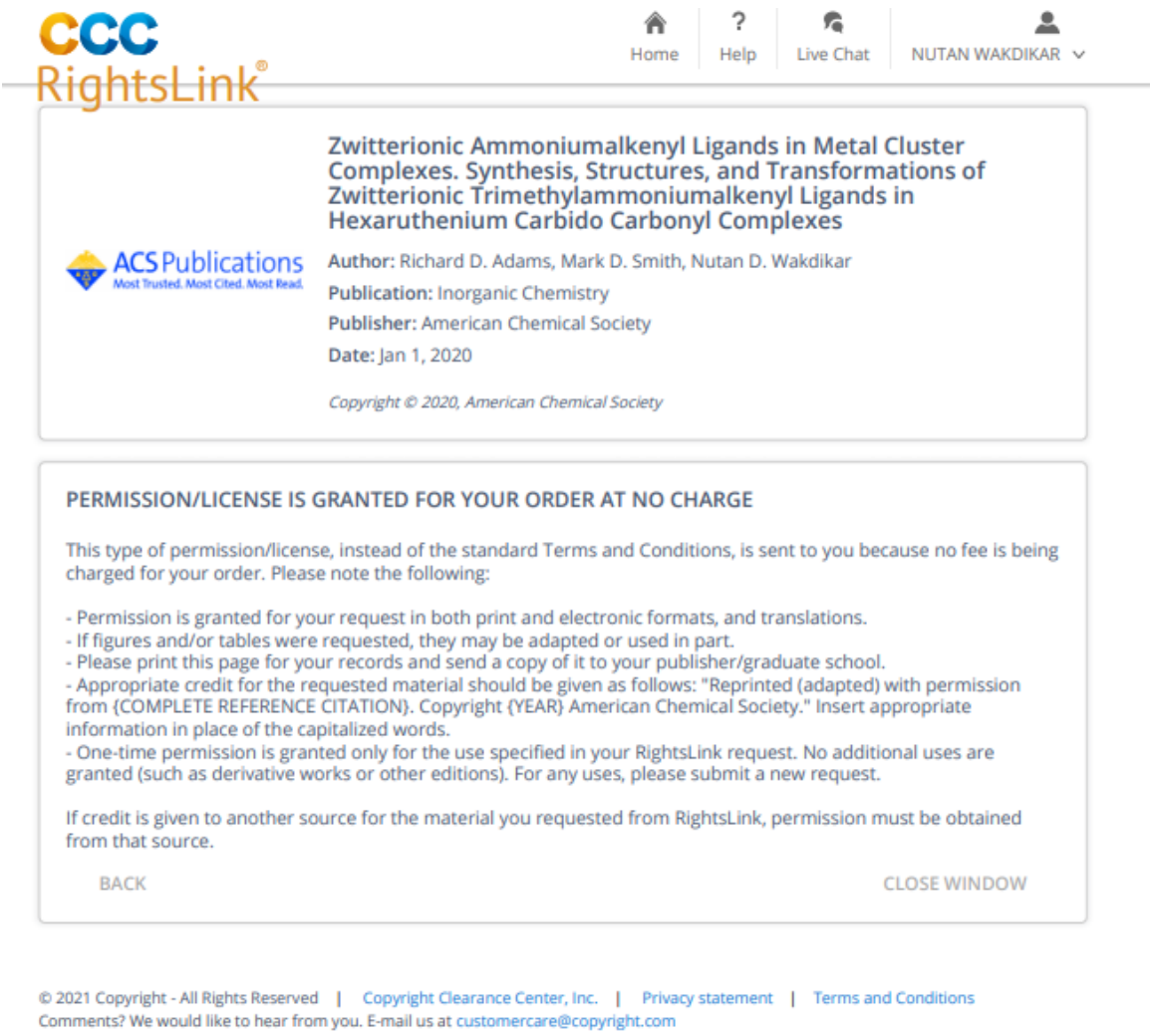

Permission for reprint from publisher of Chapter 2.

Adams, R. D.; Smith, M. D.; Wakdikar, N. D.; *Inorganic Chemistry* **2020**, *59*, 2, 1513–1521

Permission for reprint from publisher of Chapter 4.

Adams, R. D.; Pellechia, P. J.; Smith, M. D.; Tedder, J. D.; Wakdikar, N. D.; *J. Organomet. Chem.* **2019**, *898*, 120872

Permission for reprint from publisher of Chapter 5.

Adams, R. D.; Smith, M. D.; Tedder, J. D.; Wakdikar, N. D.; *J. Organomet. Chem.* **2021**, *941*, 121799